Stony Brook University

OFFICIAL COPY

The official electronic file of this thesis or dissertation is maintained by the University Libraries on behalf of The Graduate School at Stony Brook University.

© All Rights Reserved by Author.

Targeting and roles of complexins in zebrafish ribbon-containing neurons

A Dissertation Presented

by

George Zanazzi

to

The Graduate School

In Partial fulfillment of the

Requirements

For the Degree of

Doctor of Philosophy

in

Neuroscience

Stony Brook University

December 2010

Copyright by
George Zanazzi
2010

Stony Brook University

The Graduate School

George Zanazzi

We, the dissertation committee for the above candidate
for the Doctor of Philosophy degree, hereby recommend
acceptance of this dissertation.

Gary G. Matthews, Ph.D., Professor,
Department of Neurobiology and Behavior

Howard Sirotkin, Ph.D., Associate Professor,
Department of Neurobiology and Behavior

Stephen Yazulla, Ph.D., Professor,
Department of Neurobiology and Behavior

Ruth Heidelberger, M.D., Ph.D., Professor,
Department of Neurobiology and Anatomy, U. Texas Medical School at Houston

This dissertation is accepted by the Graduate School

Lawrence Martin
Dean of the Graduate School

Abstract of the Dissertation

Targeting and roles of complexins in zebrafish ribbon-containing neurons

by

George Zanazzi

Doctor of Philosophy

In

Neuroscience

Stony Brook University

2010

The primary receptor cells of the visual, auditory, vestibular and lateral line systems encode a broad range of sensory information by modulating the tonic release of the neurotransmitter glutamate in response to graded changes in membrane potential. The output synapses of these neurons are marked by structures called synaptic ribbons, which tether a pool of releasable synaptic vesicles at the active zone. Despite the importance of the ribbon in synaptic transmission, the molecular mechanisms that govern the assembly and function of the exocytotic machinery in these terminals are poorly understood. We have identified a subfamily of SNARE complex regulators, composed of complexin 3 and complexin 4, which are enriched in ribbon-containing sensory neurons. Phylogenetic analysis reveals that there are two complexin 3 paralogs and three complexin 4 paralogs in zebrafish. Complexin 3/4 is

rapidly targeted to photoreceptor presynaptic terminals in the zebrafish retina and pineal organ concomitantly with RIBEYE, a member of the CtBP family of transcriptional corepressors that is the major component of ribbons. In hair cells of the inner ear and lateral line, however, complexin 3/4 immunoreactivity clusters on the apical surfaces of hair cells, among their stereocilia. While a complexin 4a-specific antibody and riboprobe selectively label visual system ribbon-containing neurons, neuromasts and the inner ear contain complexin 4b. Complexin 4a knockdown in vivo perturbs visual background adaptation and optokinetic responses, indicating that these mutants are blind, without grossly affecting photoreceptor presynaptic architecture. Complexins may have additional functions during development since modulation of complexin 3a levels via knockdown or overexpression induces pleiotropic effects on dorsoventral patterning and eye development. Taken together, these results provide evidence for the concurrent transport and/or assembly of multiple components of the active zone in developing ribbon terminals. Members of the complexin 3/4 subfamily are enriched in these terminals in the visual system and in hair bundles of the octavolateral system, suggesting that these proteins are differentially targeted and have multiple roles in ribbon-containing sensory neurons. Furthermore, these results implicate complexin 3 and complexin 4 as candidate genes for hereditary visual, auditory, and vestibular disorders.

Dedication

This dissertation is dedicated to my mom, Marisa Zanazzi, for all of her love and support through the years.

Table of Contents

List of Figures

Chapter 1

Chapter 3

Chapter 4

Chapter 5

Chapter 6

Chapter 7

List of Tables

List of Abbreviations

aa	amino acid
ada	adenosine deaminase
AS	antisense
cat	catalog
chr	chromosome
cplx	complexin
CSK	c-src kinase
CtBP2	carboxy-terminal binding protein 2
DIG	digoxigenin
DMEM	Dulbecco's Modified Eagle's Medium
dpf	days post-fertilization
EGFP	enhanced green fluorescence protein
ERGIC-53	ER Golgi intermediate compartment 53-kD
ERGIC-53L	ER Golgi intermediate compartment 53-kD-like
FITC	fluorescein isothiocyanate
GCL	ganglion cell layer
gf	goldfish
HEK	human embryonic kidney
hpf	hours post-fertilization
hu	human
INL	inner nuclear layer
IPL	inner plexiform layer
kD	kilodalton
lman1	lectin mannose-binding 1
lman1-L	lectin mannose-binding 1-like
mc	monoclonal
mo	mouse

MO	morpholino
mpf	months post-fertilization
ONL	outer nuclear layer
OPL	outer plexiform layer
PBS	phosphate-buffered saline
pc	polyclonal
PCR	polymerase chain reaction
pin	pineal
rb	rabbit
rx3	retinal homeobox gene 3
S	sense
SDS	sodium dodecyl sulfate
sm	saccular macula
SNAP	soluble NSF attachment protein
SNARE	soluble N-ethylmaleimide–sensitive factor attachment protein receptor
TE	Tris-EDTA
wpf	weeks post-fertilization
ZIRC	Zebrafish International Resource Center

Acknowledgments

This PhD thesis was carried out in the Department of Neurobiology and Behavior at Stony Brook University. I would like to extend my deepest gratitude to everyone who supported me during my graduate study. First of all, I would like to thank my thesis advisor, Dr. Gary Matthews, for his support and guidance. Gary's work ethic, scope of scientific knowledge, and passion for research are inspirational. It truly has been a privilege to work in his lab. I would also like to thank my thesis committee, composed of Dr. Howard Sirotkin, Dr. Steve Yazulla, and Dr. Ruth Heidelberger, for their advice throughout the course of this project. Much of the work was performed in Howie's lab, and I will always be grateful for his help and encouragement.

Several investigators provided reagents that were used in this work, including Teresa Nicolson (Oregon Health and Science University), David Zenisek (Yale University), Julie Rosenbaum (Halegoua lab, Stony Brook University), Chi Bin-Chien (University of Utah), Andrew Taibi (Sirotkin lab, Stony Brook University), Joerg Leheste (currently at New York College of Osteopathic Medicine) and Rashek Kazi (Wollmuth lab, Stony Brook University) for the kind gifts of RIBEYE b polyclonal antibody, RIBEYE-binding peptide, Alexa Fluor 488 phalloidin, Tol2 kit, lacZ mRNA, zebrafish mGluR6 promoter, and HEK 293T cells, respectively. This work was supported by National Institutes of Health Grants NIH R01 EY03821 (G.M.), NIH RO3 EY014316 (G.M.), NIH F30 NS061494 (G.Z.), and an NIH MSTP fellowship (G.Z.). The text of this dissertation is, in part, a reprint of publications in *Neural Development* and *Molecular Neurobiology*. The co-author listed in the publications (G.M.) directed and supervised the research that forms the basis for this dissertation.

Thanks to the Matthews lab for providing me with a home away from home. In particular, I would like to thank Karen Wexler for assistance with preparing solutions, Diane Henry-Vanisko for invaluable help whenever a calamity befell the lab, and Wendy Akmentin for expert assistance with electron microscopy. Thanks also to Lance Sommer, Ana Vega, Thirumalini Vaithianathan, Joerg Leheste, Stephanie Burke, Lisamarie LoGiudice and the rest of the students in the lab for fun discussions. Thanks to Andrew Taibi, Richard Grady, and Laurie Mentzer in Howie's lab for assistance with zebrafish husbandry and for teaching me several useful techniques. In addition to the Matthews and

Sirotkin labs, I was adopted by the Wollmuth lab—Iehab Talukder, Mike Prodromou, Gulcan Akgul, Alexandra Corrales, Jessica Helm, Rashek Kazi, Janet Allopenna, Mike Langis, Catherine Salussolia— and I am grateful for their friendship and scientific discussions. I will miss very much our times in the lab late at night and on weekends, our dinners, and our coffee and tea breaks. Finally, the biggest thanks are reserved for John Sinnamon for his unwavering support and for his help with Western Blots. Besides being a great friend, he is a very talented scientist. John has a very bright future ahead of him in science.

Many other people at Stony Brook provided support that helped me to complete this dissertation- Paul Brehm, Gail Mandel, Joe Fetcho, Simon Halegoua, Lorne Mendell, Craig Evinger, Joel Levine, Lonnie Wollmuth, Mary Kritzer, Lorna Role, Nisson Schechter, Raafat El-Maghrabi, Catherine Waddell, Gretchen Lopez, Mayo Mertz, Sarah Canetta, Edlira Luca, Tanvir Khan, Pola Philippidou, Jack Turvin, Bing Fan, and Victor Luna. Extra special thanks goes to Diane Godden and Barbara Mummers for help with administrative matters. Thanks to Paul Fisher and Mike Frohman, the past and current MSTP directors, respectively, for bringing me to Stony Brook and making my dream of becoming a physician-scientist a reality.

Over the past 22 years, I have had the privilege to work in several laboratories with outstanding mentors and colleagues. While scientific inquiry provides many intrinsic rewards, the relationships made with these wonderful people have been just as fulfilling. I would like to thank Premila Rathnam, Brij Saxena, and Sam George at the Weill Cornell Medical College; Stephen Shochat, Stuart Young, Fan Qing, Holde Muller, Terry Desser, and Dan Rubin at the Stanford University School of Medicine; Jim Salzer, Steve Einheber, Orlando Gil, Carmen Melendez-Vasquez, William Ching, Patrice Maurel, Jose Rios, Marina Rubin, Carla Taveggia, Yulia Dzhashiashvilli, Takeshi Sakurai, Martin Grumet, Marc Lustig, David Friedlander, Ravi Tikoo, Irene Noguera, Bill Dolan, Paul Ovelheira, and Takashi Morimoto at the NYU School of Medicine. I would also like to acknowledge the guidance of Robert Sapolsky and Arthur Kornberg.

Finally, I would like to express my deepest thanks to my family for all of their support, encouragement, and love. My grandmothers, Pierina and Berta, encouraged scholarship and diligence from a young age. My Aunt Rita, Uncle Luigi, Aunt Rosa, and

cousins have always been supportive. Thanks to my brother, Sergio, and my sisters, Francesca and Cristina, for their immeasurable love and for providing several fun nephews and nieces over the course of my graduate education. Finally, thanks to my parents, Joseph and Marisa Zanazzi, for all of their sacrifices. They are my heroes.

George John Zanazzi

State University of New York at Stony Brook
Department of Neurobiology and Behavior
Centers for Molecular Medicine, Room 335
Stony Brook, New York 11794-5230

Tel: (631) 632-8648
Fax: (631) 632-4858

Education

1989 - 1993	Stanford University, Palo Alto, California Bachelor of Science, Department of Biological Sciences
2002 - present	State University of New York at Stony Brook MD-PhD, Department of Neurobiology and Behavior

Research Experience

1989	Cornell University Medical College, New York, New York Research Assistant, Department of Obstetrics and Gynecology
1991 - 1993	Stanford University School of Medicine, Palo Alto, California Research Assistant, Departments of Surgery and Radiology
1993 - 2002	New York University School of Medicine, New York, New York Research Technician, Department of Cell Biology
2002 - present	State University of New York at Stony Brook MD-PhD, Department of Neurobiology and Behavior

Publications

Young, S.W., Sidhu, M.K., Qing, F., Muller, H.H., Neuder, M., **Zanazzi, G.**, Mody, T.D., Hemmi, G., Dow, W., Mutch, J.D., Sessler, J.L. and Miller R.A. 1994. Preclinical evaluation of gadolinium (III) texaphyrin complex: a new paramagnetic contrast agent for magnetic resonance imaging. ***Invest. Radiol.*** 29: 330-338.

Desser, T.S., Rubin, D.L., Muller, H.H., Qing, F., Khodor, S., **Zanazzi, G.**, Young, S.W., Ladd, D.L., Wellons, J.A., Kellar, K.E., Toner, J.L. and Snow, R.A. 1994. Dynamics of tumor imaging with Gd-DTPA-polyethylene glycol polymers: dependence on molecular weight. ***J. Mag. Res. Imag.*** 4: 467-472.

Einheber, S., **Zanazzi, G.**, Ching, W., Scherer, S., Milner, T.A., Peles, E. and Salzer, J.L. 1997. The axonal membrane protein Caspr/neurexin IV is a component of the septate-like paranodal junctions that assemble during myelination. ***J. Cell Biol.*** 139: 1495-1506.

Gil, O.D., **Zanazzi, G.**, Struyk, A. and Salzer, J.L. 1998. Neurotrimin mediates bifunctional effects on neurite outgrowth via homophilic and heterophilic interactions. ***J. Neurosci.*** 18: 9312-9325.

Rambukkana, A., Yamada, H., **Zanazzi, G.**, Mathus, T., Salzer, J.L., Yurchenco, P.D., Campbell, K.P. and Fischetti, V.A. 1998. Role of alpha-dystroglycan as a Schwann cell receptor for Mycobacterium leprae. ***Science*** 282: 2076-2079.

Galbiati, F., Volonte, D., Gil, O., **Zanazzi, G.**, Salzer, J.L., Sargiacomo, M., Scherer, P.E., Engelman, J.A., Schlegel, A., Parenti, M., Okamoto, T. and Lisanti, M.P. 1998. Expression of caveolin-1 and -2 in differentiating PC12 cells and dorsal root ganglion neurons: caveolin-2 is up-regulated in response to cell injury. ***Proc. Natl. Acad. Sci.*** 95: 10257-10262.

Ching, W., **Zanazzi, G.**, Levinson, S.R. and Salzer, J.L. 1999. Clustering of neuronal sodium channels requires contact with myelinating Schwann cells. ***J. Neurocytol.*** 28: 295-301.

Tikoo, R., **Zanazzi, G.**, Shiffman, D., Salzer, J. and Chao, M.V. 2000. Cell cycle control of Schwann cell proliferation: role of cyclin-dependent kinase-2. ***J. Neurosci***. 20: 4627-4634.

Ng, V.∗, **Zanazzi, G.**∗, Timpl, R., Talts, I.F., Salzer, J.L., Brennan, P.J. and Rambukkana, A. 2000. Role of the cell wall phenolic glycolipid-1 in the peripheral nerve predilection of Mycobacterium leprae. ***Cell*** 103: 511-524. ∗Equal contribution.

Zanazzi, G., Einheber, S., Westreich, R., Hannocks, M.-J., Bedell-Hogan, D., Marchionni, M.A. and Salzer, J.L. 2001. Glial growth factor/neuregulin inhibits myelination and induces demyelination. ***J. Cell Biol.*** 152: 1289-1299.

Melendez-Vasquez, C., Rios, J.C., **Zanazzi, G**., Bretscher, A., Lambert, S. and Salzer, J.L. 2001. Nodes of Ranvier form in association with ERM-positive Schwann cell microvilli. ***Proc. Natl. Acad. Sci.*** 98: 1235-1240.

Lustig, M.∗, **Zanazzi, G.**∗, Sakurai, T., Lambert, S., Grumet, M. and Salzer, J.L. 2001. Nr-CAM and neurofascin interactions regulate ankyrin G and sodium channel clustering at the node of Ranvier. ***Curr. Biol.*** 11: 1864-1869. ∗Equal contribution.

Chen, S., Gil, O.D., Ren, Y.Q., **Zanazzi, G.,** Salzer, J.L. and Hillman, D. 2002. Neurotrimin expression during cerebellar development suggests roles in axon fasciculation and synaptogenesis. ***J. Neurocytol.*** 30: 927-937.

Rambukkana, A.**, Zanazzi, G.**, Tapinos, N. and Salzer, J.L. 2002. Contact-dependent induction of demyelination by Mycobacterium leprae in the absence of immune cells. ***Science*** 296: 927-931.

Gil, O.D., Zhang, L., Chen, S., Ren, Y.Q., Pimenta, A., **Zanazzi, G.**, Hillman, D., Levitt, P. and Salzer, J.L. 2002. Complementary expression and heterophilic interactions between IgLON family members neurotrimin and LAMP. ***J. Neurobiol.*** 51: 190-204.

Melendez-Vasquez, C., Carey, D.J., **Zanazzi, G.,** Reizes, O., Maurel, P., Salzer, J.L. 2005. Differential expression of proteoglycans at central and peripheral nodes of Ranvier. ***Glia*** 52: 301-308.

Taveggia, C., **Zanazzi, G.,** Petrylak, A., Yano, H., Rosenbluth, J., Einheber, S., Xu, X., Esper, R.M., Loeb, J.A., Shrager, P., Chao, M.V., Falls, D.L., Role, L., Salzer, J.L. 2005. Neuregulin-1 type III determines the ensheathment fate of axons. ***Neuron*** 47: 681-694.

Koticha, D., Maurel, P., **Zanazzi, G**., Kane-Goldsmith, N., Basak, S., Babiarz, J., Salzer, J., Grumet, M. 2006. Neurofascin interactions play a critical role in clustering sodium channels, ankyrin G and beta IV spectrin at peripheral nodes of Ranvier. ***Dev Biol.*** 293: 1-12.

Zanazzi, G., Matthews, G. 2007. A doubleheader in endocytosis. ***Neuron*** 56: 939-942.

Zanazzi, G., Matthews, G. 2009. The molecular architecture of ribbon presynaptic terminals. **Mol. Neurobiol.** 39: 130-148.

Zanazzi, G., Matthews, G. 2010. Enrichment and differential targeting of complexins 3 and 4 in ribbon-containing sensory neurons during zebrafish development. **Neural Dev.** 5:24.

Conference Presentations and Abstracts

Young, S.W., Sidhu, M.K., Qing, F., Muller, H.H., Neuder, M., **Zanazzi, G.**, Mody, T.D., Hemmi, G., Dow, W., Mutch, J.D., Sessler, J.L. and Miller R.A. 1992. Preclinical evaluation of gadolinium (III) texaphyrin complex: a new paramagnetic contrast agent for magnetic resonance imaging. Radiological Society of North America 78th Annual Meeting and Scientific Assembly.

Gil, O.D., **Zanazzi, G.**, Struyk, A. and Salzer, J. 1996. Neurotrimin, a member of a subfamily of neural cell adhesion molecules, promotes homophilic adhesion and neuronal outgrowth. ***Soc. Neurosci. Abstr.*** 22(2): 1464.

Zanazzi, G., Westreich, R., Hannocks, M.-J., Einheber, S., Teng, K., Kraemer, R., Marchionni, M. and Salzer, J. 1997. GGF/neuregulin promotes Schwann cell proliferation, inhibits myelination, and induces demyelination. ***Soc. Neurosci. Abstr.*** 23(1): 66.

Gil, O.D., **Zanazzi, G.**, Struyk, A., Zhukareva, V., Pimenta, A., Levitt, P. and Salzer, J. 1997. Heterophilic interactions between members of a family of cell adhesion molecules- LAMP, OBCAM, and Neurotrimin- that are differentially expressed in the nervous system. ***Soc. Neurosci. Abstr.*** 23(2): 1699.

Einheber, S., **Zanazzi, G.**, Ching, W., Scherer, S., Milner, T.A., Peles, E. and Salzer, J.L. 1998. A novel role for neurexins in the axonal-glial interactions of myelination. Third European meeting on glial cell function in health and disease: dialogue between glia and neurons.

Rambukkana, A., Yamada, H., **Zanazzi, G.**, Salzer, J.L., Yurchenco, P.D., Campbell, K.P. and Fischetti, V.A. 1998. Molecular mechanism of neural targeting of Mycobacterium leprae: role of the G domain of laminin-2 and its receptor alpha-dystroglycan. Thirty-third U.S.-Japan tuberculosis and leprosy research conference.

Galbiati, F., Volonte, D., Gil, O., **Zanazzi, G.**, Salzer, J.L., Sargiacomo, M., Scherer, P.E., Engelman, J.A., Schlegel, A., Parenti, M., Okamoto, T. and Lisanti, M.P. 1999. Expression of caveolin-1 and -2 in neurons. ***J. Neurochem.*** 72: 87.

Ching, W., **Zanazzi, G.**, Levinson, S.R. and Salzer, J.L. 1999. Sodium channel clustering at the node of Ranvier requires contact with myelinating Schwann cells. ***Soc. Neurosci. Abstr.*** 25(1): 999.

Lustig, M., **Zanazzi, G.**, Sakurai, T., Blanco, C., Salzer, J. and Grumet, M. 1999. Interactions of Nr-CAM are critical for clustering of ankyrin and sodium channels at the node of Ranvier. ***Soc. Neurosci. Abstr.*** 25(1): 999.

Ng, V.∗, **Zanazzi, G.**∗, Timpl, R., Talts, I.F., Salzer, J.L., Brennan, P.J. and Rambukkana, A. 2000. Role of cell wall phenolic glycolipid-1 in the neural predilection of Mycobacterium leprae.Thirty-fifth U.S.-Japan tuberculosis and leprosy research conference. ∗Equal contribution.

Maurel, P., **Zanazzi, G.**, Rambukkana, A. and Salzer, J.L. 2001. Regulation of laminin-2 chains during myelination. Conference on neuron-glial communication in neural plasticity.

Zanazzi, G., Matthews, G. 2008. Identification and characterization of complexin 3 and 4 paralogs in the zebrafish visual system. ***Soc. Neurosci. Abstr.***. Washington, DC.

Teaching Experience

2002	Principles of Cell Signaling State University of New York at Stony Brook
2003	Cell and Organ Physiology State University of New York at Stony Brook
2005	Medical Biochemistry State University of New York at Stony Brook School of Medicine

Honors and Awards

1992	Chevrolet Collegiate Scholarship Chevrolet Corporation, Omaha, Nebraska
1992	Rhodes, Marshall, and Churchill Scholarships nominations Stanford University, Palo Alto, California
1993	J.E. Wallace Sterling Award nomination for service to Stanford Stanford University, Palo Alto, California
2003	Outstanding First-Year Doctoral Student Award Dept. Neurobiology and Behavior, State University of New York at Stony Brook
2005	Dean's List School of Medicine, State University of New York at Stony Brook
2007	Ruth Kirschstein National Research Service Award, Predoctoral National Institute of Neurological Disorders and Stroke, Bethesda, MD
2007	Best Poster Award Dept. Neurobiology and Behavior, State University of New York at Stony Brook
2009	Kevin King/John Miller Travel Scholarship Award State University of New York at Stony Brook

Invited Talks

2008	Mechanisms of exocytosis at retinal ribbon synapses State University of New York at Stony Brook
2008	Roles of microRNAs in breast cancer State University of New York at Stony Brook
2009	Compound fusion- a putative exocytosis mechanism at retinal ribbon synapses State University of New York at Stony Brook

2009	A 3-year-old boy with nystagmus and head bobbing State University of New York at Stony Brook
2009	Mechanisms of synaptic vesicle fusion in ribbon-containing sensory neurons New York Metropolitan Zebrafish Club
2010	Enrichment and differential targeting of complexins 3 and 4 in ribbon-containing sensory neurons during zebrafish development State University of New York at Stony Brook

Society Memberships

1994 - present	New York Academy of Sciences
1994 - present	American Association for the Advancement of Science
1996 - present	Society for Neuroscience
2003 - present	American Physiological Society
2009 - present	American Physician Scientists Association

Chapter 1

Introduction

The primary receptor neurons of the auditory, vestibular, and visual systems encode a broad range of sensory information by transducing environmental stimuli, via specialized apical microvilli and cilia, into graded changes in membrane potential. The vulnerability of the transduction apparatus is underscored by mutations in several genes that lead to its disorganization and dysfunction in Usher Syndrome, which is the leading cause of combined blindness and deafness. Some proteins mutated in Usher Syndrome, such as myosin VIIa, are localized both in the apical and basolateral compartments of sensory receptor cells, where their distinct roles remain to be clarified. The presynaptic terminals of these cells have a molecular architecture that allows them to effectively transmit information about stimulus intensity and frequency with release modification. A protein unique to these terminals, called RIBEYE, polymerizes to form electron-dense organelles, called ribbons, which tether a halo of releasable synaptic vesicles at the active zone where glutamate release occurs in response to calcium influx through L-type channels. Despite the importance of these presynaptic terminals in visual, auditory, and vestibular function, the molecular mechanisms that underlie fast and sustained exocytosis at these synapses are not well-understood. This dissertation will discuss the development and functions of some molecular and subcellular specializations that support the transduction and transmission of sensory signals in ribbon-containing neurons. In particular, this work focuses primarily on the expression and roles of one molecular specialization, a novel subfamily of SNARE complex regulators called the complexin 3/4 subfamily, in zebrafish ribbon-containing neurons.

Photoreceptive organs in vertebrates- the retina

Vertebrate photoreceptors capture light to generate images and for non-image-forming tasks. Image-forming visual responses to environmental light occur in the retina. While the basic organization of the retina is similar among vertebrates, many structural and functional differences are necessary to encode the variable visual space that different vertebrates encounter. Since this thesis will address studies in the zebrafish retina, we will introduce here the basic cell biology and physiology of the teleost retina. The reader is referred to several excellent

monographs and reviews that provide detail on the mammalian retina (Cajal, 1894; Polyak, 1941; Rodieck, 1973; Dowling, 1987; Wässle and Boycott, 1991; Masland, 2001; Sterling, 2004; Sterling and Demb, 2004; Field and Chichilnisky, 2007).

The teleost retina consists of ten structurally and functionally distinct layers, including three somatic and two synaptic layers (Figure 1-1A). The three somatic layers are the outer nuclear layer (which contains the cell bodies of the light-sensitive photoreceptor cells – the rods and cones), the inner nuclear layer (which contains the bipolar cells as well as amacrine and horizontal cells), and the ganglion cell layer. Interspersed between the nuclear layers are the outer plexiform layer (OPL) (where photoreceptors transmit to bipolar cells and horizontal cells) and the inner plexiform layer (IPL) (where bipolar cells contact amacrine cells and/or ganglion cells). It has been estimated that there are greater than 110 classes of neurons in the teleost retina (Marc, 1999). These different cell types are utilized to create parallel circuits that encode various aspects of the visual environment.

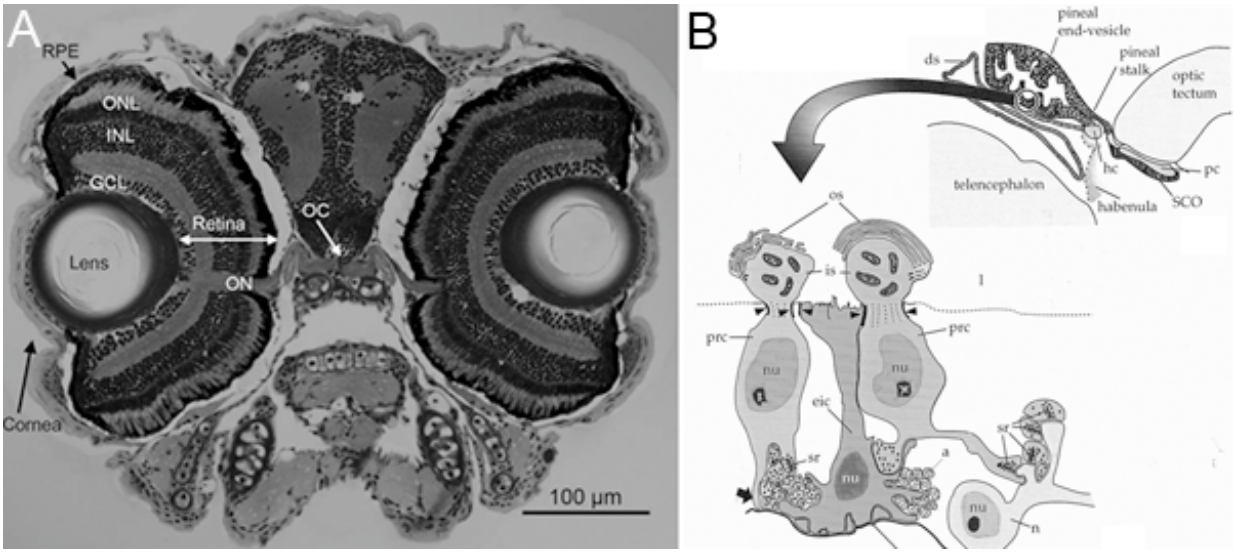

Figure 1-1. Teleosts utilize photoreceptors in the retina and pineal complex. A. Hematoxylin and eosin-stained transverse section through the eyes of a 6 dpf zebrafish larva. The retina is composed of four somatic layers-- the retinal pigment epithelium (RPE), outer nuclear layer (ONL), inner nuclear layer (INL), and ganglion cell layer (GCL), whose neurons send axons via the optic nerve (ON) through the optic chiasm (OC) to the optic tectum. Modified from Neuhauss (2010), with permission from Academic Press. B. Schematic of a teleost pineal organ and its major cell types. The outer segments (os) and inner segments (is) of photoreceptors (prc) extend medially into the pineal organ lumen (l). Photoreceptors project axons ventrolaterally, where they synapse onto pineal ganglion cells (n). Abbreviations: pineal axons (a), basal lamina (bl), dorsal sac (ds), habenular commissure (hc), nucleus (nu), posterior commissure (pc), subcommissural organ (SCO), synaptic ribbons (sr). Modified from Ekström and Meissl (1997), with permission from Springer.

When photons of light enter the eye, they traverse the entire retina and are captured by photoreceptors, which transduce the electromagnetic energy into a hyperpolarizing membrane potential. Photoreceptors come in two basic flavors- rods and cones- that differ in their light sensitivity and response kinetics. Rods are slower but more sensitive than cones, being able to detect and signal the absorption of a single photon. Cones, meanwhile, have a wide dynamic range. Therefore, rods mediate photopic vision, while cones are important for scotopic vision. To accurately sample the visual field, rods (Fadool, 2003) and cones (Marc and Sperling, 1976) are arranged in a crystalline mosaic. In adult zebrafish, a row of alternating long single blue-sensitive cones and short single ultraviolet-sensitive cones alternates with a row of red- and green-sensitive double cones such that a blue cone is always adjacent to a red cone, and a UV cone is always adjacent to a green cone (Robinson et al., 1993).

The encoding of spatial information begins at the first synapse in the retina. In the outer plexiform layer, photoreceptors make triad contacts consisting of two lateral horizontal cell processes and a central bipolar cell process (Stell, 1967). Due to their relatively depolarized state, photoreceptors tonically release glutamate in the dark (Copenhagen and Jahr, 1989), which depolarizes horizontal cells and one class of bipolar cell, termed OFF bipolars, due to the activation of ionotropic glutamate receptors (DeVries and Schwartz, 1999). Glutamate hyperpolarizes another class of bipolar cell (the ON bipolar) by binding to a metabotropic glutamate receptor, mGluR6, (Nakajima et al., 1993) and subsequently closing a cation channel that has recently been shown in mammals to be TRPM1 (Morgans et al., 2009; Shen et al., 2009; van Genderen et al., 2009). In some teleost cone ON bipolars, glutamate-mediated hyperpolarization appears to occur via glutamate-transporter-dependent chloride influx (Grant and Dowling, 1995). If a bipolar cell depolarizes in response to light stimuli in its receptive field center, it is classified as an ON-type cell, while OFF-type cells hyperpolarize in response to light stimuli in their receptive fields (Werblin and Dowling, 1969; Kaneko, 1970).

Retinal bipolar cells propagate these signals via graded changes in glutamate release in the inner plexiform layer. ON mixed rod/cone bipolar cells, termed Mb bipolars, have large presynaptic terminals in the distal IPL (sublamina b) that release glutamate in response to illumination. OFF mixed rod/cone bipolar cells, termed Ma bipolars, and OFF cone bipolar cells have small presynaptic terminals in the proximal IPL (sublamina a) that release glutamate in response to darkness (Famiglietti et al., 1977; Ishida et al., 1980; Sherry and Yazulla, 1993).

Bipolar cell terminals synapse onto a pair of postsynaptic processes (Dowling and Boycott, 1966) expressing AMPA and NMDA glutamate receptors-- two amacrine cell processes, an amacrine cell process and a ganglion cell dendrite, or two ganglion cell dendrites. Feedback in teleosts occurs via GABAergic amacrine cells (Marc et al., 1978; Tachibana and Kaneko, 1987; Yazulla et al., 1987) and extracellular protons (Palmer et al., 2003). Integrated signals are transmitted out of the retina by ganglion cells, projecting via the optic nerve to the retina's main target, the optic tectum.

Photoreceptive organs in vertebrates- the pineal complex

According to comparative morphological analyses, the pineal was originally a double organ, possibly evolving from the upper eyes of the postulated four-eyed protovertebrate. In reptiles, frogs and some fish species, the extracranial organ (the parietal eye) directly senses solar radiation and the intracranial organ (the pineal organ) is a luminance detector (reviewed in Vigh et al., 2002). Mammals have a single pineal organ, and it is indirectly photosensitive. Retinal ganglion cell axons synapse onto the suprachiasmatic nuclei, which project to the lateral hypothalamus. Neurons from the paraventricular nucleus of the hypothalamus send afferents to the intermediolateral column of the upper thoracic cord, which is the origin of preganglionic fibers to the superior cervical ganglia (SCG). The mammalian pineal is innervated by sympathetic fibers from the SCG (Kappers, 1960).

In most teleosts, the pineal complex consists of intracranial pineal and parapineal organs (reviewed in Ekström and Meissl, 1997). Between the telencephalon and optic tectum, the teleost pineal organ end-vesicle lies in a recess under a non-pigmented area of the skull (termed the pineal window), adjacent to the smaller parapineal. Below the pineal window, photoreceptors send out axons ventrolaterally that terminate in neuropil (Figure 1-1B). While little is known about intrapineal circuitry, there is evidence for interneurons (see Ekström and Meissl, 1997 for review) and large, peripheral projection neurons that are called pineal ganglion cells. Photoreceptors are known to synapse upon each other and on pineal ganglion cells (reviewed in Vollrath, 1981; Reiter, 1981-1982). Pineal photoreceptors and ganglion cells send afferent fibers via the pineal tract to several targets, some of which also receive retinal inputs. Targets include the habenula, pretectal nuclei, preoptic nuclei, and dorsal thalamus (Korf and Wagner, 1981; Ekström, 1984; Yáñez et al., 2009).

Both the pineal and parapineal organs are photosensitive (Dodt, 1963; Tabata et al., 1975; Meissl et al., 1986; Marchiafava and Kusmic, 1993), with light inhibiting tonic spike discharges from these organs. Indeed, spontaneous pineal firing rates are highest at night and lowest during the day (see Vigh, 2002). Pineal photoreceptor membrane potentials vacillate between -20 and -60 mV (dark-adapted to light-adapted) (Meissl and Ekström, 1988). Light-induced hyperpolarization is graded with increasing light intensity until saturation, and then is constant (Meissl and Ekström, 1988). The light intensity range and response times are wider and slower, respectively, for the pineal organ compared to the retina (Meissl et al., 1986; Meissl and Ekström, 1988). Therefore, although the pineal cannot discriminate between rapidly changing light stimuli, it is an ideal sensor of ambient illumination and thereby measures day length.

Pineal photoreceptors have an endogenous circadian oscillator, entrained to the photoperiod (Yokoyama et al., 1978), that drives melatonin (n-acetyl-5-methoxytryptamine) synthesis and secretion at night. Melatonin is a pleiotropic indoleamine originally identified by Lerner et al. (1958) as the activity that lightens young amphibian larvae by aggregating pigment (Lerner and Case, 1959). The vast majority of pineal research over the past half-century has focused on the effects of melatonin, which can reverse some of the effects of pinealectomy on sleep, locomotor activity, shoaling behavior, thermal preference, and skin pigmentation/color change (reviewed in Falcón, 2007). In Chapter 5 of this thesis, we will discuss the zebrafish pineal's effects on skin pigmentation, in particular its role in dorsal melanophore trafficking.

Octavolateral receptors in vertebrates- the inner ear

Vertebrate hair cells are mechanoreceptors that detect pressure waves to encode auditory, vestibular, and/ or hydrodynamic information. The anatomy of the octavolateral system varies among vertebrates (for review, see Lewis et al., 1985). In this part of the introduction, we will review the topography of the teleost inner ear organs and their processing of vestibular and auditory signals. For an in-depth discussion of the mammalian inner ear, please see Corti, 1851; Retzius, 1884; Lewis et al., 1985; Lim, 1986; von Békésy, 1989; Eatock and Lysakowski, 2006; Fettiplace and Hackney, 2006; Brown et al., 2008; Schwander et al., 2010.

The adult zebrafish inner ear contains three semicircular canals (anterior, posterior and lateral), three otolithic organs (utricle, saccule and lagena), and the macula neglecta (Figure 1-2A). The main components of the teleost vestibular system, the semicircular canals and utricle,

are located in the dorsal part of the inner ear. Within the widest part of each semicircular canal, the ampulla, is a conical patch of hair cells called a crista. Head rotation displaces the apical surfaces of the hair cells, which are embedded in a gelatinous cupula, due to the inertia of endolymph in the semicircular canals. Deflection of the apical stereocilia by a few angstroms toward the kinocilium can depolarize the hair cell to effect basolateral neurotransmitter release upon an afferent fiber of the VIIIth cranial nerve that projects to medulla octaval nuclei (for review, see Hudspeth, 1989; Popper and Fay, 1993; Abbas and Whitfield, 2010).

The main components of the adult teleost auditory system, the saccule and the lagena, are located in the ventral part of the inner ear. These two organs, along with the utricle and the macula neglecta, each contain a sensory patch of hair cells called a macula. While the hair cells in the macula neglecta are embedded in a cupula, the other three organs are covered by a calcified otolith that is displaced when encountering a pressure wave. As a result, the apical stereocilia are displaced, leading to a graded change in the hair cell membrane potential and subsequent change in tonic neurotransmitter release (reviewed in Hudspeth, 1989; Popper and Fay, 1993; Abbas and Whitfield, 2010). The amplitude and the duration of the pressure wave are encoded in the action potentials of the VIIIth cranial nerve (reviewed in Fuchs and Parsons, 2006), and activity may be regulated by inhibitory cholinergic feedback onto the hair cell (Furukawa, 1981).

Teleosts primarily use the saccule to detect sound waves (frequencies between approximately 10–4000 Hz for goldfish) and the utricle to encode information about horizontal linear acceleration (with an effective stimulus of approximately 1 Hz) (reviewed in Popper and Fay, 1993; Abbas and Whitfield, 2010). However, there is some overlap in both organs (reviewed in Popper and Fay, 1993). For example, the utricle also detects higher frequencies (Fay, 1984), and projections from the utricle eventually go to both auditory nuclei in the dorsal medulla and vestibular nuclei in the ventral medulla (Tomchik and Lu, 2005). In the larval zebrafish, only the utricular and saccular maculae (and the three cristae) are present (Figure 1-2B).

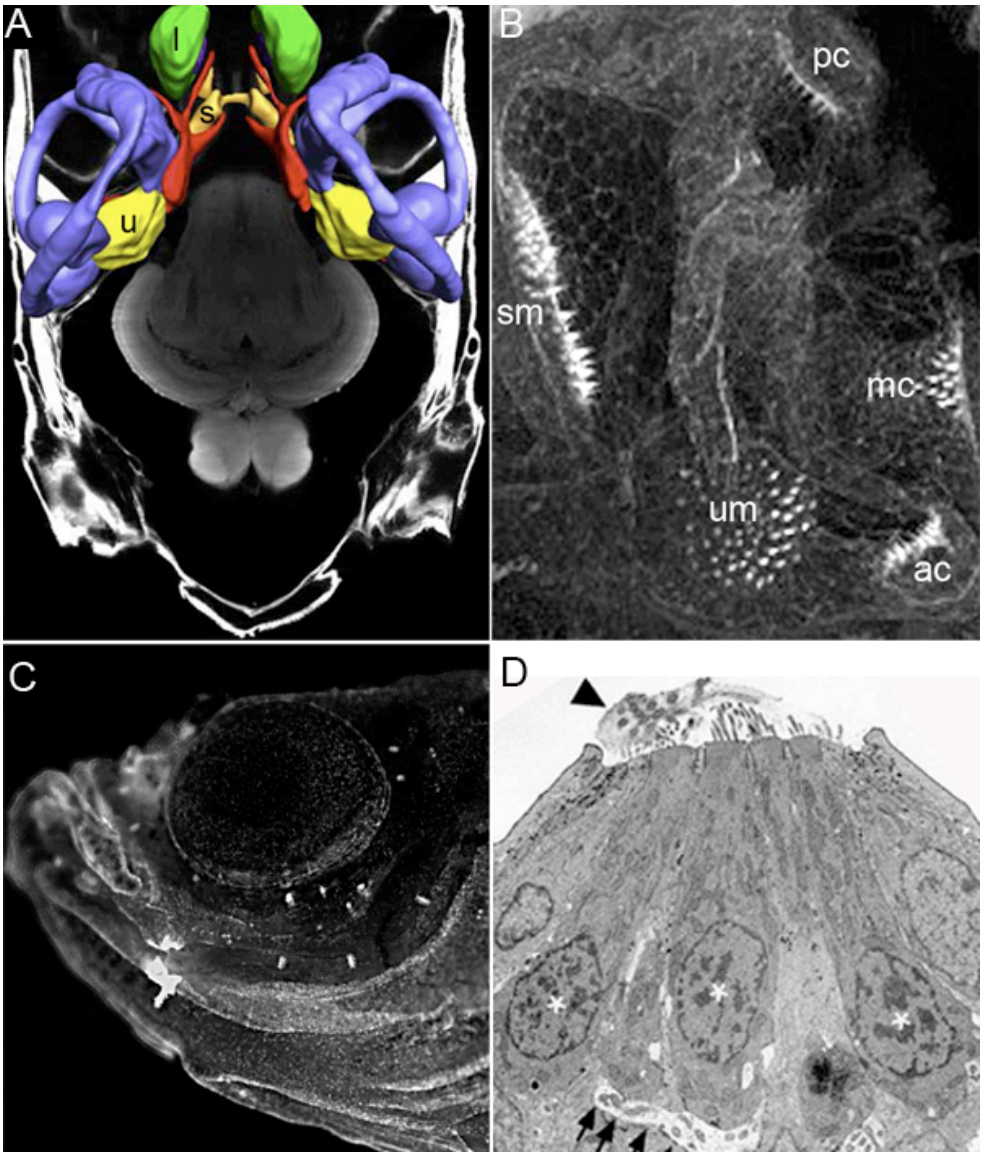

Figure 1-2. Zebrafish utilize hair cells in the inner ear and lateral lines. A. Thin-sheet laser imaging micrograph of a longitudinal section through the head of a 6-8 wpf *casper* zebrafish. A three-dimensional isosurface reconstruction of the two inner ears containing the semicircular canals (blue), utricle (yellow), cranial nerve VIII (red), saccule and transverse canal (gold), and lagena (green) is shown. Abbreviations: utricle (u), saccule (s), lagena (l). Modified from Abbas and Whitfield (2010), with permission from Academic Press. B. Confocal micrograph of a 5 dpf zebrafish inner ear stained with phalloidin-FITC to reveal the actin-rich stereocilia on the apical surfaces of five sensory patches of hair cells-the utricular and saccular maculae (um, sm) and the anterior, medial, and posterior cristae (ac, lc, pc). Modified from Whitfield et al. (2002), with permission from Wiley. C. Epifluorescence micrograph of an adult zebrafish labeled with AM1-43 shows several neuromasts around the eye. D. Transmission electron micrograph of a 5 dpf zebrafish lateral line neuromast indicates the presence of several hair cells with stereocilia and kinocilia embedded in a cupula (arrowhead). Asterisks point to some hair cell nuclei. An afferent nerve fiber (arrows) contacts the basal surfaces of two hair cells. Modified from Murakami et al. (2003), with permission from Elsevier.

Octavolateral receptors in vertebrates- the lateral lines

An additional mechanosensory system found in fish, larval amphibians, and adult aquatic amphibians is the lateral line, which detects low-frequency water movements (Schulze, 1861) to avoid obstacles (Hassan, 1989) and predators (Blaxter and Fuiman, 1989), detect prey (Hoekstra and Janssen, 1985), and for shoaling (Dijkgraaf, 1963) schooling (Pitcher et al., 1976), and rheotaxis (Montgomery et al., 1997). While the lateral line may have evolved into an electrosensory system in some fish (Lissmann and Mullinger, 1968) it has disappeared from non-aquatic vertebrates.

The teleost lateral line system consists of neuromasts, located superficially within the epidermis (Figure 1-2C) and/or within grooves or canals, and their afferent and efferent connections. A neuromast organ (Figure 1-2D) contains 20-30 hair cells divided into two populations, such that the apical stereocilia of the two populations are oriented 180° relative to each other (Flock and Wersall, 1962; López-Schier et al., 2004). A hair cell of one orientation forms a synapse on its basolateral surface with an afferent bipolar neuron (Nagiel et al., 2008) whose cell soma is located in a cranial ganglion. The amplitude of the stimulus and the orientation of the hair cell rapidly modulate the tonic firing rate of these neurons, which is 1-80 spikes/second (Gorner, 1963; Bleckmann and Topp, 1981). These neurons can phase lock onto a small stimulus (0.02 mm amplitude) at low frequency (50-100 Hz) (Bleckmann and Topp, 1981).

An anterior ganglion (located between the eye and the ear) collects sensory information from cranial neuromasts, while a posterior ganglion (located posterior to the ear) collects sensory information from trunk and tail neuromasts (Metcalfe et al., 1985; Northcutt, 1989). Both ganglia send central projections into a somatotopic rostrocaudal column in the hindbrain (Claas and Munz, 1981; Alexandre and Ghysen, 1999). Efferent fibers primarily from hindbrain octavolateralis neurons (Metcalfe, 1985) directly regulate neuromast hair cell sensitivity (Roberts and Meredith, 1989).

Apical organelles in visual and octavolateral receptor cells

To transduce their specific stimuli, photoreceptors and hair cells elaborate distinct apical organelles. Photoreceptors have outer segments that contain many flattened membrane disks densely packed (25,000 molecules/μm^2) (Sung and Chuang, 2010) with visual pigment (Figure 1-3A). In rods, photoisomerization of the visual pigment, rhodopsin, changes it to metarhodopsin

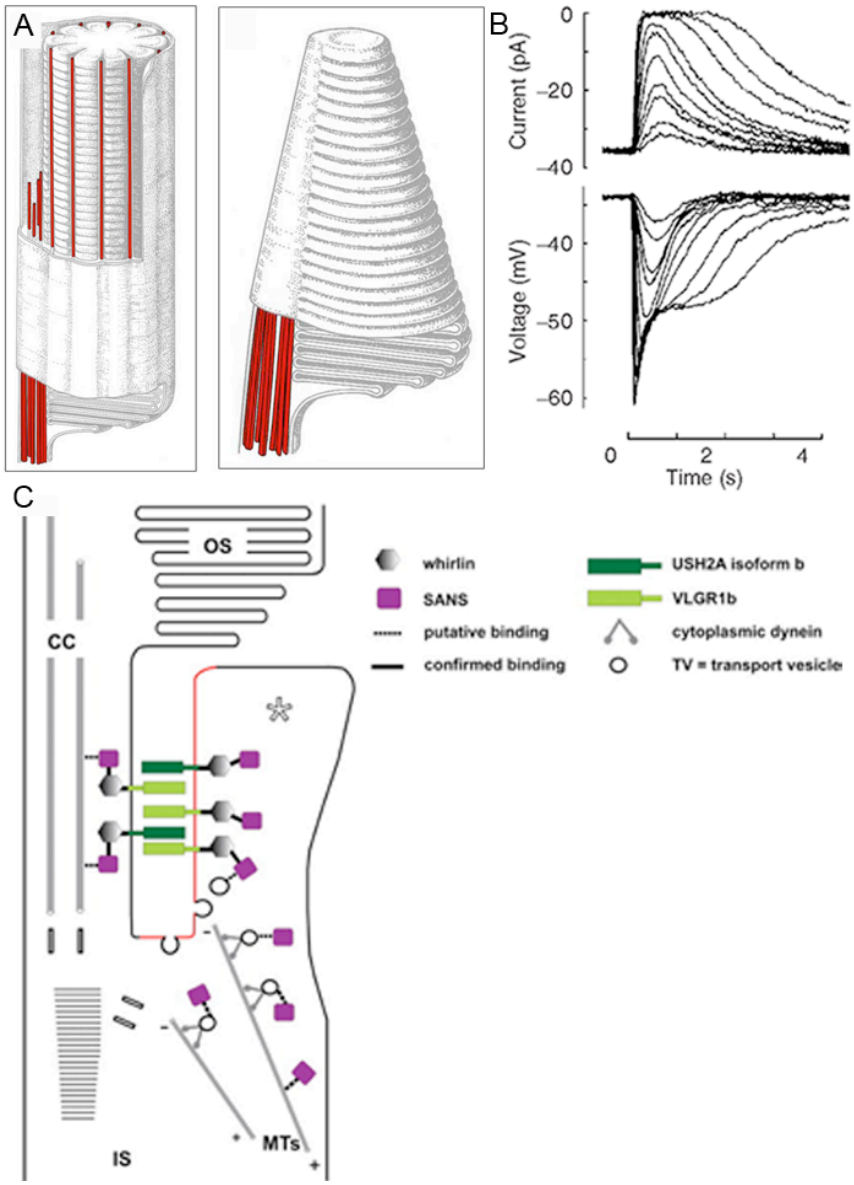

Figure 1-3 Structure and function of the photoreceptor apical cilium. A. Illustration of rod (left) and cone (right) outer segments. While the cone outer segment consists entirely of tightly packed, double-folded membranes contiguous with the plasma membrane, the rod outer segment contains both free-floating disks and infoldings of the plasma membrane. Microtubules are shown in red. Modified from Kennedy and Malicki (2009), with permission from Wiley. B. Suction-pipette recordings of outward membrane current (upper panel) and membrane potential (lower panel) of tiger salamander rod outer segments in response to brief light flashes of increasing intensity. Outer segment membrane contains channels that hyperpolarize the photoreceptor in response to light. Modified from Luo et al. (2009), with permission from Academic Press. C. Schematic showing the molecular architecture of the periciliary compartment in photoreceptors. Several proteins mutated in Usher syndrome localize to this compartment found between the outer and inner segments. Abbreviations- CC, connecting cilium; IS, inner segment; MTs, microtubules; OS, outer segment. Modified from Maerker et al. (2008), with permission from Oxford University Press.

II. Metarhodopsin II binds to transducin and promotes the exchange of bound GDP for GTP. This activates a phosphodiesterase, which hydrolyzes cGMP. Cyclic nucleotide-gated channels close, resulting in photoreceptor hyperpolarization (reviewed in Stryer, 1986; Burns and Baylor, 2001; Sung and Chuang, 2010). With increasing light intensity, hyperpolarization increases in a graded manner until it saturates (Baylor et al., 1984; Figure 1-3B).

TRP channels have been proposed as candidates for the mechanosensitive cation channel. Knockdown of NompC/Trpn1 in zebrafish leads to morphants with auditory and vestibular defects, a loss of evoked microphonic potentials and lack of transduction-dependent endocytosis of FM1-43 (Sidi et al., 2003). However, no mammalian NompC/Trpn1 gene has yet been identified. In addition, while TRPA1/ANKTM1 localizes to hair bundle tips and is involved in mechanotransduction, mouse mutants lack auditory and vestibular defects (Corey et al., 2004). Despite much effort, therefore, the identity of the mechanotransduction channel is still unclear.

A ciliary axoneme, with a 9+0 microtubule configuration, connects the outer segment with the inner segment (Figure 1-3C). Several proteins mutated in Usher syndromes, such as whirlin, SANS, and VLGR1b, may form fibrous links in the ridge between the connecting cilium and the microvilli (called calycal processes) that protrude from the top of the inner segment (Maerker et al., 2008). These links are analogous to the lateral and ankle links that form between apical hair cell microvilli (see below). Substantial vesicle transport and fusion occurs in this ridge as transport cargo (such as opsin) is transferred to the ciliary transport machinery (for review, see Kennedy and Malicki, 2009).

The hair cell is also polarized, with an apical hair bundle consisting of numerous, actin-rich, interconnected stereocilia whose lengths progressively increase closer to the kinocilium (Figure 1-4A, B) (for recent reviews, please see Dror and Avraham, 2009; Gillespie and Müller, 2009; Petit and Richardson, 2009; Schwander et al., 2010). The stiff stereocilia and kinocilium are anchored in an actin-rich cuticular plate, which is surrounded by an actin belt attached to tight junctions. Depending upon the direction of the pressure wave, the stereocilia pivot around their insertion point either towards the kinocilium (leading to depolarization of the hair cell by triggering the opening of nonselective cation channels) or away from the kinocilium (leading to hyperpolarization). Fast calcium imaging has localized the transduction channel to the bottom of the stereocilia tips (Figure 1-4F) (Beurg et al., 2009). The stereocilia and kinocilium are interconnected by thin, extracellular, lateral and oblique filaments called tip links, horizontal top

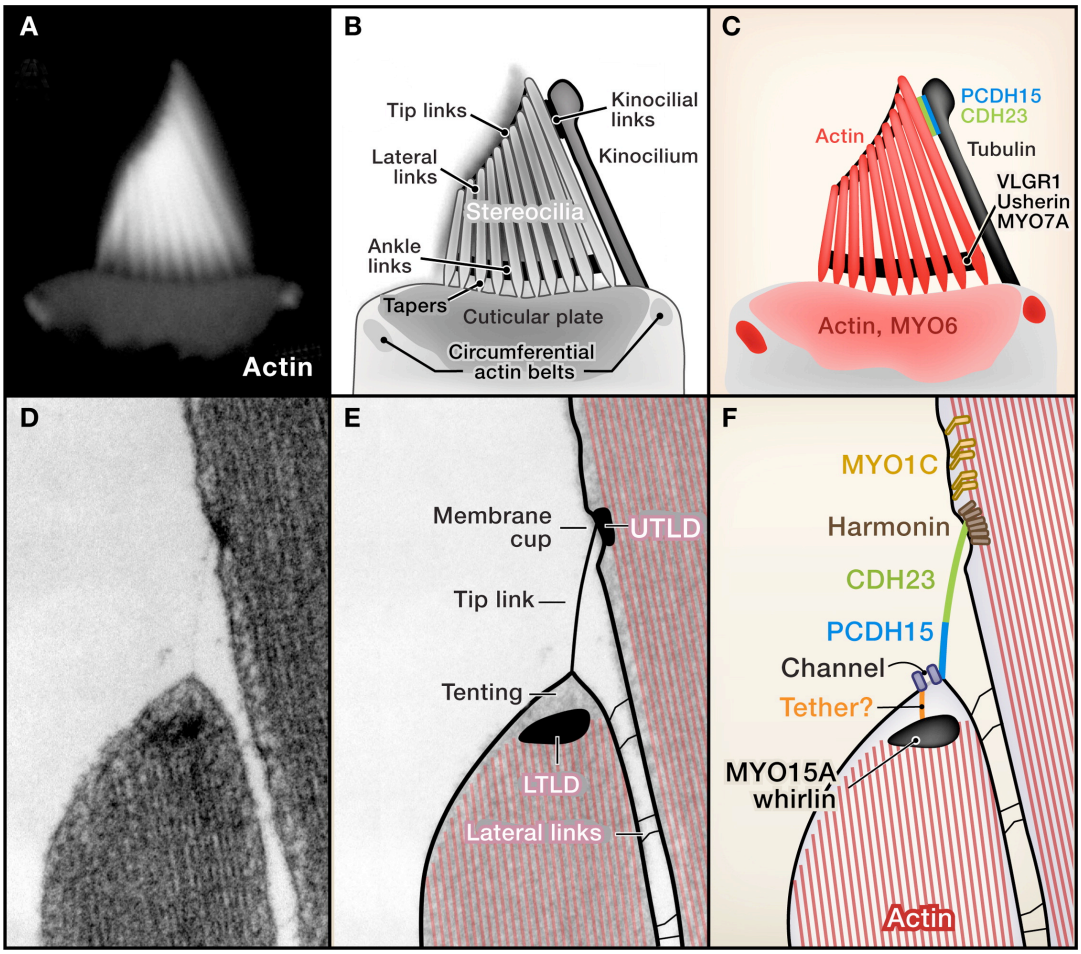

Figure 1-4. Apical stereocilia mediate auditory and vestibular mechanotransduction in hair cells. A-C. An apical bullfrog hair cell bundle stained with phalloidin (A) and schematized to show subcellular structures (B) and some of their associated molecules (C). D-F. Two adjacent hair cell stereocilia shown by high-magnification transmission electron microscopy (D) and schematized to show subcellular structures (E) and some associated molecules (F). Abbreviations- cadherin 23 (CDH23), LTLD (lower tip link density), myosin 1C (MYO1C), myosin 6 (MYO6), myosin 7A (MYO7A), myosin 15A (MYO15A), protocadherin15 (PCDH15), upper tip link density (UTLD), very large G protein-coupled receptor 1 (VLGR1). Reproduced from Gillespie and Müller (2009), with permission from Cell Press.

connectors, shaft connectors and ankle links (reviewed in Nayak et al., 2007). The classical model for mechanotransduction channel gating involves the springing open of the channel by directly connected tip links (Figure 1-4D-F) (Pickles et al., 1984). Cadherin23 localizes to the tip links, and mutations cause deafness and balance disorders in zebrafish, mice, and humans (Bolz et al., 2001; Siemens et al., 2004; Sollner et al., 2004). The tip link may also include protocadherin 15 homodimers that adhere to cadherin 23 homodimers (Ahmed et al., 2006; Kazmierczak et al., 2007). However, the tip link identity remains controversial since cadherin 23,

but not tip links, disappear in adult mice (reviewed in Geleoc and Holt, 2009).

Several additional proteins, including lateral links and motor proteins, have key roles in hair bundle integrity and mechanotransduction. VLGR1, usherin, whirlin and myosin VIIa are ankle links (Figure 1-4C) (Adato et al., 2005; Delprat et al., 2005; McGee et al., 2006; Michalski et al., 2007) that are mutated in several forms of Usher syndrome (for recent review, see Yan and Liu, 2010). The zebrafish mutant called *mariner*, in which myosin VIIa is mutated, provides a nice example of the pathophysiological consequences of ankle link perturbation. In these mutants, the short hair bundles are splayed such that the kinocilia and stereocilia detach from each other (Ernest et al. 2000). Myosin VIIa, as well as myosin Ic, myosin XVa, and myosin VI may have additional functions on the apical surface of the hair cell, including adaptation, regulation of actin flow, protein transport, and endocytosis (Rzadzinska et al., 2004; Belyantsevaet al., 2005; Delprat et al., 2005; Kikkawa et al., 2005; Stauffer et al., 2005; Schneider et al., 2006). Some proteins mutated in Usher Syndrome, such as myosin VIIa, are also localized to the basolateral compartment, i.e., the presynaptic terminal, of hair cells and photoreceptors (el-Amraoui et al., 1996), where their distinct roles remain to be clarified.

The synaptic ribbon is an organelle, composed primarily of RIBEYE/CtBP2, which tethers vesicles

The synapses of vertebrate sensory receptor cells transmit a broad range of information with high fidelity over a prolonged period of time. The synaptic terminals of all of these sensory neurons share a specialized organelle, the synaptic ribbon (Figure 1-5). Also termed synaptic bodies or dense bodies, ribbons are proteinaceous organelles that tether large numbers of synaptic vesicles near the active zone where neurotransmitter release occurs. The importance of the ribbon in synaptic transmission was revealed with the discovery of visual (Dick et al., 2003; Van Epps et al., 2004) and auditory (Khimich et al., 2005) deficits in mutants that lack anchored ribbons. Over the past two decades, substantial progress has been made in the characterization of the proteomes of ribbon presynaptic terminals, and investigations of mouse and zebrafish mutants that affect ribbons have provided new insights into their functions (for review, see Heidelberger et al., 2005; Moser et al., 2006; Zanazzi and Matthews, 2009; Matthews and Fuchs, 2010).

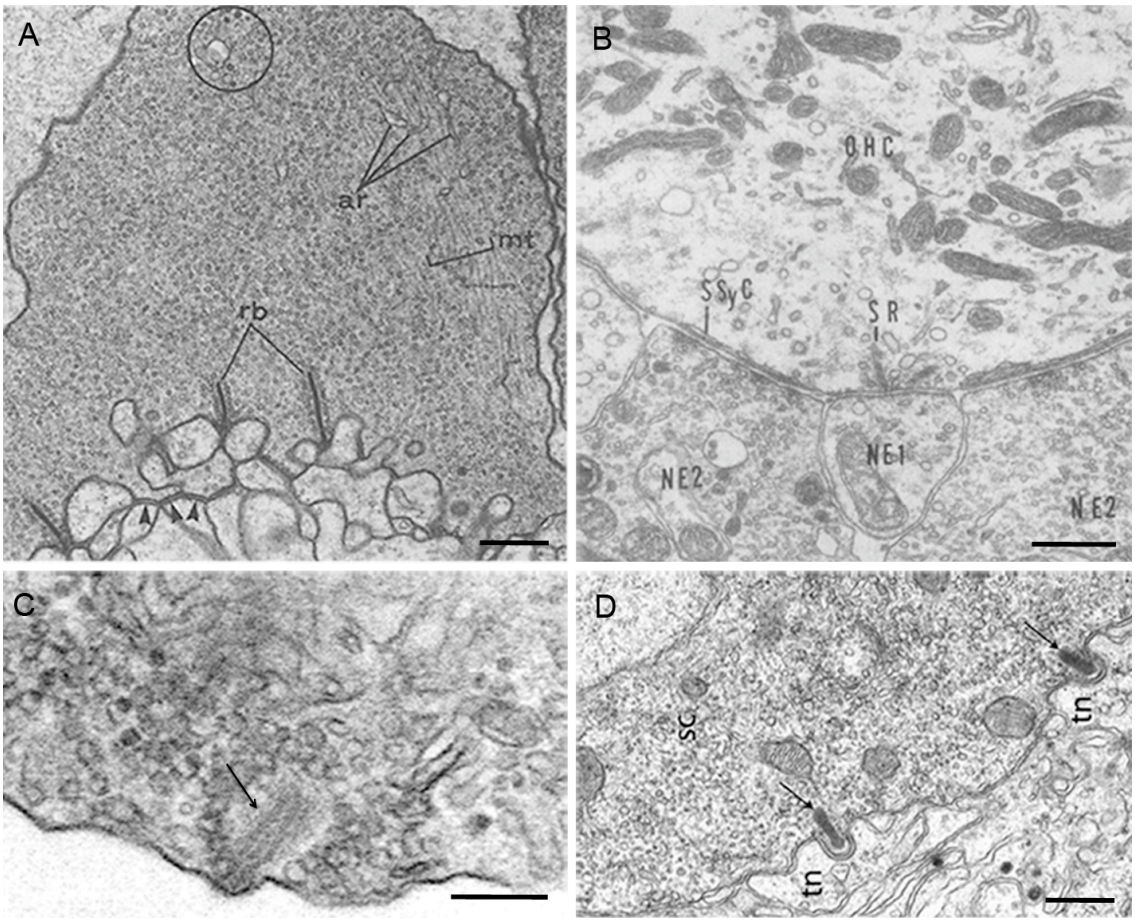

Figure 1-5. Examples of ribbon presynaptic terminals. A. Electron micrograph of a turtle cone presynaptic terminal is shown. Postsynaptic processes are apposed to ribbons (rb) and basal junctions (arrowheads) in the terminal. The large population of synaptic vesicles is a hallmark of most ribbon presynaptic terminals. Other organelles in this terminal include microtubules (mt), agranular reticulum (ar), and vacuoles (circle). Figure modified from Schaeffer and Raviola (1978), with permission from The Rockefeller University Press. B. Electron micrograph of the basal portion of a guinea pig outer hair cell (OHC), which makes contact with afferent (NE1) and efferent (NE2) nerve fibers. Two synaptic ribbons (SR) are directly apposed to the afferent nerve fiber, while subsynaptic cisterns (SSyC) are opposite the efferent nerve fibers. A relative paucity of synaptic vesicles and abundant mitochondria also characterize the OHC ribbon terminal. Figure modified from Saito (1980), with permission from Elsevier. C. Electron micrograph shows a goldfish bipolar cell synaptic ribbon (arrow) at high magnification. Three distinct laminae can be observed in this ribbon. D. Electron micrograph of an elephantfish promormyromast. These sensory organs of the lateral line contain electroreceptors (sc) that synapse onto terminal neural boutons (tn). Ribbons (arrows) nestle within invaginating synapses. Also present in the electroreceptor terminal are numerous synaptic vesicles and mitochondria. Panel modified from Denizot et al. (2007) with permission from Wiley. Scale bars, 0.5 μm (A, B, and D), 0.15 μm (C). Figure reproduced from Zanazzi and Matthews (2009), with permission from Springer.

Synaptic ribbons were originally identified in electron micrographs as electron-dense, osmiophilic structures surrounded by vesicles in the presynaptic terminals of photoreceptors and hair cells (Sjöstrand, 1953; De Robertis and Franchi, 1956; Sjöstrand, 1958; see Figure 1-6). These heterogeneous organelles vary in shape, size, and number of tethered vesicles depending on activity. Enzymatic digestion of ribbons suggested they are proteinaceous (Bunt et al., 1971). The logjam in molecular characterization of the ribbon was broken by Schmitz and colleagues (2000), who used partial purification of retinal ribbons to identify RIBEYE as a specific and major component of the ribbon (Figure 1-6). RIBEYE contains a serine- and proline-rich amino-terminal A domain and a carboxyl-terminal B domain that is identical to all but the N-terminal 20 residues of CtBP2, a transcriptional repressor related to D-isomer-specific 2-hydroxyacid dehydrogenases. Consistent with the notion that synaptic ribbons are vertebrate specializations, no RIBEYE orthologs exist in the Drosophila and C. elegans genomes. However, vesicles are associated with ribbon-like structures called T-bars at active zones of many synapses in Drosophila (reviewed in Prokop and Meinertzhagen, 2006), suggesting that invertebrates possess alternative molecular mechanisms to achieve the synaptic function of ribbons. The molecular composition of T-bar ribbons is not yet known. Besides retinal ribbon synapses, RIBEYE appears to be expressed only in vertebrate pinealocytes (Schmitz et al., 2000) and hair cells (Zenisek et al., 2003). Immunoelectron micrographs reveal that RIBEYE localizes to the ribbon (tom Dieck et al., 2005). It has been estimated that RIBEYE (possibly in association with CtBP1) constitutes 64-69% of the total volume of a goldfish bipolar cell ribbon (Zenisek et al., 2004).

Although a RIBEYE knockout has not yet been reported, zebrafish with decreased levels of a RIBEYE ortholog have an impaired optokinetic response and retinal ribbon abnormalities (Wan et al., 2005). It is unclear whether the aberrant ribbons in these morphants result from specific defects in ribbon formation or from secondary effects of abnormal bipolar cell development and increased apoptosis. RIBEYE can polymerize via interactions between its A and B domains to form vesicle-associated structures reminiscent of spherical synaptic ribbons. NAD(H) may promote the assembly of synaptic ribbons by favoring homotypic, and inhibiting heterotypic, interactions between these domains. Additional proteins may be necessary to generate plate-like ribbons from the spheres (Magupalli et al., 2008).

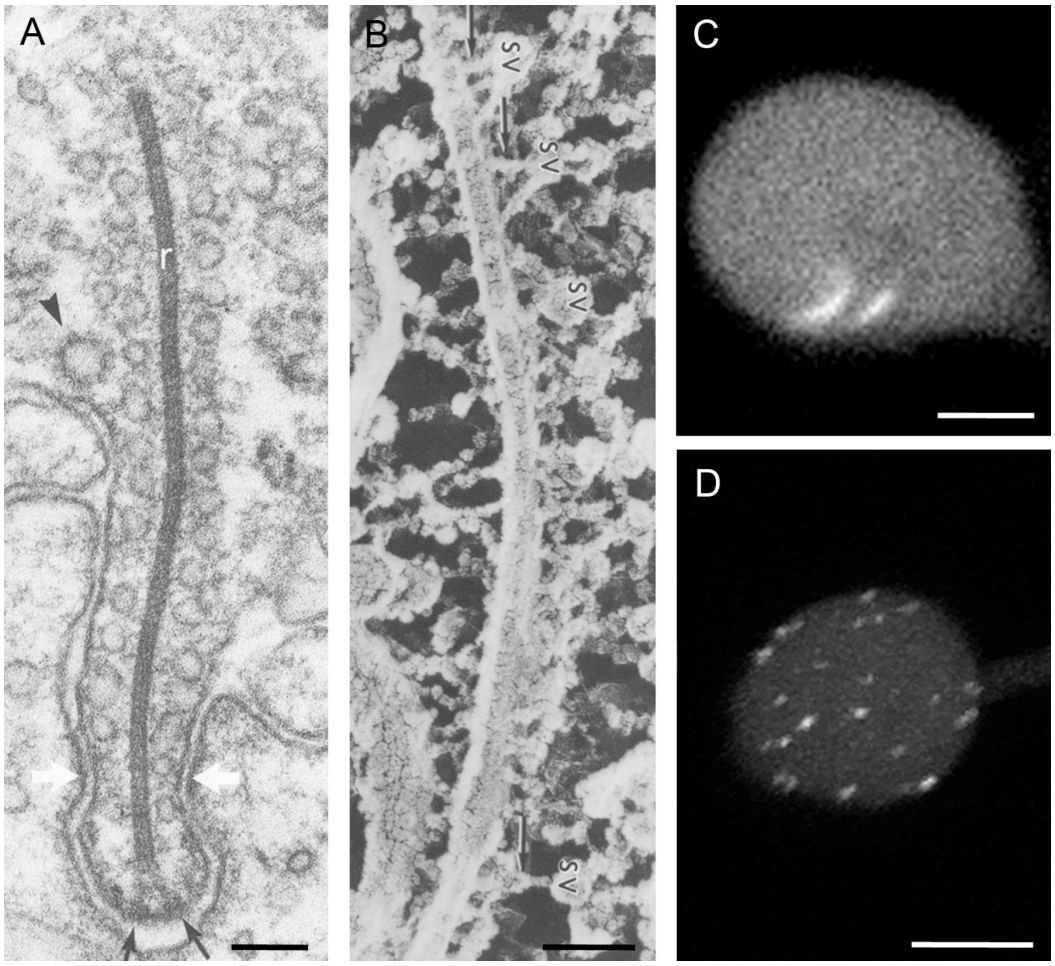

Figure 1-6. Synaptic ribbons are cytoskeletal organelles, composed primarily of RIBEYE, that tether vesicles. A. An electron micrograph of a skate electroreceptor ribbon synapse. The ribbon (r), which appears electron-dense and laminar, is located in an evagination of the presynaptic plasma membrane flanked by postsynaptic processes. Vesicles are attached to the surface of the ribbon except at its base, which is connected to osmiophilic aggregates on the plasma membrane (black arrows). Postsynaptic densities are most prominent adjacent to the constrictions in the presynaptic plasma membrane (white arrows). Coated vesicles (arrowhead) are found lateral to the ribbon and its active zones. Figure modified from Sejnowski and Yodlowski (1982) with permission from Chapman and Hall. B. Freeze-etched replica of a cross-fractured frog photoreceptor synaptic ribbon and its surrounding environment. Synaptic vesicles (SV) are tethered to the ribbon by filaments (arrows). Figure modified from Usukura and Yamada (1987), with permission from Springer. C. Confocal micrograph of a goldfish cone presynaptic terminal filled with a fluorescent RIBEYE-binding peptide is shown. Ultrastructural analysis confirmed that the two long, curvilinear structures were synaptic ribbons (data not shown). D. Several ribbons in a three-dimensional reconstruction from optical sections through the synaptic terminal of a goldfish bipolar cell dialyzed via a whole cell patch pipette with the fluorescent RIBEYE-binding peptide. Scale bars, 0.1 μm (A, B), 2.5 μm (C), 5 μm (D). Figure reproduced from Zanazzi and Matthews (2009), with permission from Springer.

Mechanisms of exocytosis at ribbon presynaptic terminals

Ultrastructural evidence suggests that vesicles fuse at active zones lateral to presumptive calcium channels at synapses where ribbons nestle within an evagination of the plasma membrane (Gray and Pease, 1971; see Figure 1-7). Imaging of vesicles labeled with FM dye confirmed that ribbon-associated vesicles undergo exocytosis (LoGiudice et al., 2008). It is believed that the vesicles docked at the plasma membrane constitute the readily releasable pool that exocytoses first, with a time constant of 0.5 milliseconds in goldfish MB1 bipolar cells (Mennerick and Matthews, 1996). Capacitance measurements have also identified a slower component of exocytosis that corresponds, in goldfish MB1 bipolars, to the total number of vesicles attached to ribbons (von Gersdorff et al., 1996). The morphological correlate for this slower releasable pool is currently unclear at other ribbon synapses and may reflect the exocytosis of vesicles on the ribbon combined with those at ectopic sites (Nouvian et al., 2006).

The precise cellular and molecular mechanisms underlying ribbon-associated exocytosis are not yet known. As described earlier, the ribbon has been suggested to function like a conveyor belt, moving vesicles toward the active zone in response to depolarization (Bunt, 1971). In potential support of this model, the motor protein KIF3A has been localized to ribbons (Muresan et al., 1999). However, several pieces of evidence suggest that ribbons act more like a safety belt than a conveyor belt (reviewed in Parsons and Sterling, 2003). In particular, the entire releasable pool at the synaptic ribbon can be discharged within 1-2 milliseconds (Heidelberger et al., 1994; Heidelberger, 1998), which is much faster than the rates that could be achieved with a molecular motor (Gilbert, 2001). Furthermore, the addition of ATP-γS to retinal bipolar cell terminals does not affect the initial bout of exocytosis (Heidelberger et al., 2002), although it does abolish pool refilling. The safety belt model postulates that vesicles are held in close proximity at the ribbon and may undergo compound fusion on this scaffold. Indeed, vesicles are immobilized at bipolar cell ribbons (LoGiudice et al., 2008), where they may undergo compound fusion in response to a strong stimulus (Matthews and Sterling, 2008). Compound fusion may be one mechanism through which the ribbon coordinates multivesicular release, which has been reported at hair cell (Glowatzki and Fuchs, 2002) and bipolar cell (Singer et al., 2004) terminals. Another mechanism for multivesicular release may be the exocytosis of large endosomes, but this occurs with a substantial delay after stimulation (Coggins et al., 2007).

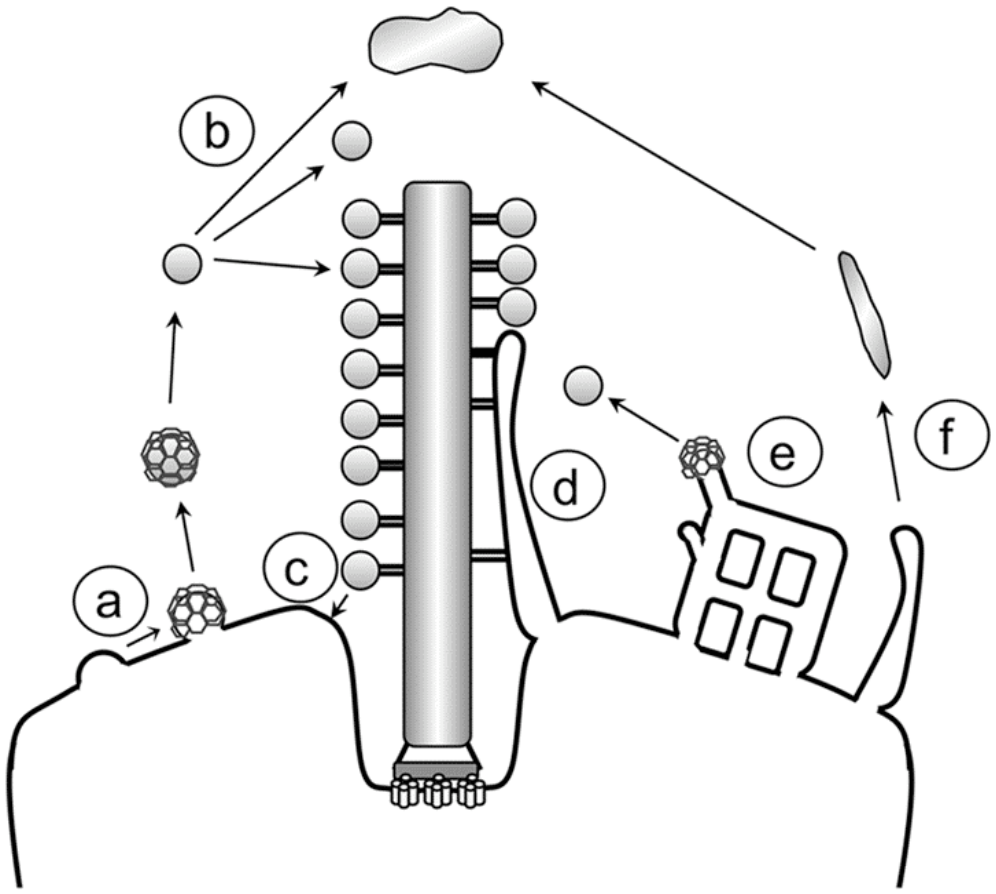

Figure 1-7. Events in the synaptic vesicle cycle near the ribbon. Clathrin-mediated endocytosis (a) retrieves vesicles that can either coalesce with a presynaptic cistern (b, top arrow) or enter either the reserve (middle arrow) or releasable (bottom arrow) pools. Single (c) or multiple (d) ribbon-associated vesicles fuse with the plasma membrane lateral to L-type voltage-gated calcium channels. Vesicle retrieval may also occur from large anastomosing tubules (e) or directly via large endosomes (f). Figure reproduced from Zanazzi and Matthews (2009), with permission from Springer.

Membrane fusion events are driven by the formation of trans-complexes of SNARE proteins. One membrane contains an R-SNARE/v-SNARE protein such as synaptobrevin/VAMP that provides an alpha helix to the trans-complex. The other membrane contains two Q-SNARE/t-SNARE proteins such as syntaxin and SNAP-25 that contribute a total of three alpha helices to the complex. Specific isoforms of the three core members of the SNARE complex are differentially distributed in ribbon presynaptic terminals (for review, see Zanazzi and Matthews, 2009). For example, syntaxin 1 is present in hair cells (Safieddine and Wenthold, 1999) and pinealocytes (Redecker, 1996; Redecker et al., 1996), but absent from retinal ribbon synapses

(Ullrich and Südhof, 1994). Instead, photoreceptor and bipolar cell terminals express the b isoform (Curtis et al., 2008) of syntaxin 3 (Morgans et al., 1996). It remains to be determined precisely how syntaxin 3b and other specific SNARE protein isoforms contribute to homotypic and heterotypic vesicle fusion events at ribbon terminals, although a recent study revealed that a syntaxin 3b peptide can block exocytosis in goldfish bipolar cells (Curtis et al., 2010).

At conventional terminals, trans-SNARE complexes appear to be stabilized in a fusion-ready state before calcium enters the presynaptic terminal and binds to synaptotagmin 1. This calcium sensor then interacts simultaneously with phospholipid membranes and the assembled SNARE complex to promote fusion (reviewed in Rizo and Rosenmund, 2008). At ribbon synapses, however, the regulation of the calcium-triggering step is poorly understood. Several pieces of evidence suggest that many ribbon terminals utilize a sensor other than a vesicular synaptotagmin (i.e., synaptotagmin 1 or 2). First, 1-2 μM calcium induces tonic exocytosis at photoreceptor (Rieke and Schwartz, 1996) and bipolar cell (Lagnado et al., 1996) terminals. This calcium concentration is much lower than that needed for binding of synaptotagmin 1 or 2 to calcium (half maximal binding at 200 μM). Indeed, synaptotagmin 3 binds calcium with much higher affinity (half maximal binding at 1 μM, Li et al., 1995). Secondly, the sensor for phasic release from MB1 goldfish bipolar cells does not display the calcium-binding affinity of a classical vesicular synaptotagmin (reviewed in Heidelberger et al., 2003). Consistent with this finding, these bipolar cells express synaptotagmin 3 and lack synaptotagmin 1/2 (Berntson and Morgans, 2003). Third, rat and guinea pig cochlear hair cells lack synaptotagmins 1, 2, 3, and 5. Rather, they express several nonvesicular synaptotagmins—4, 6, 7, 8, and 9— with high calcium affinity (Safieddine and Wenthold, 1999). The physiological importance of these synaptotagmins in hair cell synaptic vesicle fusion is not yet known.

The complexins are important regulators of synaptic vesicle exocytosis

Besides synaptotagmin, a second protein is known to bind an assembled SNARE complex and regulate fast, calcium-triggered exocytosis at conventional presynaptic terminals. Complexin was originally identified in rat brain extracts, together with synaptotagmin and calcium channels, by co-immunoprecipitation with anti-syntaxin and anti-SNAP25/anti-rab3a antibodies (Saisu et al., 1991). The complexins comprise a family of small, hydrophilic, negatively charged proteins found in invertebrates and vertebrates. While invertebrate genomes

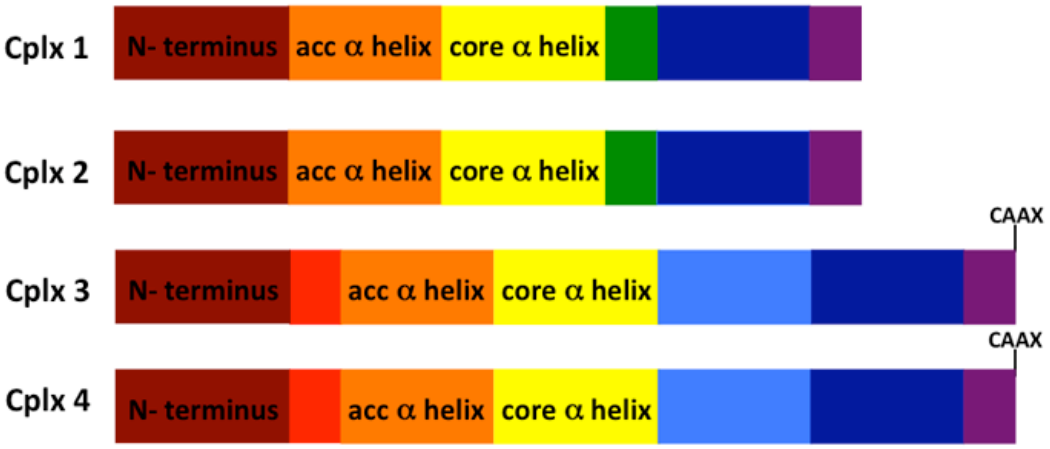

Figure 1-8. Structural features of the complexin protein family. Complexins (cplx) consist of an amino terminal domain, an accessory alpha helix, a core alpha helix that binds to an assembled SNARE complex, followed by a carboxy terminus. The red and green boxes denote glycine and alanine-rich regions. Complexins 3 and 4 differ from complexins 1 and 2 in several respects, including the presence of an insert within the carboxy terminus (light blue box) and a post-translational prenylation motif (CAAX) at the carboxy terminus that is important for membrane targeting.

have one or two complexins, mammals have four complexins (Figure 1-8) that can be grouped into two subfamilies based upon structural features and expression patterns (Ishizuka et al., 1995; McMahon et al., 1995; Takahashi et al., 1995; Tokumaru et al., 2001; Reim et al., 2005). Complexins 1 and 2 share approximately 80% amino acid identity and are enriched at conventional synapses (Ishizuka et al., 1995; McMahon et al., 1995; Takahashi et al., 1995). In the retina, antibodies directed against complexin 1/2 labeled amacrine cells, horizontal cells, and ganglion cells, but not photoreceptors or bipolar cells (Hirano et al., 2005).

Meanwhile, mammalian complexins 3 and 4 are homologous to each other (~ 60% amino acid identity), but not to the complexin 1/2 subfamily (~ 25%). All members of the complexin 3/4 subfamily share a post-translational prenylation motif (CAAX) at the carboxy terminus that is important for membrane targeting. This motif is not present in the complexin 1/2 subfamily, but is found in some invertebrate complexins (Reim et al., 2005). Retinal ribbon synapses selectively express the complexin 3/4 subfamily (Hirano et al., 2005; Reim et al., 2005). Mammalian complexin 3 localizes primarily to rod bipolar cell, cone photoreceptor, and rod photoreceptor terminals, while mammalian complexin 4 is expressed in cone bipolar cell and rod photoreceptor terminals (Reim et al., 2005). Besides retinal ribbon synapses, complexin 3 also localizes to the cortex, hippocampus, inferior colliculus, and striatum at low levels (Reim et al.,

2005).

Despite their differences, all complexins appear to bind specifically and rapidly, via a central alpha helix, to an assembled SNARE complex (Figure 1-9) (Pabst et al., 2000; Hu et al., 2002; Bowen et al., 2005; Reim et al., 2005). Crystal structures of complexin/SNARE complexes revealed that the complexin central alpha helix binds, in an antiparallel fashion, in the groove between the syntaxin and synaptobrevin alpha helices in the 4-helix bundle of the SNARE complex (Bracher et al., 2002; Chen et al., 2002). Recent studies indicate that complexin 1 can also bind, with lower affinity, to the t-SNARE heterodimer (Guan et al., 2008; Weninger et al., 2008; Yoon et al., 2008).

The roles of complexins in synaptic vesicle fusion are very controversial. Early work suggested that complexin inhibits exocytosis (for review, see Brose, 2008). For example, microinjection of complexin 2 or anti-complexin 2 in Aplysia buccal ganglion neurons inhibited or promoted exocytosis, respectively (Ono et al., 1998). Transfection of complexin 1 or complexin 2 in PC12 cells suppressed exocytosis of human growth hormone and acetylcholine (Itakura et al., 1999). Some more recent studies are also consistent with the view of complexin as a fusion clamp. For example, lentiviral overexpression of a fusion protein consisting of complexin 1-synaptobrevin 2-Venus impairs evoked exocytosis in cultured rodent cortical neurons (Tang et al., 2006). In addition, the Rothman group has shown that ectopic expression of any full-length complexin in HeLa cells with extracellular SNAREs inhibits cell-cell fusion (Giraudo et al., 2006; Giraudo et al., 2008). Using another distinct in vitro system, Schaub et al. (2006) and Chicka and Chapman (2009) showed that complexin 1 blocks fusion of liposomes coated with SNAREs. Finally, deletion of most of the coding region of Drosophila *complexin* resulted in a greater than 20-fold increase in miniature postsynaptic potentials at the neuromuscular junction, indicating that complexin blocks spontaneous synaptic vesicle fusion in Drosophila (Huntwork and Littleton, 2007). Taken together, these results suggested a model whereby trans-SNARE complexes appear to be clamped or stabilized in a fusion-ready state by complexin before calcium enters the presynaptic terminal and binds to synaptotagmin. This calcium sensor then interacts simultaneously with phospholipid membranes and the assembled SNARE complex to relieve the complexin clamp and promote fusion (however, see McMahon et al., 1995 and Chicka and Chapman, 2009) for a different view of complexin-synaptotagmin interactions).

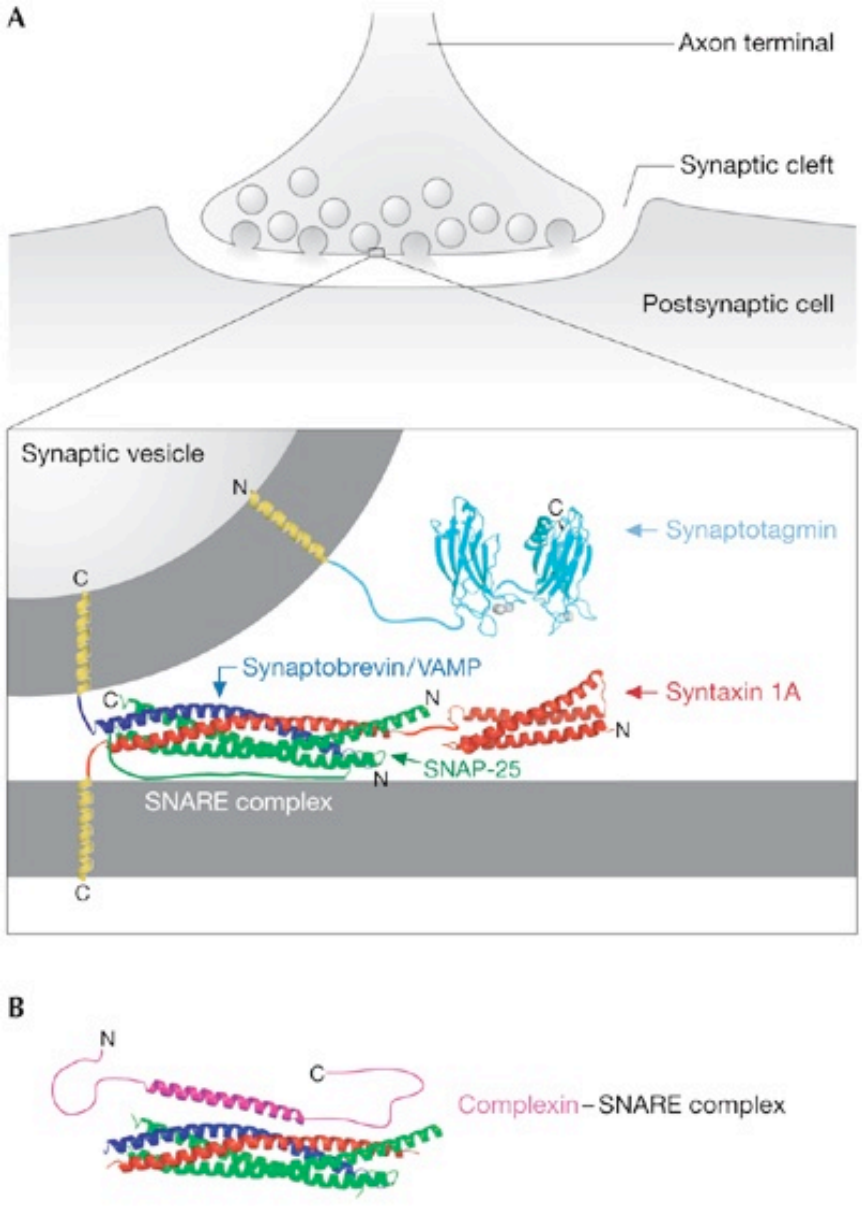

Figure 1-9. Structures of proteins required for the fast, calcium-stimulated release of neurotransmitters. A. The SNARE complex (Protein Data Bank (PDB) ID 1SFC, Sutton et al. (1998) and the C2A and C2B domains of synaptotagmin I (PDB IDs 1BYN, Shao et al. (1998); and 1K5W, Fernandez et al., (2001, respectively) are required at sites of synaptic vesicle fusion on the presynaptic plasma membrane. B. Complexin bound to the SNARE complex (PDB ID 1KIL, Chen et al. (2002). The transmembrane domains and unstructured regions are modelled in the figure. Amino- and carboxy-terminal ends of each protein are indicated. Reproduced from Carr and Munson (2007), with permission from Macmillan Publishers Ltd.

In direct contrast to these results, other studies support the hypothesis that complexin promotes exocytosis. Tokumaru et al. (2001) identified a peptide from squid complexin that blocks the interaction between complexin and the SNARE complex. When microinjected into the squid giant synapse, this peptide inhibits exocytosis (Tokumaru et al., 2001). Substantial evidence from null mutants also suggests that complexins promote evoked exocytosis. In the aforementioned Drosophila mutant, synchronous release of transmitter is decreased (Huntwork and Littleton, 2007). Similarly, patch clamp recordings from hippocampal neurons of complexin 1/2 double knockout mice revealed a 66% decrease in evoked, excitatory post-synaptic current (EPSC) amplitude. It was determined that vesicular release probabilities and calcium sensitivity were decreased in these neurons (Reim et al., 2001). In complexin 1/2/3 triple knockout mice, evoked exocytosis from hippocampal and striatal neurons is also impaired (Xue et al., 2008).

Over the past three years, several groups have attempted to reconcile the debate over whether complexins promote or inhibit exocytosis. While several mechanistic details remain to be firmly established, it now appears that complexins can both promote and inhibit exocytosis depending upon several factors, including complexin domain utilization, isoforms, levels, and localization. These factors are integrated to regulate synaptic vesicle exocytosis. A breakthrough in the field was made by Xue et al. (2007) with the report of inhibitory activity by an accessory alpha helix in complexin (see Figure 1-8), which prevents full zippering of the SNARE complex (Giraudo et al., 2009), and stimulatory activity in the amino terminus. The domain activities, and their sums, vary in their strengths depending upon species such that Drosophila complexin is mainly inhibitory and rodent complexin 1 is mainly facilitatory (Xue et al., 2009). In vitro experiments suggest that exocytosis levels vary inversely with complexin levels (Yoon et al., 2008; An et al., 2010) and localization at the fusion pore (An et al., 2010).

Most of the aforementioned work on complexin's physiological roles has examined mammalian complexin 1/2 and invertebrate complexin. Little is known about the functions of complexins 3 and 4. Rodent complexins 3 and 4 can rescue the defect in calcium-triggered transmitter release in hippocampal neurons from complexin 1/2 double knockout mice (Reim et al., 2005). However, liposome (Malsam et al., 2009) and HeLa cell (Giraudo et al., 2008) fusion assays revealed that complexins 3 and 4 can inhibit exocytosis. At the beginning of my dissertation work, nothing was known about the functions of complexins 3 and 4 in ribbon-containing neurons. Recently, Reim et al. (2009) reported that mice with targeted disruptions of

the complexin 3 and 4 genes exhibit vision deficits and disorganized photoreceptor terminals containing floating ribbons. My work, performed concurrently primarily in zebrafish, has confirmed the importance of complexin 3/4 in visual system function and revealed novel functions and targeting of the complexins during development.

Chapter 2

Methods

Zebrafish husbandry and tissue processing

All procedures were approved by the Institutional Animal Care and Use Committee at the State University of New York at Stony Brook. Wildtype zebrafish (*Danio rerio*) obtained from a local pet store (Fetcho and O'Malley, 1995) were propagated by natural matings and maintained on a controlled cycle of 13 hours of light and 11 hours of darkness at 28.5°C in system water (Westerfield, 2000). Adult wildtype and transgenic zebrafish were maintained at an average density of 5 fish per 2 liter tank. Onset of fertilization was approximately 9:30 AM (30 minutes after lights were turned on). Embryos and young larvae were staged as previously described (Kimmel et al., 1995). Larval zebrafish for whole mount in situ hybridization were raised in 0.003% 1-phenyl-2-thiourea (Sigma-Aldrich) starting at 8 hpf to prevent pigmentation.

Before overnight fixation at 4°C with 4% paraformaldehyde (Electron Microscopy Sciences, Hatfield, PA), zebrafish were anesthetized with 0.168 mg/ml tricaine (Sigma-Aldrich Chemical Co., St. Louis, MO). For in situ hybridization, fixed zebrafish were washed extensively in phosphate-buffered saline (PBS) and stored in methanol at -20°C until use. For immunocytochemistry, fixed zebrafish were washed extensively in PBS, cryoprotected in 30% sucrose until equilibrated, embedded in M-1 matrix (Shandon Lipshaw, Pittsburgh, PA) and frozen at -80°C. Tissue was sectioned at 20-30 μm with a Leica CM1850 cryostat (Leica Microsystems, Bannockburn, IL) with a chamber temperature of -20°C to -22°C and then stored at either -20°C or -80°C.

For isolation of zebrafish retinal RNA from freshly dissected eyes, adult zebrafish were decapitated, enucleated, and the lens and vitreous were extracted in cold, oxygenated, low-calcium solution containing (in mM): NaCl (102), KCl (2.5), $MgCl_2$ (1), $CaCl_2$ (0.5), glucose (10), and HEPES (10), pH 7.4. The retinae were removed from the eyecups, separated from retinal pigment epithelium, and incubated for 25 minutes in 500 units/ml hyaluronidase (Worthington Biochemical Corp., Lakewood, NJ) at room temperature to remove residual vitreous. Retinae were rapidly frozen on dry ice, and poly(A)+ RNA was obtained with the Micro Poly A+ Pure kit (Applied Biosystems, Foster City, CA).

Mouse husbandry and tissue processing

Adult C57BL/6 mice (Taconic, Hudson, NY) were euthanized by CO_2 inhalation, decapitated, and brains were removed for access to the inner ears. The utricles were isolated from the cochleas in PBS, fixed for two hours in 4% paraformaldehyde at 4°C, washed extensively in PBS, and cryoprotected in 30% sucrose overnight. Adult mice were also enucleated and the lens and vitreous were extracted in cold, oxygenated, solution (denoted 2.5 calcium mouse HEPES) containing (in mM): NaCl (135), KCl (5), $MgCl_2$ (1), $CaCl_2$ (2.5), glucose (10), and HEPES (10), pH 7.4. Retinae were removed from the eyecups, and some were placed in cold SDS sample buffer or fixed in 4% paraformaldehyde overnight at 4°C. These retinae were cryoprotected in 30% sucrose overnight, embedded in M-1 matrix and sectioned as described for zebrafish.

To isolate living adult mouse bipolar cells, retinae were removed from the eyecups, and each retina was cut into six pieces. The pieces were transferred into a vial with cold 2.5 calcium mouse HEPES solution containing 2.7 mM D-cysteine hydrochloride hydrate and 21 units/ml papain at room temperature for 28 minutes. After washing several times in 2.5 calcium mouse HEPES solution, the retinal pieces were stored at room temperature in an oxygenated environment. A piece of retina was triturated via a small-bore Pasteur pipette, and the dissociated cells were plated onto glass-bottomed dishes containing 2.5 calcium mouse HEPES solution for recording. Cells were allowed to settle and bind to the glass-bottomed dishes for 35 minutes. After a couple of gentle washes, the dishes were put under the microscope objectives.

Cloning and sequence analysis

The nucleotide sequences of mouse complexin 3 (GenBank:AY264290), human complexin 3 (GenBank:AY286501), mouse complexin 4 (GenBank:AY264291), and human complexin 4 (GenBank:AY286502) (Reim et al., 2005) were used in BLAST searches of the zebrafish genome in the ENSEMBL and GenBank databases. Five putative orthologs were identified in the zebrafish ENSEMBL database (Zv7) – ENSDARG00000062508, ENSDARG00000067826, ENSDARG00000059978, ENSDARG00000059486, and ENSDARG00000069963. To determine whether these genes are expressed in zebrafish, the following primers (which were expected to span multiple introns) were designed – (ENSDARG00000062508 forward) 5'-CGCGACTAACGTTAGGAATT-3'

(ENSDARG00000062508 reverse) 5'-AAAATCACCTCTGATCCTTG-3'
(ENSDARG00000067826 forward) 5'-GAGGAGATGAATCTACATCAC-3'
(ENSDARG00000067826 reverse) 5'-CTCCTAGAACAATATTAGCATC-3'
(ENSDARG00000059978 forward) 5'-ATGGCGTTTTTAATCAAAAGTATGG-3'
(ENSDARG00000059978 reverse) 5'-CTACATGACAGAACATTTCTCCTCG-3'
(ENSDARG00000059486 forward) 5'-GCTTCACATTCATTGTGATCAGCC-3'
(ENSDARG00000059486 reverse) 5'-GGTCTCGAGGGATTGGAATGAC-3'
(ENSDARG00000069963 forward) 5'-CAGTGTTACCTGTGCAGCTC-3'
(ENSDARG00000069963 reverse) 5'-CTCTCACATTAGCTGCACTCC-3'

Reverse transcription (RT) of adult zebrafish retina poly(A)+ RNA was carried out with Superscript II reverse transcriptase (Invitrogen, Carlsbad, CA). PCR was performed with Platinum *Taq* DNA polymerase (Invitrogen), 1 μl of reverse-transcribed cDNA (or non-RT control), and 10 pmol of primers. The PCR protocol consisted of 95°C for 5 minutes, followed by 30 cycles of 95°C, 45°C, and 72°C for 1 minute each, ending with 72°C for 4 minutes. PCR products of approximate expected sizes, obtained with all five primer pairs, were gel-purified, subcloned in pGEM-T Easy, and sequenced. Comparison of these cDNA clones with the aforementioned annotated genes in the zebrafish ENSEMBL database via BLAST revealed >95% nucleotide identity for four of the genes (ENSDARG00000067826 was the exception).

Alignment of the cDNA clones and the aforementioned mammalian complexins 3 and 4 were performed with ClustalW in Molecular Biology Workbench (http://workbench.sdsc.edu). Based on this multiple alignment, an unrooted phylogenetic tree was generated via the neighbor joining method and visualized with TreeView (http://taxonomy.zoology.gla.ac.uk/rod/treeview.html). Bootstrap values supporting each node were calculated from 2000 trials. Based on phylogenetic analysis, the cDNA clone most similar to ENSDARG00000062508 was named *cplx 3a,* ENSDARG00000067826 was named *cplx 3b*, ENSDARG00000059978 was named *cplx 4a,* ENSDARG00000059486 was named *cplx 4b* and ENSDARG00000069963 was named *cplx 4c*. The sequences of the isolated cDNA clones have been deposited (GenBank:GU174497, GU174498, GU174499, GU174500, and GU174501 for zebrafish complexins 3a, 3b, 4a, 4b, and 4c, respectively).

In silico analysis of the following genes were performed based on sequence in the ENSEMBL database (Zv8)—human *cplx 3* (ENSG00000213578), human *cplx 4*

(ENSG00000166569), mouse *cplx 3* (ENSMUSG00000039714), mouse *cplx 4* (ENSMUSG00000024519), zebrafish *cplx 3a* (ENSDARG00000062508), zebrafish *cplx 4a* (ENSDARG00000059978). Proteomic analysis of the cplx3/4 subfamily was performed in Molecular Biology Workbench with the PROSEARCH and PFSCAN algorithms.

Construction and expression of myc-tagged complexins

Complexins 3a, 3b, 4a, 4b, and 4c were each fused in-frame with the myc tag from pCMV-Tag3b using the In-Fusion Dry-Down PCR Cloning Kit (Clontech Labs, Mountain View, CA) according to the manufacturer's instructions. 50 pmol of the following primers were used to amplify 100 ng full-length complexins for eventual fusion with linearized pCMV-Tag3b-
(complexin 3a forward)5'-GAGCCCGGGCGGATCCATGGCTTTTATGTTGAAACACATG-3'
(complexin 3a reverse) 5'-GCAGCCCGGGGGATCCCTACATGACATCACACTTCTCGGC-3'
(complexin 3b forward) 5'-GAGCCCGGGCGGATCCATGGCTTTTATGGTGAAACACGTA-3'
(complexin 3b reverse) 5'-GCAGCCCGGGGGATCCTCACATGACGCAGCACTTCTCA-3'
(complexin 4a forward) 5'-GAGCCCGGGCGGATCCATGGCGTTTTTAATCAAAAGTATG-3'
(complexin 4a reverse) 5'-GCAGCCCGGGGGATCCCTACATGACAGAACATTTCTCCTC-3'
(complexin 4b forward) 5'-GAGCCCGGGCGGATCCATGTCTCATGATGGGATGTCC-3'
(complexin 4b reverse) 5'-GCAGCCCGGGGGATCCTCACATGACGGTGCATTTCTC-3'
(complexin 4c forward) 5'-GAGCCCGGGCGGATCCATGGCGTTCCTTCTGCAGCAG-3'
(complexin 4c reverse)5'-GCAGCCCGGGGGATCCTCACATCAAGACACATTTTTCTTCC-3'

HEK 293T cells were grown in Dulbecco's Modified Eagle's Medium (DMEM, Invitrogen) supplemented with 10% fetal bovine serum (HyClone Labs, Logan, UT) and glutamine (Invitrogen) in a humidified incubator containing 5% CO_2 and 95% air at 37°C. Cells on 100 mm dishes were transfected with Lipofectamine (Invitrogen) and 8 μg of a complexin-myc construct or pCMV-Tag3b. After 24 hours, the cells were trypsinized, plated onto poly-L-lysine-coated glass coverslips, and maintained for an additional 24 hours before processing for immunocytochemistry.

Immunocytochemistry

HEK 293T cells were washed with PBS for five minutes, fixed with 4% paraformaldehyde for 15 minutes at room temperature, washed with PBS, permeabilized and

blocked with PBS+ 0.3% Triton X-100+ 6% normal goat serum (Jackson ImmunoResearch) at room temperature for 2 hours. The coverslips were then incubated overnight at room temperature with anti-myc and either anti-complexin 3 or anti-complexin 4 diluted in the blocking solution. In parallel, coverslips from each cell line were incubated solely with anti-myc, anti-complexin 3, anti-complexin 4, or the blocking solution. All of the coverslips were then washed three times with blocking solution and incubated for one hour at room temperature with affinity-purified, Alexa Fluor 488-conjugated goat anti–rabbit IgG and Alexa Fluor 546-conjugated goat anti–mouse IgG (Jackson ImmunoResearch, West Grove, PA) diluted 1:200 in the blocking solution. Finally, the coverslips were washed three times in PBS, once in distilled water, and mounted in Vectashield (Vector Laboratories, Burlingame, CA).

Sections and wholemounts were washed with PBS and blocked for 2 hours at room temperature as described for the HEK293T cells. Primary antibodies (see Table 2-1 for complete list) were added to fresh blocking solution, and slides were incubated overnight at room temperature. For labeling of actin, Alexa Fluor 488 phalloidin (Invitrogen) was diluted 1:50 and incubated overnight with primary antibodies. After three washes, species-specific secondary antibodies were added for 1 hour at room temperature. Sections and wholemounts were washed three times with PBS, rinsed with water, and coverslipped in Vectashield.

For labeling of neuromasts, adult zebrafish were bathed in 3.0 μM AM1-43 in system water for 30 minutes and imaged. Zebrafish larvae were bathed in 3.0 μM AM1-43 in embryo medium for 30–45 seconds (Seiler and Nicolson, 1999). After several washes in embryo medium. larvae were anesthetized with tricaine, fixed with 4% paraformaldehyde for 2 hours at room temperature, and cryoprotected in 30% sucrose overnight as described earlier. Larvae were sectioned sagittally at 30 μm, dried at room temperature, washed with PBS, and permeabilized with 0.3% Triton X-100 for 1 hour 15 minutes. Sections were then blocked for 2 hours with PBS + 6% normal goat serum, and incubated overnight with primary antibodies in the blocking solution. Slides were processed the next day as described above, except for the use of affinity-purified, Alexa Fluor 546-conjugated goat anti–rabbit IgG (Jackson ImmunoResearch) to detect complexins.

antibody	type	dilution	source	immunogen	characterization of specificity
complexin 3	rb pc	1:10,000	Synaptic Systems cat#122 302	full-length ms complexin 3	Immunofluorescence of heterologous cells expressing complexin isoforms; Western Blot
complexin 4	rb pc	1:75,000	Synaptic Systems cat#122 402	full-length ms complexin 4	Immunofluorescence of heterologous cells expressing complexin isoforms; immunofluorescence of morphant visual system
zpr 1/FRet43	ms mc	1:400	ZIRC	adult zf retinal cells	Immunofluorescence of zf retina
zn 1	ms mc	1:40	ZIRC	homogenized 1-5 dpf whole zf or membrane or basal lamina fractions	Immunofluorescence of zf inner ear
PKC	ms mc	1:1,000	BD Biosciences Pharmingen cat#554207	bovine full-length PKC	Immunofluorescence of gf retina
myc	ms mc	1:250	Zymed Laboratories cat#13-2500	hu c-myc aa 408-439	Antibody reacts specifically to hu c-myc aa 410-419
ribeye b	rb pc	1:500	Dr. T. Nicolson	zf ribeye b aa 133-483	Immunofluorescence of zf hair cells
CtBP2	ms mc	1:1,000	BD Biosciences Pharmingen cat#612044	ms CtBP2 aa 361-445	Western Blot with retinal homogenates reveals expected bands of 120 and 110 kD

Table 2-1. Primary antibodies used in this study. Cat#, catalog number; CtBP 2, carboxy-terminal binding protein 2; gf, goldfish; hu, human; mc, monoclonal; mo, mouse; pc, polyclonal; PKC, protein kinase C; rb, rabbit; zf, zebrafish; ZIRC, Zebrafish International Resource Center.

Confocal microscopy and image analysis

Images were acquired with either a FluoView 300 laser scanning confocal microscope running Olympus FluoView 5.0 or an Olympus FluoView FV1000 laser scanning confocal microscope running Olympus10-ASW software (Olympus America, Center Valley, PA). For the

Olympus FluoView FV300 confocal, images were collected with an Olympus UPlan-Apochromat 60x NA 1.20 objective or a Zeiss Fluar 10x NA 0.5 objective. For the Olympus FluoView FV1000 confocal, images were collected with an Olympus Plan-Apochromat 60x NA 1.42 objective or an Olympus UPlan-S Apochromat 10x NA 0.4 objective.

For all double-labeling experiments, sequential scans were taken to reduce cross-talk. For most experiments, a series of confocal optical sections (with a step size of 0.5-2.0 μm) was taken through the entire tissue section and a planar projection was generated. Images were passed through a median filter, and exported to ImageJ64 (NIH, Bethesda, MD) and Photoshop CS3 (Adobe Systems Inc., San Jose, CA), where levels were increased to reflect the original captures in FluoView.

To quantitate the zebrafish complexin 3/4 reactivity profiles of the rabbit polyclonal anti-complexin 3 and anti-complexin 4 antibodies, fifty random fields of transfected HEK 293T cells were photographed from a representative of triplicate experiments for each cell line. All images were taken within the dynamic range of the photomultiplier, and identical gain and offset settings were used when imaging complexin (and myc) antibody immunoreactivity between cell lines. For each field, confocal z-stacks were taken through the entire cell with a step size of 2 μm, and the middle three optical sections were chosen to make a z-projection for each cell. These projections were encircled in ImageJ, and the mean pixel intensities were measured for both channels. Background fluorescence, which was obtained by measuring the mean pixel intensity for both channels in a region outside of a cell, was subtracted from the pixel intensity measurements. To compare the immunoreactivity of a complexin antibody directly, we calculated mean fluorescence ratios for each complexin paralog by dividing the corrected mean complexin antibody fluorescence intensity by the corrected mean myc fluorescence intensity. Student's t-tests were performed with Microsoft Excel 2008, with $p < 0.05$ considered to be statistically significant.

Western blot

Total protein extracts were prepared from freshly isolated adult mouse and zebrafish retinae. Zebrafish extract was made in hypotonic lysis buffer (with protease inhibitors) and loaded at 200 μg, while mouse extract was loaded at 100 μg in SDS-sample buffer (with protease inhibitors). Proteins were size-fractionated by 15% SDS–PAGE and transferred to nitrocellulose

membranes. The blot was probed with anti-complexin 3/4 antibody (1:1000) in TBST + 2.5 % milk overnight, followed by DyLight 800 conjugated anti-rabbit IgG (Rockland Immunochemicals, Gilbertsville, PA). Fluorescence was detected with the Odyssey Imaging System (LI-COR Biosciences, Lincoln, NE).

In situ hybridization

With the high degree of nucleic acid homology over the coding regions of the zebrafish complexin 3 and 4 paralogs, we designed probes (300-400 nucleotides) that would recognize portions of the 5'UTR for each gene. By consulting the aforementioned genomic sequences in the zebrafish ENSEMBL database, the following primers were generated to pull out fragments of 5'UTR and the amino termini for each gene-

(complexin 3a forward/AS) 5'-CAGCAACAGCAAGCATAAAAC-3'
(complexin 3a reverse/AS) 5'-AATTAACCCTCACTAAAGGGACTGTTCTTCAA-3'
(complexin 3a forward/S) 5'-TAATACGACTCACTATAGGCAGCAACAGCAAGC-3'
(complexin 3a reverse/S) 5'-GACTGTTCTTCAATAAATTCC-3'
(complexin 3b forward/AS) 5'-CTCCAGATGGATGTTGTATAG-3'
(complexin 3b reverse/AS) 5'-AATTAACCCTCACTAAAGGGTTGCTTAACACT-3'
(complexin 3b forward/S) 5'-TAATACGACTCACTATAGGCCAGATGGATGTTG-3'
(complexin 3b reverse/S) 5'-AGATTTCTCCCCTTCAGGTT-3'
(complexin 4a forward/AS) 5'-AGTCAACAGTGTGTCCTTGA-3'
(complexin 4a reverse/AS) 5'-ATTAACCCTCACTAAAGGGATTAGGGGTCTCC-3'
(complexin 4a forward/S) 5'-TAATACGACTCACTATAGGAGTCAACAGTGT-3'
(complexin 4a reverse/S) 5'-TTAGGGGTCTCCTCTTCAGC-3'
(complexin 4b forward/AS) 5'-GGCCCAGGTCACTGTCAGGAT-3'
(complexin 4b reverse/AS) 5'-AATTAACCCTCACTAAAGGCATGAGACATTTT-3'
(complexin 4b forward/S) 5'-TAATACGACTCACTATAGGGGCCCAGGTCACT-3'
(complexin 4b reverse/S) 5'-CATGAGACATTTTTGATTAGC-3'
(complexin 4c forward/AS) 5'-AAGGAGAGTTTGTGTTGACG-3'
(complexin 4c reverse/AS) 5'-AATTAACCCTCACTAAAGGCCTCCGCCATCTT-3'
(complexin 4c forward/S) 5'-TAATACGACTCACTATAGGAAGGAGAGTTTGT-3'
(complexin 4c reverse/S) 5'-CCTCCGCCATCTTCATCTTC-3'

For additional controls, zebrafish red cone opsin antisense and sense primers were designed as follows-

(red cone opsin forward/AS) 5'-AGGGTCCCAATTACCACATTGCC-3'

(red cone opsin reverse/AS) 5'-AATTAACCCTCACTAAAGGATTCCTGTGGATC-3'

(red cone opsin forward/S) 5'-TAATACGACTCACTATAGGGTCCCAATTACCA-3'

(red cone opsin reverse/S) 5'-TTCCTGTGGATCTTAAGTCA-3'

Note that a T7 RNA polymerase primer site was incorporated into all forward/sense (S) primers, while a T3 RNA polymerase primer site was incorporated into the reverse/antisense (AS) primers.

RT-PCR was performed with adult retina cDNA as described in "Cloning and sequence analyses." PCR products were obtained with reverse-transcribed (RT) cDNA, but not with no RT control samples from adult retina. These products were cloned into pGEM-TEasy and sequenced. Digoxigenin-labeled sense and antisense RNA probes were then synthesized with the appropriate RNA polymerase (T7 and T3, respectively) (Roche, Nutley, NJ) from the gel-purified (Qiaex Gel Extraction Kit, QIAGEN, Valencia, CA) PCR products. Probes were purified with NucAway Spin columns (Ambion, Austin, TX) and examined on a denaturing RNA agarose gel to confirm the presence of a single band.

Whole mount in situ hybridizations were performed essentially as described (Thisse and Thisse, 2008). In brief, larvae were removed from methanol and rehydrated with successive 5-minute incubations of increasing amounts of PBS. Following 4x 5-minute incubations in PBS + 0.1% Tween 20 (PBST), larvae were incubated with 10 μg/ml proteinase K (Roche) for 55 minutes and then re-fixed for 20 minutes at room temperature. After 5 washes in PBST, larvae were blocked with prehybridization solution (50% formamide, 5x SSC, 0.1% Tween 20, 9.2 μM citric acid pH 6.0, 50 μg/ml heparin, 500 μg/ml yeast tRNA) for 2 hours at 70°C. Probe (0.25 ng/μl) was added to fresh prehybridization solution, and larvae were incubated at 70°C overnight. Increasing amounts of 2x SSC were then added for 15 minutes apiece at 70°C, followed by 2 washings with 0.2x SSC for 30 minutes apiece. Successively increasing amounts of PBST were added at room temperature for 10 minutes each, followed by blocking with 2% goat serum and 2 mg/ml BSA fraction V (Sigma-Aldrich) in PBST for 3 hours at room temperature. Larvae were incubated overnight at 4°C with preadsorbed anti-digoxigenin antibody coupled to alkaline phosphatase (diluted 1:5000) (Roche) in blocking solution. Larvae

were washed several times, and the color reaction was performed by adding 0.225 mg/ml nitroblue tetrazolium (NBT) and 0.175 mg/ml 5-bromo-4-chloro-3-indoyl-phosphate (BCIP) (both from Sigma-Aldrich) in 100 mM Tris-HCl pH 9.5, 50 mM $MgCl_2$, 100 mM NaCl, 0.1% Tween 20. After approximately 30-60 minutes, the reaction was stopped with PBS pH 5.5 + 1 mM EDTA. Larvae were photographed using a Zeiss Axiocam mounted on a Zeiss Axioplan microscope with a Zeiss Plan Apochromat 20x 0.75 NA objective (Carl Zeiss Microimaging, Thornwood, NY).

RNA dot blot

RNA dot blots were prepared as described (Hodge, 1998) with some modifications. In brief, positively charged nylon membrane (Roche) was air-dried after washing with DEPC-treated water and 10x SSC. 25 μl of either full-length complexin 3b mRNA (800 pg/μl) or yeast RNA (Ambion, 800 pg/μl) was denatured at 65°C for 5 minutes in diluent consisting of 49 μl formamide + 16 μl 37% formaldehyde + 10 μl 10x MOPS. The RNA was then cooled on ice and added to 100 μl ice-cold 20x SSC. 2 μl of RNA was spotted on a 1 cm^2 -square of nylon membrane, dried, and UV crosslinked for 90 seconds.

The RNA-containing nylon membranes were pre-hybridized at 68°C for 1 hour with 6x SSC + 5% Denhardt's solution + 0.5% SDS + 100 μg/ml ss DNA + 50% formamide. The pre-hybridization solution was replaced with 200 μl of fresh pre-hybridization solution containing 100 ng of denatured, DIG-labeled RNA probe, and hybridization was performed at 68°C for 6 hours. The membranes were then washed twice (5 minutes per wash) with 2x SSC + 0.1% SDS at room temperature. This was followed by two washes (15 minutes pre wash) at 68*C with 0.1x SSC + 0.1% SDS.

Immunological detection of hybridization was performed, with anti-digoxigenin antibody coupled to alkaline phosphatase, via chemiluminescence with the CSPD substrate (Roche) according to the manufacturer's instructions. Blots were exposed to X-ray film for 15 minutes at room temperature.

Morpholino antisense oligonucleotide and mRNA microinjections

Morpholino antisense oligonucleotides were designed to block the initiation of translation or affect pre-mRNA splicing to prevent the production of full-length complexin protein. All

morpholinos were purchased from Gene Tools (Philomath, OR), reconstituted in nuclease-free water to a stock concentration of 33-66 μg/μl, aliquoted and stored at –80°C. A morpholino antisense oligonucleotide (5'-CCTCTTACCTCAGTTACAATTTATA-3') directed against a human beta-globin intron mutation was used as a negative control. Morpholino solutions were diluted to a final concentration of 2-20 ng/nl with 0.2 M KCl and 2 mg/ml phenol red. 0.5 nl of a morpholino solution was pressure-injected into one-cell-stage zebrafish embryos treated with 2 mg/ml pronase (Sigma-Aldrich) (Londin et al., 2005) for 3 minutes to remove chorions. An additional negative control condition consisted of dechorionated zebrafish embryos that were not injected. Zebrafish embryos were then raised at 25.5 °C (for complexin 3a and complexin 3b morphants) or at 28.5 °C (for complexin 4a morphants) in embryo medium (0.346 mg/ml sodium bicarbonate supplemented with Hanks Solution #1, Hanks Solution #2, Hanks Solution #4, Hanks Solution #5 (Westerfield, 2000), and penicillin-streptomycin (Invitrogen). The day after injection, embryos were switched to embryo water (10 ml reverse osmosis (RO) water + 3 mg Instant Ocean + 10 μl methylene blue (1mg/ml)), which was replaced daily thereafter.

To knock down the expression of complexin 3a, a morpholino (5'-GTATCGTCCAATTCACTCTGGTAAT-3') was used to block the splicing out of intron 2, leading to the incorporation of a stop codon after exon 2. To confirm the incorporation of intron 2 (and the stop codon), RNA was first isolated from pools of 12 larvae at 4.5 dpf (either not injected fish, control morpholino-injected fish, cplx 3a morpholino-injected fish that were morphologically normal, and cplx 3a morpholino-injected fish that were morphologically abnormal) using an RNAeasy Mini Kit (QIAGEN). The RNA pools were then reverse transcribed, as described above. Finally, RT-PCR was performed as described above with primers zf 62508f (5'-CACATGATAGGAGGGCAGC-3') and zf 62508r (5'-TCTGTTTCAGGTCCTCGAGG-3'), which anneal to exons 1 and 3, respectively, in complexin 3a. PCR products were gel-purified, subcloned into pGEMTEasy and sequenced.

To knock down complexin 3b protein expression, a morpholino (5'-CTACGTGTTTCACCATAAAAGCCAT-3') was designed to target the translation start site of complexin 3b. To knock down complexin 4a protein expression, a morpholino antisense oligonucleotide (5'-AAACGCCATTATTTACCACGCCGGA-3') complementary to the translation start site of the complexin 4a gene was utilized. In addition, a second morpholino (5'-TCTCTAGCTTGATGCCAAGTTGCGA-3') was designed to target the 5' untranslated region of

complexin 4a.

For the synthesis of full-length complexin capped mRNA, 1 μg of linearized DNA was incubated at 37°C for 2 hours with NTPs/CAP, reaction buffer, and T7 or SP6 RNA polymerase enzyme mix (mMESSAGE mMACHINE kit; Ambion). For full-length complexin 3a mRNA, complexin 3a in pGEMTEasy (in the 3' to 5' orientation) was linearized with PstI and used as a template for the T7 RNA polymerase. For full-length complexin 4a mRNA, complexin 4a in pGEMTEasy (in the 3' to 5' orientation) was linearized with NcoI and used as a template for the SP6 RNA polymerase. Capped mRNA was then purified, using an RNeasy MinElute Cleanup kit (QIAGEN), and resuspended in nuclease-free water. Embryos were injected at the 1-cell stage with 50 pg of complexin 3a mRNA, 50 pg lacZ mRNA, or 50 pg complexin 4a mRNA in 0.5 nl.

Transmission electron microscopy

Zebrafish embryos and larvae were fixed in 4% paraformaldehyde and 0.2% glutaraldehyde (Electron Microscopy Sciences) in 0.13 M phosphate buffer (pH 7.4) at 4°C overnight. Three rinses with 0.13 M phosphate buffer were followed by post-fixation with 1% osmium tetroxide and 1.5% potassium ferrocyanide in 0.1 M phosphate buffer for 30 minutes at room temperature. Zebrafish were washed three times with 0.13 M phosphate buffer and then dehydrated with 50% ethanol for 5 minutes, followed by 70% ethanol for 5 minutes, and three changes of 100% ethanol (2 minutes per incubation). Embedding was initiated in Embed 812 (Electron Microscopy Sciences) at room temperature with 50% ethanol + 50% Embed 812 for 30 minutes, followed by 25% ethanol + 75% Embed 812 for 90 minutes, followed by 100% Embed 812 for 3 hours. Embedding was accelerated overnight at room temperature in a resin consisting of 44.6% Embed 812 + 35.7% dodecyl succinic anhydride (DDSA) + 17.9% nadic methyl anhydride (NMA) + 1.8% 2, 4, 6-tri (dimethylaminomethyl) phenol (DMP30). The resin was replaced with fresh resin, and incubated at 60°C for 48 hours.

Serial semithin sections (1 μm) were cut on a Reichert Ultracut E ultramicrotome, and stained with toluidine blue for light microscopic examination. Ultrathin sections (60–90 nm) were cut, mounted on formvar-coated nickel grids, and stained with 2% methanolic uranyl acetate for 8 minutes and 0.3% aqueous lead citrate for 3 minutes. To analyze cell ultrastructure, stained ultrathin sections were examined with a JEOL 1200 EX electron microscope operating at

80 kV (JEOL, Peabody, MA) and photographed at 15, 000x. Photographs were then digitized and analyzed using Adobe Photoshop CS3 and Image J64.

Optokinetic response assay

The optokinetic response of zebrafish larvae in response to moving, alternating black and white stripes, was measured as described (Brockerhoff, 2006). In brief, 4-5 dpf zebrafish larvae were placed, with their dorsal sides up, in a 35-mm diameter Petri dish, filled with 5% methylcellulose (Sigma-Aldrich), positioned at the center of the stereomicroscope stage (above the light source). Concentric with the dish was an opaque drum (7.0 cm in diameter and 3.5 cm in height) lined with paper containing alternating vertical black and white stripes (1 cm in width). The drum was rotated clockwise around the vertical axis by a motor at a velocity of 36 degrees/second. The numbers of eye movements, consisting of smooth pursuit followed by a saccade, were counted over the course of 1 minute following the start of the rotating drum.

Melanophore response to extrinsic stimuli

Zebrafish embryos and larvae were examined on a Zeiss SteREO Discovery.V20 stereomicroscope equipped with an Axiocam camera and AxioVision Rel 4.8 software. Representative zebrafish were individually immobilized by placing them in small wells cut out of a thin, 2% agar layer in a 100-mm diameter Petri dish (the "imaging chamber"). Dorsal and lateral views were photographed. To examine whether melanophores in complexin 4a morphants were functional, control morphant and complexin 4a morphant fish were transferred to labelled 35-mm diameter Petri dishes, and then incubated with 10^{-3} M epinephrine in embryo medium (Sigma-Aldrich) for 15 minutes at room temperature. At the end of the incubation period, the zebrafish were transferred back to the imaging chamber and photographed. To examine the effects of ambient light levels, light-adapted embryos and larvae were first photographed as described above. These fish were then dark or light-adapted for a minimum of 1 hour at 28.5°C. At the end of this period, embryos and larvae were photographed in the imaging chambers. Since tricaine leads to the dispersion of melanosomes (Sheets et al., 2007), all of the time-lapse experiments were performed on non-anesthetized zebrafish.

In addition to these time-lapse experiments, other experiments were performed in which the melanophores of fixed embryos and larvae were analyzed. In these experiments, zebrafish

were rapidly fixed overnight in 4% paraformaldehyde at 4°C. After several washed in PBS, individual fish were transferred to an imaging chamber and photographed as described above.

Generation of transgenic zebrafish expressing sypHy

pHluorin cDNA (either 1, 2, or 4 copies) in pcDNA3 provided by Y. Zhu (Salk Institute, La Jolla, CA) was blunt-ligated into an intraterminal loop of synaptophysin. This fusion construct (sypHy) was used as a template for PCR with an attB1-containing forward primer (5'-GGGGACAAGTTTGTACAAAAAAGCAGGCTCCATGGATGTTGCCAACCAGTTGGTC-3') and attB2-containing reverse primer (5'-GGGGACCACTTTGTACAAGAAAGCTGGGTCTCACATCTCGTTGGAGAAGGATGT-3'). The PCR protocol was: 95°C for 5 minutes, 25 cycles of 95°C (1 minute), 55°C (1 minute), and 68°C (4 minutes), and 68°C for 4 minutes. An equimolar amount of purified PCR product and Gateway donor vector pDONR 221 were combined with BP Clonase II enzyme mix (Invitrogen) for 2 hours to promote recombination. The reaction was terminated with Proteinase K for 10 minutes at 37°C. One Shot Top10 phage-resistant competent cells (Invitrogen) were then transformed with the recombination products to obtain middle entry clones that contain sypHy with 1, 2, or 4 copies of pHluorin (designated as pME-1x sypHy, pME-2x sypHy, pME-4x sypHy).

To generate a 5' entry clone containing the zebrafish mGluR6 promoter, an intermediate 5' entry clone containing the pBluescriptII KS+ multiple cloning site was first synthesized. This was done by amplifying the multiple cloning site from pBluescriptII KS+ with an attB4-containing forward primer (5'-GGGGACAACTTTGTATAGAAAAGTTGCCGTAATACGACTCACTATAGGGCGA-3') and attB1-containing reverse primer (5'-GGGGACTGCTTTTTTGTACAAACTTGGAATTAACCCTCACTAAAGGGAACA-3'). The PCR protocol, subsequent BP reaction, and transformation were performed as described above, except for the use of pDONR P4-P1R rather than pDONR221 in the BP reaction. The intermediate 5' entry clone (designated p5E-MCS opp) was digested with NotI + XhoI and ligated to the zebrafish mGluR6 promoter, which had been cut out of mGluR6-EYFP-ISceI (generated previously by J. Leheste, Matthews lab) with NotI + XhoI. This 5' entry clone was designated as p5E-mGluR6.

p5E-mGluR6, a sypHy middle entry clone (either pME-1x sypHy, pME-2x sypHy, or pME-4x sypHy) and a 3' entry clone containing the SV40 late polyA signal (designated p3E-polyA, C. Bin-Chien, University of Utah School of Medicine, Salt Lake City, UT) were combined together with a Tol2 transposon-containing destination vector which also contains a cardiac myosin light chain 2:EGFP transgenesis marker (designated pDestTol2CG2, C. Bin-Chien) in an LR recombination reaction. Equimolar amounts of the vectors were added to LR Clonase II enzyme and buffer mix, which was kept overnight at room temperature. The reaction was terminated with Proteinase K for 10 minutes at 37°C. OneShotTop10 competent cells were transformed to obtain clear bacterial colonies with the appropriate clones (named mGluR6-1x sypHy-polyA, mGluR6-2x sypHy-polyA, and mGluR6-4x sypHy-polyA).

To generate inducible sypHy-containing constructs, the sypHy middle entry clones were combined in an LR reaction with a 5' entry clone containing a heat shock promoter (designated p5E-hsp70l, C. Bin-Chien), p3E-polyA, and pDestTol2CG2. OneShotTop10 competent cells were transformed to obtain clear bacterial colonies with the appropriate clones (named hsp70-1x sypHy-polyA, hsp70-2x sypHy-polyA, and hsp70-4x sypHy-polyA).

Capped transposase mRNA was synthesized with the SP6 RNA polymerase (mMessage mMachine), as described above, using pCS2FA-transposase (C. Bin-Chien) linearized with NotI as template. One-cell-stage, dechorionated zebrafish embryos were microinjected with 0.5 nl of a mixture of the sypHy-containing vector (e.g., hsp70 -1x sypHy-polyA) (final concentration of ~5-15 ng/μl) and transposase mRNA (final concentration of ~5 ng/μl). Embryos were maintained at 25.5°C in embryo medium and embryo water. Approximately 1.25 days after injection, embryonic zebrafish were initially screened for green fluorescence in the heart using either a Leica MZ APO stereomicroscope, a Zeiss SteREO Discovery.V20 stereomicroscope or an Olympus SZX/2 stereomicroscope. mGluR6 lines with GFP in the heart were re-screened at 5 dpf for green fluorescence emanating from the eye. Hsp70 fish with GFP in the heart were heat-shocked at 2 dpf by transferring embryos from 25.5°C to 37°C for 1 hour in pre-warmed embryo water, and then maintained again at 25.5 °C. These zebrafish were then re-screened for green fluorescence in the eye at 3 dpf. Founders were outcrossed, starting at 3 mpf, to wildtype zebrafish. Progeny with GFP in the heart and eye were obtained with the hsp70-1x sypHy-polyA and mGluR6-1x sypHy-polyA transgenes. Stable lines containing the hsp70-1x sypHy-polyA were crossed to other hsp70-1x sypHy-polyA stable lines to obtain homozygotes.

Patch clamping and imaging

Recordings were performed with an EPC-9 amplifier and PULSE software (HEKA Instruments, Southboro, MA) in voltage-clamp mode. Mouse bipolar cell somata were patch-clamped at -60 mV and dialyzed with cesium gluconate solution containing (in mM): Cs-gluconate (120), TEA-Cl (10), HEPES (20), NMDG–EGTA (0.2), $MgCl_2$ (3), Na_2ATP (2), GTP (0.5), supplemented with 30 μM fluorescent RIBEYE-binding peptide (rhodamine-EQTVPVDLSVARPR-COOH) (Zenisek et al., 2004) and 1 mM fluorescent complexin 3 SNARE-binding domain peptide (HiLyte Fluor 488-ATLRSHFRDKYRLPK-COOH). The complexin 3 SNARE-binding domain peptide was visualized with a 488 nm argon laser, SDM570 dichroic mirror, and BA510IF and BA530IF emission filters. Rhodamine-RIBEYE-binding peptide was visualized with a 543 helium-neon laser and a 605BP emission filter. Approximately 1-2 minutes after going whole-cell, confocal z stacks were obtained of the living bipolar cell terminals dialyzed with these peptides. Data analysis was initially performed in Fluoview, and data were then exported into Microsoft Excel 2008.

In additional experiments, dissociated mouse bipolar cells were plated onto glass coverslips, allowed to attach for 35 minutes, and then fixed for 15 minutes with 4% paraformaldehyde. Cells were permeabilized and blocked with PBS+ 0.3% Triton X-100 + 6% normal goat serum for 30 minutes at room temperature. Cells were subsequently incubated in blocking solution with anti-CtBP2 (1:1000) and 1 mM complexin 3 peptide for 1 hour. Finally, cells were incubated with blocking solution supplemented with goat anti-mouse conjugated to Alexa Fluor 546 secondary antibody for 1 hour, washed with water, and mounted in Vectashield. As a negative control, some coverslips were incubated with an equivalent molar amount of Alexa Fluor 488 goat anti-rabbit. Confocal z stacks were obtained of the fixed and labeled bipolar cells.

Chapter 3

Enrichment of complexins 3 and 4 in ribbon-containing sensory neurons

Introduction

Photosensitive and non-cutaneous mechanosensitive neurons transduce stimuli, via specialized sensory cilia and microvilli on their apical surfaces, into graded membrane potentials. A rod or cone photoreceptor elaborates, from a primary cilium, vast quantities of plasma membrane that contain opsins and the rest of the transduction machinery (reviewed in Kennedy and Malicki, 2009). Less well-developed outer segments are also present in pineal complex photoreceptors in anamniotes and sauropsids (reviewed in Ekström and Meissl, 1997). Developing mechanosensory hair bundles, on the other hand, consist of a kinocilium and actin-rich stereocilia embedded in a cuticular plate and interconnected with proteinaceous linkages (reviewed in Nicolson, 2005; Nayak et al., 2007). In teleosts such as zebrafish, mechanosensory hair cells are located in sensory patches of inner ear epithelia (maculae and cristae) and in neuromasts of the lateral lines (reviewed in Nicolson, 2005). Defects in the assembly of hair cell bundles and photoreceptor outer segments can lead to receptor cell degeneration and sensory deficits (reviewed in Nicolson, 2005; Nayak et al., 2007; Kennedy and Malicki, 2009).

The presynaptic terminals of receptor cells in the visual and octavolateral systems have an architecture that allows them to effectively transmit information about stimulus intensity and frequency with release modification. Synaptic vesicle exocytosis occurs at active zones that contain ribbons. These pleiomorphic organelles, composed primarily of a unique protein called RIBEYE, tether a halo of releasable vesicles (reviewed in Schmitz, 2009; Zanazzi and Matthews, 2009). Teleost genomes contain two *RIBEYE* genes, *RIBEYE a* and *RIBEYE b*, that are differentially expressed in zebrafish (Wan et al., 2005). The importance of the ribbon in synaptic transmission is underscored by the loss of vision (Dick et al., 2003; Van Epps et al., 2004) and hearing (Khimich et al., 2005) in zebrafish and mouse mutants that lack anchored ribbons. Despite this, the molecular mechanisms that contribute to exocytosis in ribbon terminals are poorly understood.

Although the molecular architectures of ribbon and conventional terminals are similar, specific isoforms of synaptic vesicle proteins have been identified at some ribbon synapses (reviewed in Schmitz, 2009; Zanazzi and Matthews, 2009). For example, adult mammalian

retinal ribbon synapses selectively express the complexin 3/4 subfamily (Hirano et al., 2005; Reim et al., 2005). The mammalian complexins are a family of small, hydrophilic proteins encoded by four genes that can be grouped into two subfamilies based upon sequence identity and expression patterns (Ishizuka et al., 1995; McMahon et al., 1995; Takahashi et al., 1995; Reim et al., 2005). Complexins 1 and 2 share approximately 80% amino acid identity, and are enriched at conventional synapses (Ishizuka et al., 1995; McMahon et al., 1995; Takahashi et al., 1995) where they appear to activate and stabilize the SNARE complex in a fusion-ready state before calcium enters the terminal and binds to synaptotagmin (reviewed in Südhof and Rothman, 2009). Meanwhile, mammalian complexins 3 and 4 are homologous to each other (~ 60% amino acid identity), but not to the complexin 1/2 subfamily (~ 25%). Mammalian complexin 3 localizes primarily to rod bipolar cell and cone photoreceptor terminals, while mammalian complexin 4 is expressed in cone bipolar cell and rod photoreceptor terminals (Reim et al., 2005). In confirmation of their importance in retinal ribbon synaptic transmission, mice with targeted disruptions of the complexin 3 and 4 genes exhibit vision deficits and disorganized photoreceptor terminals containing floating ribbons (Reim et al., 2009).

Here, we report the cloning of the zebrafish complexin 3/4 orthologs and their expression in sensory ribbon-containing neurons in the adult zebrafish. By searching the ENSEMBL and GenBank databases, we identified and subsequently cloned five zebrafish orthologs that show 50-75% amino acid identity with mammalian complexins 3 and 4. Phylogenetic analysis reveals two complexin 3 orthologs and three complexin 4 orthologs. Utilizing a polyclonal antibody that recognizes all five zebrafish orthologs, we demonstrate that these proteins are enriched in the lateral border of the adult zebrafish pineal organ and in the outer plexiform layer (OPL) and inner plexiform layer (IPL) of the adult zebrafish retina. Complexin 3/4 overlaps with zpr 1/FRet 43 in terminals of double cone photoreceptors in the OPL and pineal, and with protein kinase C (PKC) in ON bipolar cell terminals in the IPL. Hair cells of the octavolateral system display complexin 3/4 immunoreactivity among their apical stereocilia rather than in their basolateral presynaptic terminals. While complexin 4a may be the predominant complexin 3/4 isoform in visual system ribbon presynaptic terminals, it is not expressed in octavolateral hair cells. Taken together, these results define an evolutionarily conserved subfamily that is enriched in different domains of many ribbon-containing neurons.

Results

Cloning, phylogenetic, and syntenic analyses of zebrafish complexin 3 and 4 orthologs

By searching the zebrafish ENSEMBL and GenBank sequence databases, we identified five zebrafish orthologs of mammalian complexins 3 and 4. The full-length coding sequences of each zebrafish ortholog were then amplified by PCR from retina cDNA. Translation of the putative open reading frames within the amplified PCR products predicted proteins that range, with one exception, from 155–159 amino acids in length (Figure 3-1A). The five zebrafish orthologs show approximately 50-75% amino acid identity with human and mouse complexins 3 and 4 (Table 3-1, Table 3-2). Alignment of these proteins reveals striking amino acid identity adjacent to, and within, the putative core alpha helices (RDAQFTQRKAERATLRSHFRDKY in mouse complexin 3) that may mediate binding to SNARE complexes (Reim et al., 2005). Members of the complexin 3/4 subfamily share two motifs not present in the complexin 1/2 subfamily—a prenylation motif (CAAX) at the carboxy terminus that is important for membrane targeting (Reim et al., 2005), and a putative bipartite nuclear localization signal (RKAERATLRSHFRDKYRL in mouse complexin 3) that almost completely overlaps with the putative SNARE-binding core alpha helix. Taken together, the sequence identity and conserved structural features suggest a novel vertebrate subfamily consisting of complexin 3 and 4 isoforms.

To confirm that the zebrafish clones are orthologs of mammalian complexins 3 and 4, we analyzed their phylogenetic and syntenic relationships. The aligned amino acid sequences of zebrafish, human, and mouse complexin 3 and 4 orthologs were used to construct a phylogenetic tree (Figure 3-1B). While two zebrafish orthologs cluster with mammalian complexin 3, three zebrafish orthologs resemble mammalian complexin 4. The percent identity between the zebrafish complexin 3a protein and either the mouse or human complexin 3 is 63%, while the percent identity between zebrafish complexin 3b and either mouse or human complexin 3 is 67-68%. In addition to sequence identity, zebrafish and mammalian complexin 3 proteins each contain a PAZ domain, which binds to nucleic acids (Lingel et al., 2003; Song et al., 2003; Yan et al., 2003). Zebrafish complexins 4a and 4b share more identity with mammalian complexin 4 (66-73%) than complexin 3 (53-57%). Zebrafish complexin 4c is the most divergent member of this subfamily, sharing 50% identity with either mouse or human complexin 3 and 57% identity

A

```
                5         15        25        35        45
zf cplx 3a  MAFMLKHMIG GQLKDLTGGL ---EEKPEGE -KTEAAAKGM TQEEFEQYQQ
zf cplx 3b  MAFMVKHVVG GHLKNLTGGL T--EEKPEGE -KSEAAAKGM TQEEFEQYQQ
zf cplx 4a  MAFLIKSMVG NPLKGMGLGG G-DEKAEEET PKDPAAAAGM TREEYEEYQK
zf cplx 4b  ---------- ---------- ---------- ----MSHDGM SREEYEEYQK
zf cplx 4c  MAFLLQQMLG DKLKNMT--G GNSEEDEDGG GKETAASKGM SREEFEEYQK
hu cplx 3   MAFMVKTMVG GQLKNLTGSL GGGEDKGDGD -KSAAEAQGM SREEYEEYQK
hu cplx 4   MAFLMKSMIS NQVKNLGFGG GSEENKEEGG ASDPAAAQGM TREEYEEYQK
mo cplx 3   MAFMVKSMVG GQLKNLTGSL GGGEDKGDGD -KSAAEAQGM SREEYEEYQK
mo cplx 4   MAFFVKNMIS NQVKNLGFGG GSEEKKEEGG TSDPAAAKGM TREEYEEYQK

               55        65        75        85        95
zf cplx 3a  QLAEEKLERD ANFAQKKAER ATVRSHFREK YRLPKSELDD TQIQAAADDV
zf cplx 3b  QLEEEKEERD ANFAQKKAER ATVRSHFRDK YRLPKNEVDD TQIQAARDDV
zf cplx 4a  QLVEEKMERD ADFLHKKAER ATLRVCLREK YRLPKSEQDE NMLQMAGDDV
zf cplx 4b  QMVEEKMERD AEFATKKAER ACLRTCLREK YRIPKSEQDE IMLQQAGDDI
zf cplx 4c  QLIEEKITRD KEFATKKAER ANLRVLLRDK YRLPQSAQDD ATVQMAGDDL
hu cplx 3   QLVEEKMERD AQFTQRKAER ATLRSHFRDK YRLPKNETDE SQIQMAGGDV
hu cplx 4   QMIEEKMERD AAFTQKKAER ACLRVHLREK YRLPKSEMDE NQIQMAGDDV
mo cplx 3   QLVEEKMERD AQFTQRKAER ATLRSHFRDK YRLPKNETDE SQIQLAGGDV
mo cplx 4   QMIEEKMERD AAFTQKKAER ACLRVHLRDK YRLPKSEMDE TQIQLAGDDV

              105       115       125       135       145
zf cplx 3a  ELPTELAKMI AEDNQEEEHK QSVLGQITNI QNVDMDQLKE KAQSTLEDLK
zf cplx 3b  ELPTELAKMI AQDNQEEEQK QSVLGQLTNI QNVDMGHLKD KAQATLEDLK
zf cplx 4a  DVPEELLKMV DEDATEEEEK DSIMGQIQNL QNMDMDQIKE KASATLTEMK
zf cplx 4b  DVPEELVKMV DGEAPQEEEN PSIMAQMQNL QNMDVGQLKE KAQATLVEMK
zf cplx 4c  DIPEELAKMV DEEEEQEELN DSFLGKLQNM D-VDFDSIKA KAQSTMTEVK
hu cplx 3   ELPRELAKMI EEDTEEEEEK ASVLGQLASL PGLNLGSLKD KAQATLGDLK
hu cplx 4   DLPEDLRKMV DEDQEEEEDK DSILGQIQNL QNMDLDTIKE KAQATFTEIK
mo cplx 3   ELPRELAKMI EEDTEEEEDK ASVLGQLASL PGLDLSSLKD KAQTTLGDLK
mo cplx 4   DLPEDLRKMV DEDQDEEEEK DSILGQLQNL QNMDLDTIKE KAQATFTEIK

              155
zf cplx 3a  QTAE-KCDVM
zf cplx 3b  NSAE-KCCVM
zf cplx 4a  SKAEEKCSVM
zf cplx 4b  SKAEEKCTVM
zf cplx 4c  QAAEEKCVLM
hu cplx 3   QSAE-KCHVM
hu cplx 4   QTAEQKCSVM
mo cplx 3   QSAE-KCHIM
mo cplx 4   QSAEQKCSVM
```

B

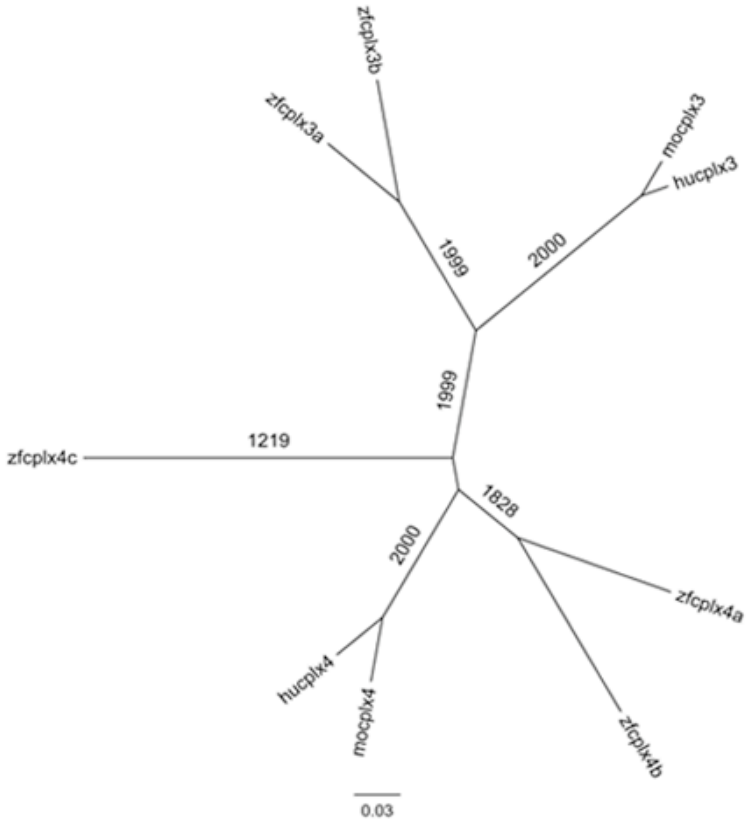

Figure 3-1. The zebrafish genome contains two complexin 3 orthologs and three complexin 4 orthologs. A. The deduced amino acid sequences of mouse (mo), human (hu), and zebrafish (zf) complexins (cplx) 3 and 4 are aligned with ClustalW. The shaded regions highlight evolutionarily conserved amino acids. Complexins 3 and 4 are highly homologous to each other (50-75% amino acid identity), but not to the complexin 1/2 subfamily (~25%). The Genbank accession numbers are GU174497 for zf cplx 3a, GU174498 for zf cplx 3b, GU174499 for zf cplx 4a, GU174500 for zf cplx 4b, GU174501 for zf cplx 4c, NP_001025176 for hu cplx 3, NP_857637 for hu cplx 4, NP_666335 for mo cplx 3, NP_663468 for mo cplx 4. B. An unrooted phylogram of vertebrate complexin 3 and 4 proteins was constructed with the neighbor joining method, and bootstrap values were calculated from 2000 trials. Branch length is proportional to evolutionary divergence. Zebrafish complexins 3a and 3b segregate closely with mammalian complexin 3, and zebrafish complexins 4a and 4b segregate closely with mammalian complexin 4. A fifth paralog is designated zebrafish complexin 4c given its relatively closer distance to mammalian complexin 4 isoforms. Cplx, complexin; hu, human; mo, mouse; zf, zebrafish. Reproduced from Zanazzi and Matthews (2010) with permission from BioMed Central.

	zf cplx3a	zf cplx3b	zf cplx4a	zf cplx4b
zf cplx3b	85	---	---	---
zf cplx4a	59	55	---	---
zf cplx4b	53	52	76	---
zf cplx4c	53	50	57	59

Table 3-1. Amino acid identities (%) between zebrafish complexin 3 and 4 paralogs. Cplx, complexin; zf, zebrafish.

	hu cplx3	ms cplx3	hu cplx4	ms cplx4
zf cplx3a	63	63	61	61
zf cplx3b	68	67	56	60
zf cplx4a	57	56	73	71
zf cplx4b	56	53	66	66
zf cplx4c	50	50	57	57

Table 3-2. Amino acid identities (%) between complexin 3 and 4 orthologs. Cplx, complexin; hu, human; ms, mouse; zf, zebrafish.

with either mouse or human complexin 4. The five zebrafish orthologs of mammalian complexins 3 and 4 indicate the presence of several *cplx* gene duplication events in the evolutionary history of this teleost.

The gene structure for vertebrate *cplx 3/4* subfamily members appears highly conserved, with three exons separated by two introns (Figure 3-2A). The second exon, which contains the sequence that encodes the putative core helix of the SNARE-binding domain, has an invariant length of 88 nucleotides in all examined *cplx 3/4* orthologs. This strict preservation of exon size throughout evolution underscores an important functional role for this module. Furthermore, these results suggest that *cplx 3* and *cplx 4* resulted from the duplication of a common ancestor. In potential support of this hypothesis, synteny analysis reveals conserved relationships between genes surrounding mammalian *cplx 3* and *cplx 4* and some of their zebrafish orthologs. For example, the *lectin mannose-binding 1 (LMAN1)/ER Golgi intermediate compartment 53-kD (ERGIC-53)* and *retina and anterior neural fold homeobox (RAX)* genes surround *cplx 4* on human and mouse chromosome 18 (Figure 3-2B). Similarly, c*plx 4a* on zebrafish chromosome 21 is surrounded by orthologs of *LMAN1/ERGIC-53 and RAX*. A gene in the *LMAN1/ERGIC-53* family, called *LMAN1L/ERGIC-53L,* and the *CSK tyrosine kinase* are situated 5' to *cplx 3* on human chromosome 15 and mouse chromosome 9. A *CSK* ortholog is present 5' to *cplx 3a* on zebrafish chromosome 25, but an *LMAN1L/ERGIC-53L* ortholog has not yet been detected in the zebrafish genome. The presence of *LMAN1/ERGIC-53* or *LMAN1L/ERGIC-53L* immediately 5' to all examined mammalian *cplx 3/4* genes, as well as zebrafish *cplx 4a*, suggests an ancestral unit composed of an *LMAN/LMAN1-L* family member and a *cplx 3/4*.

Enrichment of complexin 3/4 in visual system ribbon terminals in adult zebrafish

Previous studies have revealed that complexins 3 and 4 are expressed in the adult mammalian retina, primarily in ribbon presynaptic terminals (Reim et al., 2005; Reim et al., 2009). A polyclonal antibody raised against mouse complexin 3 labeled cone photoreceptor and rod bipolar cell terminals, while a polyclonal antibody directed against mouse complexin 4 labeled rod photoreceptor and cone bipolar cell terminals (Reim et al., 2005). We have confirmed the findings of Reim et al. (2005) that the polyclonal antibody directed against mouse complexin 3 labels large cone pedicles in the adult mouse retinal OPL and many terminals of the

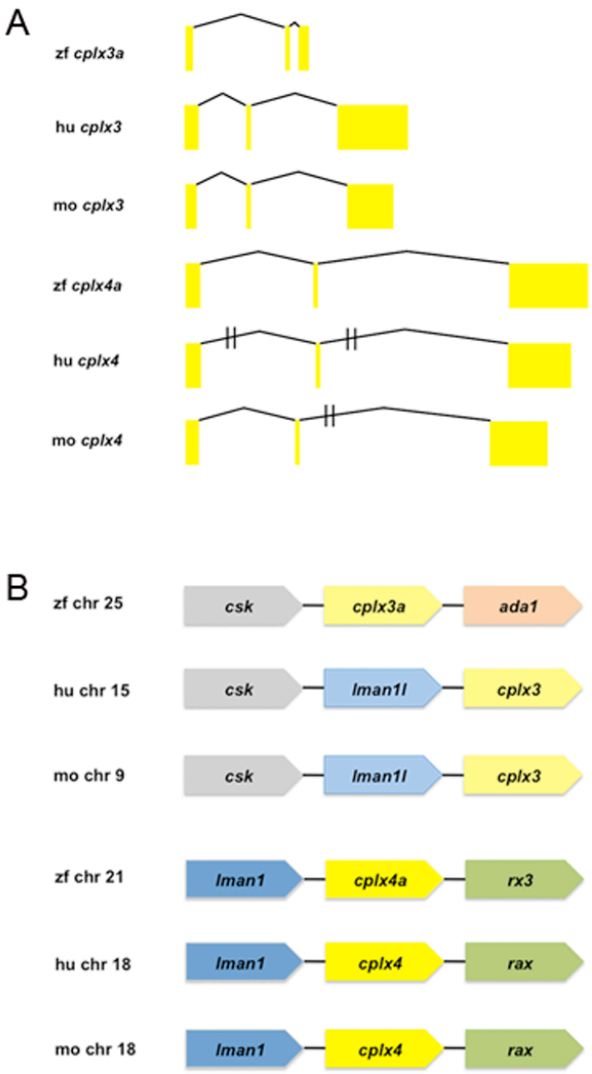

Figure 3-2. Exon-intron organization of orthologous mammalian and zebrafish *cplx 3* and *cplx 4* genes and their syntenic relationships. A. The gene structures for human, mouse, and some zebrafish *cplx 3* and *4* orthologs are shown. Exons are denoted by yellow boxes, while introns are indicated with connecting lines. The lengths of the exons and introns are drawn to scale, except for human and mouse *cplx 4*. *Cplx 3/4* gene structure is highly conserved, with three exons interrupted by two introns. The length of the second exon, which encodes part of the putative SNARE-binding domain, is exactly 88 nucleotides in all species examined. B. Syntenic relationships of zebrafish, human, and mouse *cplx 3/4* orthologs are shown. The genomic architectures of mammalian *cplx 3* orthologs and mammalian *cplx 4* orthologs are conserved. Human and mouse *cplx 3* are preceded by *CSK* and *LMAN1l*, while human and mouse *cplx 4* are bounded by *LMAN1* and *RAX*. Zebrafish *cplx 3a* is preceded by a zebrafish ortholog of *CSK*. Zebrafish *cplx 4a* is bordered by *LMAN* and *RX3*, which is the zebrafish ortholog of mammalian *RAX*. Ada, adenosine deaminase; chr, chromosome; cplx, complexin; CSK, c-src kinase; hu, human; LMAN1, lectin mannose-binding 1; LMAN1l, lectin mannose-binding 1-like; mo, mouse; RAX, retina and anterior neural fold homeobox gene; rx3, retinal homeobox gene 3; zf, zebrafish. Modified from Zanazzi and Matthews (2010), with permission from BioMed Central.

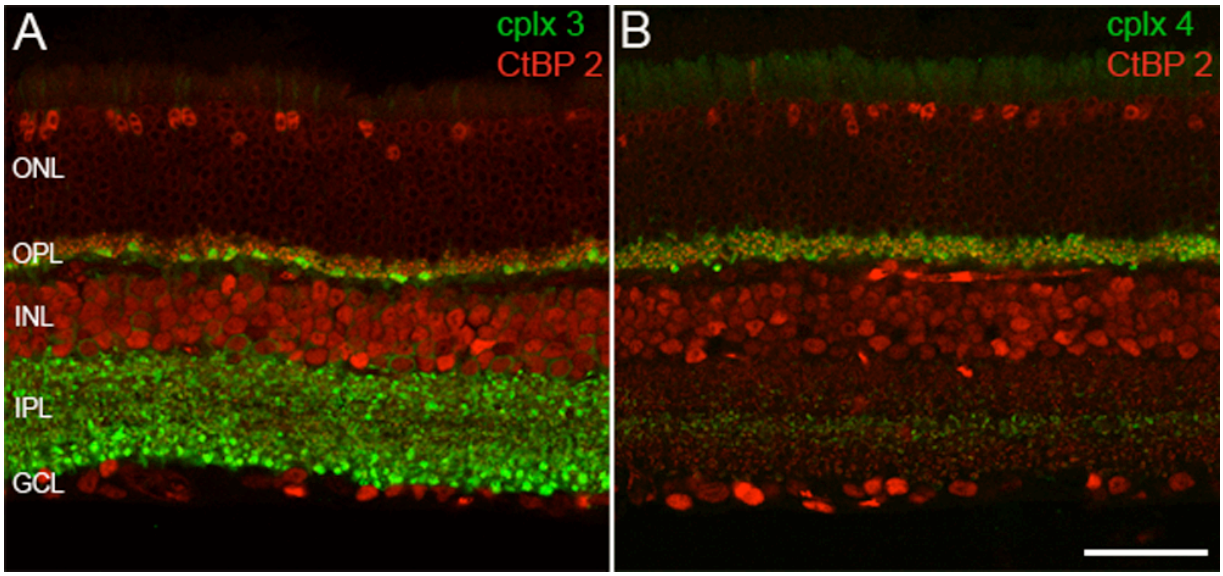

Figure 3-3. Complementary expression of complexin 3 and complexin 4 in ribbon presynaptic terminals of adult mouse retina. Adult mouse retinal sections are labeled with anti-carboxy-terminal binding protein 2 (CtBP 2, red) and either anti-complexin 3 (green, A) or anti-complexin 4 (green, B). Since CtBP2 and RIBEYE are transcribed from the same gene (Schmitz et al., 2000), anti-CtBP2 can be used to label synaptic ribbons. A low-magnification confocal projection through a retinal section stained with anti-complexin 3 and anti-CtBP 2 (A) reveals complexin 3 expression in large, putative cone pedicles of the OPL and throughout most of the IPL, especially in the large, putative bipolar cell terminals in sublamina b. Panel B shows that complexin 4 is found throughout the OPL in small terminals, which may be rod spherules, and in a thin band in the IPL that lacks complexin 3. Scale bar= 50 μm. ONL, outer nuclear layer; OPL, outer plexiform layer; INL, inner nuclear layer; IPL, inner plexiform layer; GCL, ganglion cell layer. Reproduced from Zanazzi and Matthews (2010) with permission from BioMed Central.

IPL (Figure 3-3A). Furthermore, the polyclonal antibody directed against mouse complexin 4 labels small terminals, suggestive of rod spherules, in a wide band in the OPL and small terminals in a thin band of the IPL (Figure 3-3B).

To determine whether these antibodies recognize the zebrafish complexin 3/4 orthologs, we transfected HEK 293T cells (which do not endogenously express complexins 3 or 4, data not shown) with individual myc-tagged, full-length complexins and performed immunocytochemistry with the polyclonal antibodies. In parallel, we visualized expression of the fusion proteins with a monoclonal anti-myc antibody. Figure 3-4 contains micrographs of representative cells transfected with complexin 3a (Figure 3-4A, B), complexin 3b (Figure 3-4C, D), complexin 4a (Figure 3-4E, F), complexin 4b (Figure 3-4G, H), and complexin 4c (Figure 3-4I, J) and stained with the polyclonal antibody raised against mouse complexin 3 (Figure 3-4A, C, E, G, I) and the anti-myc monoclonal (Figure 3-4B, D, F, H, J). These results demonstrate that

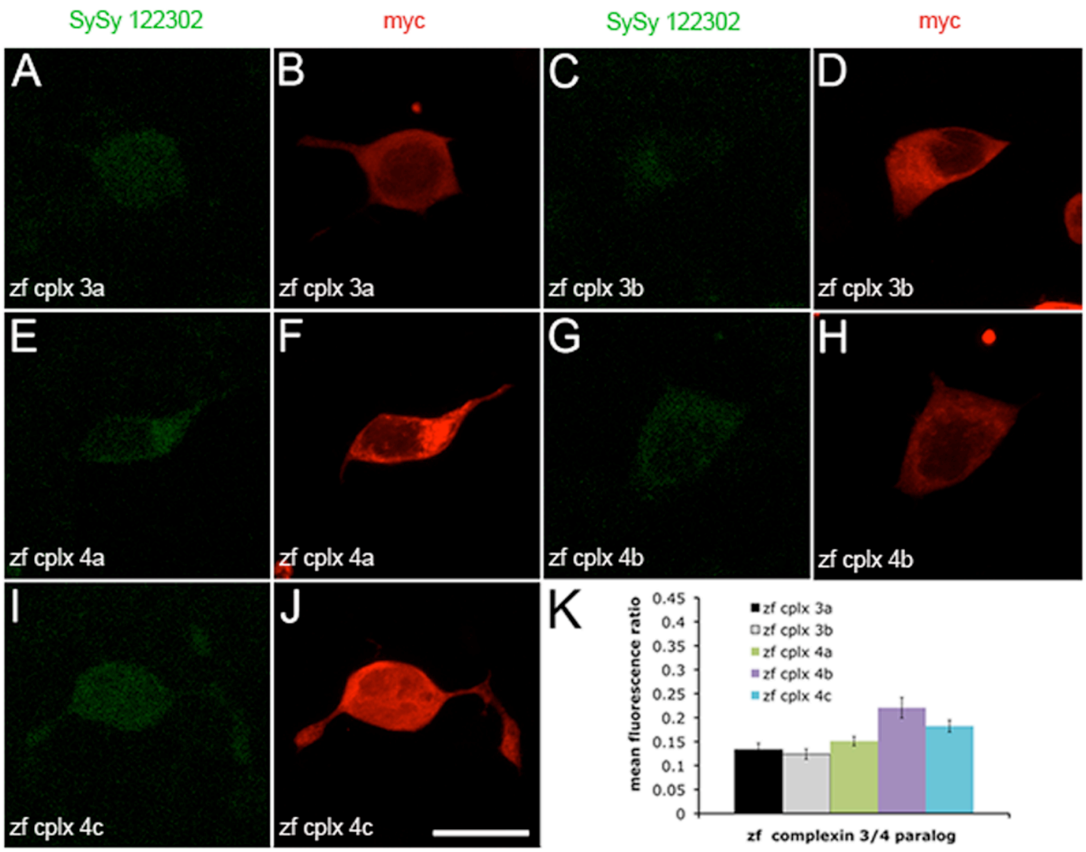

Figure 3-4. Identification of a pan-immunoreactive polyclonal antibody that recognizes zebrafish complexins 3 and 4. HEK 293T cells were transfected with myc-tagged, full-length zebrafish complexin 3a (A and B), 3b (C and D), 4a (E and F), 4b (G and H), or 4c (I and J). After 48 hours, cells were fixed with 4% paraformaldehyde and stained with a rabbit polyclonal antibody directed against mammalian complexin 3 (Synaptic Systems antibody 122302) (A, C, E, G, I) and a mouse monoclonal anti-myc antibody (B, D, F, H, J). This experiment was done in triplicate with a complexin antibody dilution of 1:10,000, and fifty random cells from one experiment were randomly selected for quantitation. The mean green fluorescence intensity for each cell was divided by the mean red fluorescence intensity. Panel K shows the mean fluorescence ratios and SEM for each cell line, revealing that this antibody recognizes all five isoforms. Scale bar= 25 μm. Reproduced from Zanazzi and Matthews (2010) with permission from BioMed Central.

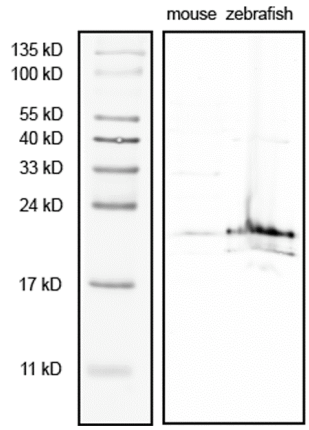

Figure 3-5. The complexin 3/4 antibody predominantly recognizes an approximately 20 kD band on Western Blots. Adult mouse and zebrafish retinae were lysed in sample buffer containing protease inhibitors. 100 μg of mouse extract and 200 μg of zebrafish extract were fractionated by 15% SDS-PAGE, blotted onto nitrocellulose, and probed with the complexin 3/4 polyclonal. A 20 kD band is apparent in both mouse and zebrafish lysates. A minor band of approximately 17 kD can also be observed in the zebrafish extract. Reproduced from Zanazzi and Matthews (2010) with permission from BioMed Central.

this polyclonal antibody recognizes all five zebrafish orthologs at a dilution of 1:10,000 (the dilution used in Reim et al. (2005) to stain mouse retina), and are quantitated in Figure 3-4K. HEK 293T cells transfected with the expression vector did not exhibit any immunoreactivity when incubated with the complexin polyclonal antibody (data not shown). This antibody detects predominantly a 20 kD band on Western Blots of adult mouse and zebrafish retina, indicating that the complexin antibody recognizes proteins of the predicted molecular weight (Figure 3-5).

The pan-complexin 3/4 antibody was then used to examine the expression of this subfamily in the adult zebrafish nervous system. As in adult mammals (Reim et al., 2005), complexin 3/4 is most highly expressed in the retina in adult zebrafish (Figure 3-6). Striking complexin 3/4 immunoreactivity (green) can be observed throughout the retinal OPL and IPL, but not in the outer nuclear layer (ONL), inner nuclear layer (INL), or ganglion cell layer (GCL) (Figure 3-6). In the OPL, complexin 3/4 co-localizes with a marker of double cone photoreceptors, called zpr 1/FRet 43 (Larison and Bremiller, 1990; Yazulla and Studholme, 2001), in their terminals, but is not restricted to these terminals (data not shown). In the IPL, complexin 3/4 appears in both sublamina a and sublamina b, overlapping with protein kinase C (red) in ON bipolar cell terminals (Negishi et al., 1988) (Figure 3-6). Besides the retina, complexin 3/4 is most highly expressed in the pineal complex in the adult zebrafish nervous

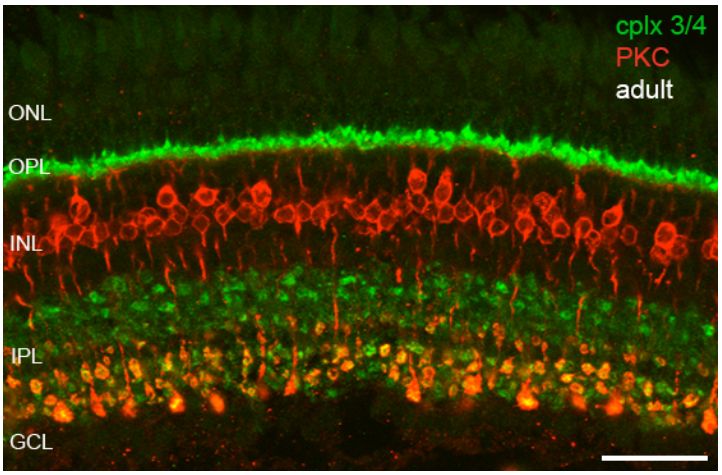

Figure 3-6. Enrichment of complexin 3/4 in adult zebrafish retinal photoreceptor and bipolar cell terminals. Adult zebrafish sections were stained with anti-complexin 3/4 (green) and anti-protein kinase C (PKC, red) to label ON bipolar cells in the retina. This confocal micrograph shows that complexin 3/4 localizes to the plexiform layers, but not the somatic layers, of the adult retina. Complexin 3/4 is found in the terminals of several types of photoreceptors and bipolar cells. Overlap of complexin 3/4 with PKC in the distal IPL confirms their presence in ON bipolar cell terminals. ONL, outer nuclear layer; OPL, outer plexiform layer; INL, inner nuclear layer; IPL, inner plexiform layer; GCL, ganglion cell layer. Scale bar= 30 μm.

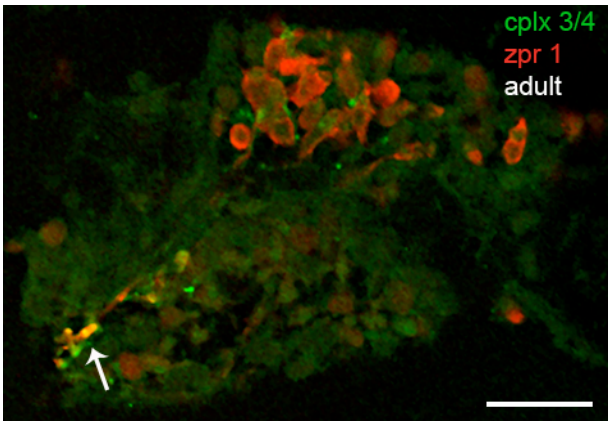

Figure 3-7. Complexin 3/4 is also enriched in photoreceptor processes and terminals of the adult zebrafish pineal organ. Coronal sections of adult zebrafish were stained with the anti-complexin 3/4 antibody (green) and anti-zpr 1/FRet 43 (red). Besides the retina, the pineal organ has the most complexin 3/4 immunoreactivity, which sometimes can be observed in double cone photoreceptor processes and terminals (arrow). Dorsal is toward the top of this confocal micrograph. Scale bar= 25 μm.

system. Complexin 3/4 concentrates in zpr 1/FRet 43-positive processes and terminals at the ventrolateral border of the pineal organ (arrow, Figure 3-7). Taken together, these results indicate that complexin 3/4 delineates many ribbon-containing sensory neurons in the adult zebrafish visual system.

Complexin 3/4 immunoreactivity in lateral line hair cells in adult zebrafish

To determine whether members of the complexin 3/4 subfamily are also expressed in sensory hair cells, we compared the distribution of complexin 3/4 immunoreactivity with that of fluorophore-tagged phalloidin, which labels actin-rich stereociliary bundles. Dozens of neuromasts decorate the outer surface of adult zebrafish. Figure 3-8 shows a cranial neuromast oriented such that the apical surface is toward the top and the basal surface is toward the bottom of the image. Surprisingly, complexin 3/4 immunoreactivity (red, arrows) is apparent among the hair bundles on the apical surface (bright green). The basal cytoplasm exhibits very weak complexin 3/4 immunoreactivity (arrowheads). Lack of complexin at the zebrafish hair cell ribbon synapse is consistent with Strenzke et al. (2009), who did not detect complexin at rodent hair cell synapses. However, the localization of complexin 3/4 among hair cell stereocilia is a novel finding. To determine the complexin isoform(s) in hair cells and visual system ribbon-containing neurons, we performed immunocytochemistry with another polyclonal antibody (detailed below) and in situ hybridization with paralog-specific riboprobes (see Chapter 4).

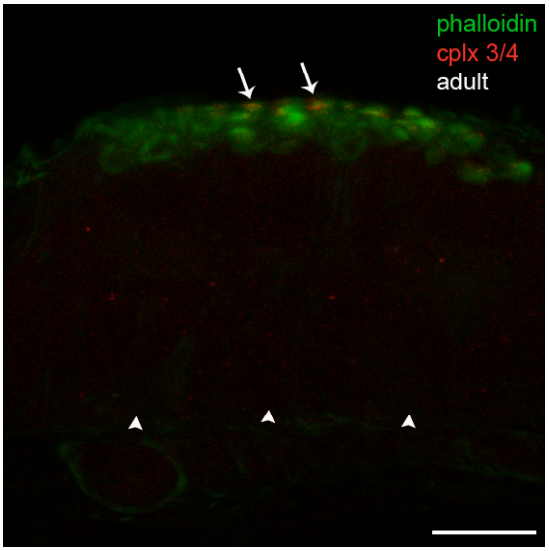

Figure 3-8. Complexin 3/4 localizes to stereocilia but not presynaptic terminals in adult zebrafish hair cells. Coronal zebrafish sections were labeled with anti-complexin 3/4 (red) and phalloidin Alexa 488 (green). This confocal micrograph shows a superficial cranial neuromast. Arrows point to prominent complexin 3/4 immunoreactivity, interspersed among stereocilia, on the apical surfaces of hair cells. Arrowheads demarcate the basal surface of the neuromast, which lacks complexins. Scale bar= 10 μm.

Complexin 4a specifically marks visual system ribbon presynaptic terminals

To determine the immunoreactivity profile for the polyclonal antibody directed against mouse complexin 4 (Reim et al., 2005), we performed the immunofluorescence assay with the transfected HEK 293T cells that express individual complexin 3/4 isoforms. As can be seen in Figure 3-9, the complexin 4 polyclonal antibody (when used at a dilution of 1:75,000) preferentially recognizes zebrafish complexin 4a. Panels B, D, F, H, and J show representative HEK 293T cells transfected with myc-tagged, full-length complexins 3a, 3b, 4a, 4b, and 4c, respectively, and labeled with the anti-myc monoclonal antibody. Panels A, C, E, G, and I contain the same cells incubated with the complexin 4 polyclonal antibody. The myc-tagged complexin 4a cell line (Figure 3-9E, F) exhibited strong immunoreactivity with the complexin 4 antibody (Figure 3-9E). These results are quantitated in panel K and demonstrate that the polyclonal antibody directed against mouse complexin 4 is relatively selective for complexin 4a in zebrafish.

Staining of adult zebrafish sections with the complexin 4a antibody and anti-zpr 1/FRet 43 reveals abundant expression of complexin 4a in the retinal plexiform layers and in the pineal organ (Figure 3-10A). Complexin 4a appears to be primarily restricted to the presynaptic terminals of retinal double cone photoreceptors in the OPL (Figure 3-10B). In the retinal IPL, complexin 4a is detectable in sublamina a and in PKC-positive presynaptic terminals in sublamina b (Figure 3-10C). Higher magnification of the large MB1 bipolar cell terminals reveals that complexin 4a is primarily membrane-associated in these terminals (Figure 3-10D).

We also examined the adult zebrafish pineal organ and cranial neuromasts to begin to pinpoint the complexin 3/4 isoforms expressed by these organs. As shown in Figure 3-11, complexin 4a is abundantly expressed in pineal neuropil. On the other hand, complexin 4a is not expressed in neuromast hair cells (Figure 3-12). The latter result suggests that one or more of the remaining complexin 3/4 paralogs is expressed among hair cell stereocilia.

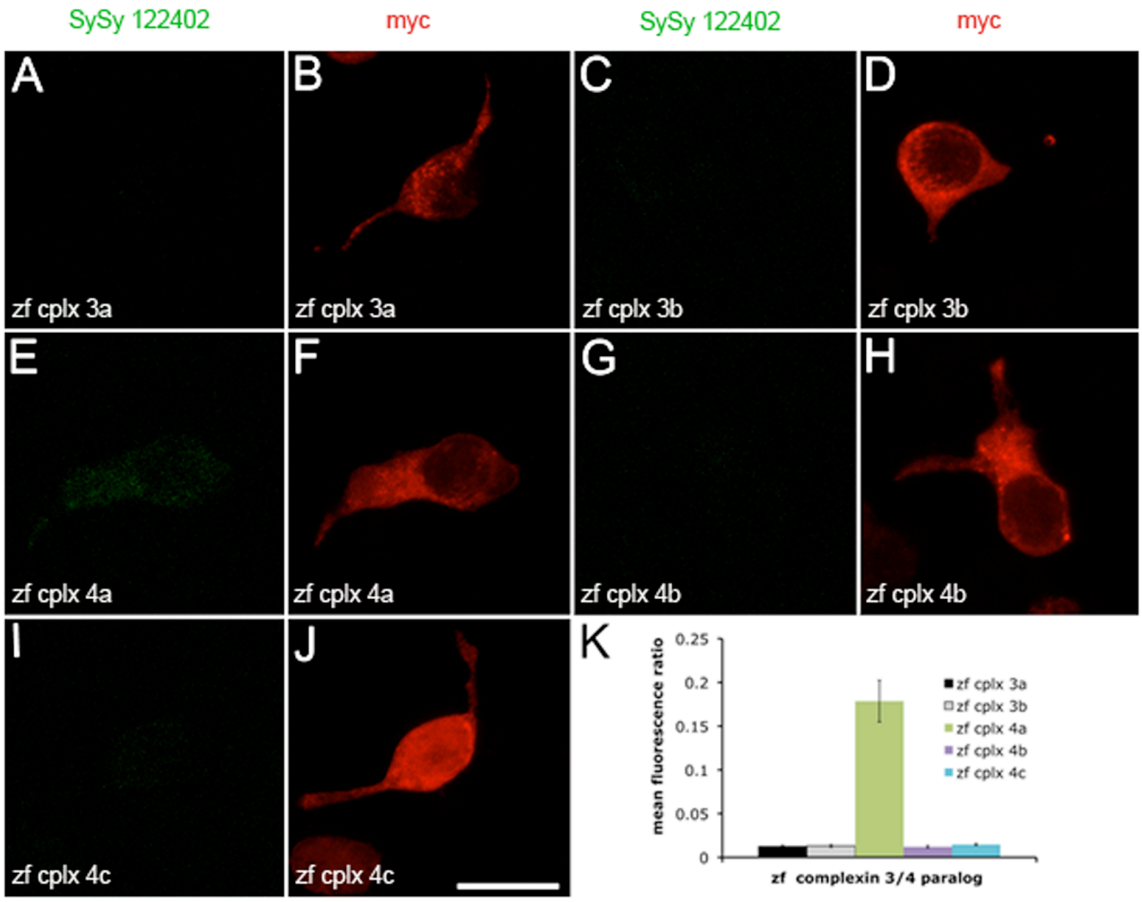

Figure 3-9. Identification of a polyclonal antibody that preferentially recognizes zebrafish complexin 4a. HEK 293T cells were transfected with myc-tagged, full-length zebrafish complexin 3a (A and B), 3b (C and D), 4a (E and F), 4b (G and H), or 4c (I and J). These transiently transfected cells were stained with the mouse monoclonal anti-myc antibody (B, D, F, H, J) and a rabbit polyclonal antibody directed against mammalian complexin 4 (A, C, E, G, I). Panels E and F show complexin and myc immunoreactivity, respectively, in a representative cell transfected with zf cplx4a-myc. This experiment was done in triplicate with a complexin antibody dilution of 1:10,000, and fifty random cells from one experiment were randomly selected for quantitation. The mean green fluorescence intensity for each cell was divided by the mean red fluorescence intensity. Panel K shows that this antibody preferentially recognizes zebrafish complexin 4a (unpaired Student's t- test, $p<.0001$). Scale bar= 25 μm. Reproduced from Zanazzi and Matthews (2010) with permission from BioMed Central.

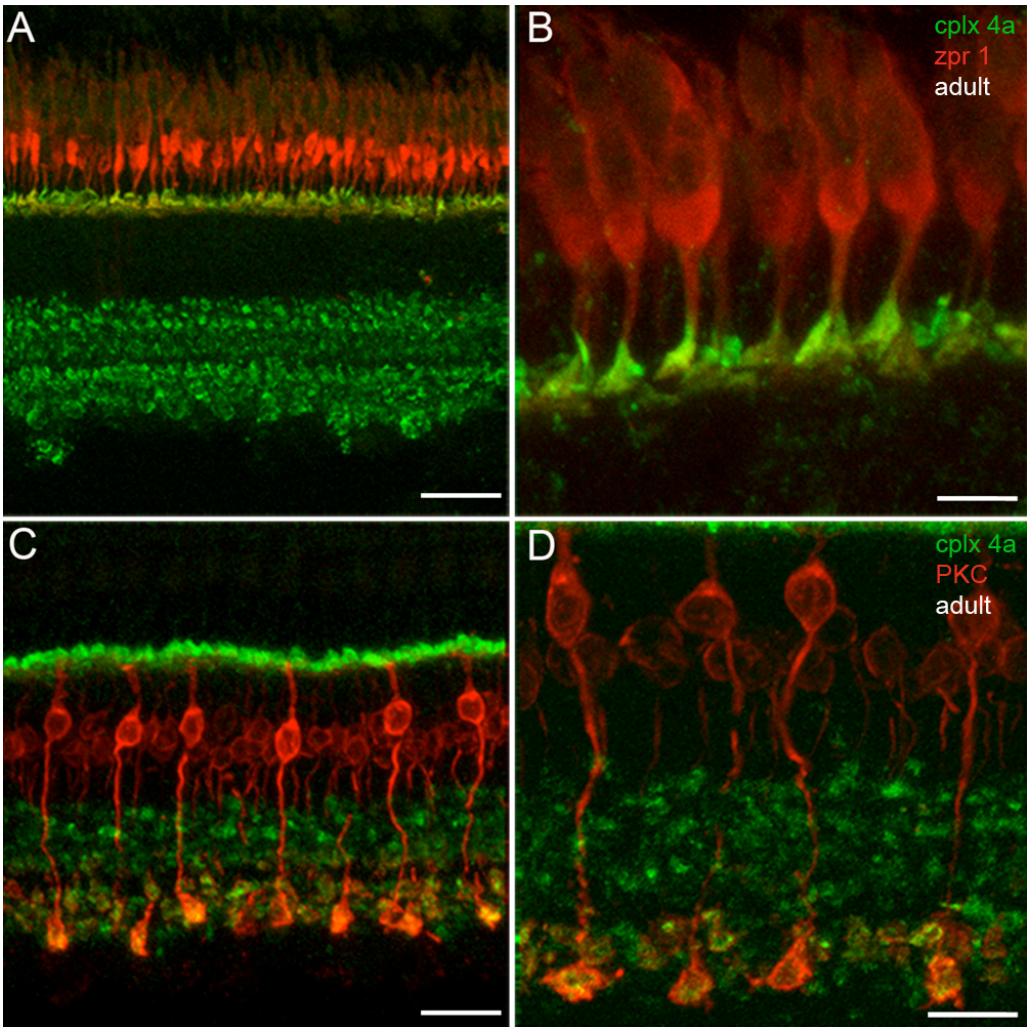

Figure 3-10. Complexin 4a is a predominant isoform in retinal bipolar cell and double cone photoreceptor terminals. A. A confocal projection of a light-adapted adult zebrafish retinal section stained in green with anti-complexin 4a (1:75,000) and in red with anti-zpr 1/FRet 43. B. A higher magnification image of the double cone photoreceptors shows complexin 4a restricted primarily to their terminals. C. A confocal projection of another retinal section stained in red with anti-PKC and in green anti-complexin 4a. The yellow in panels C and D show that there is focal overlap in the bipolar cell terminal.

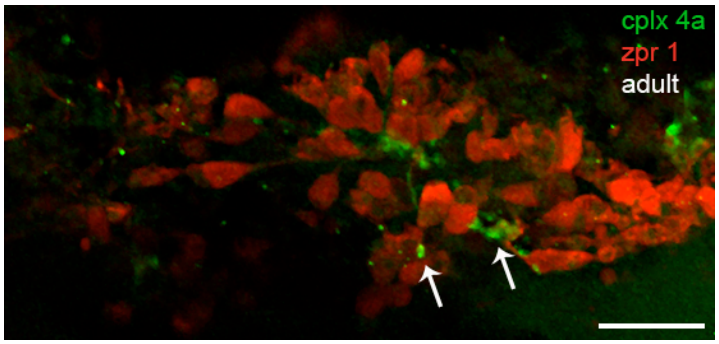

Figure 3-11. Complexin 4a expression in the adult zebrafish pineal. Confocal micrograph of a coronal section through much of the adult zebrafish pineal organ labeled with anti-zpr 1/FRet 43 (red) and anti-complexin 4a (green). Note the presence of complexin 4a in processes and terminals (arrows) that are zpr 1/FRet 43-negative. Scale bar= 25 μm.

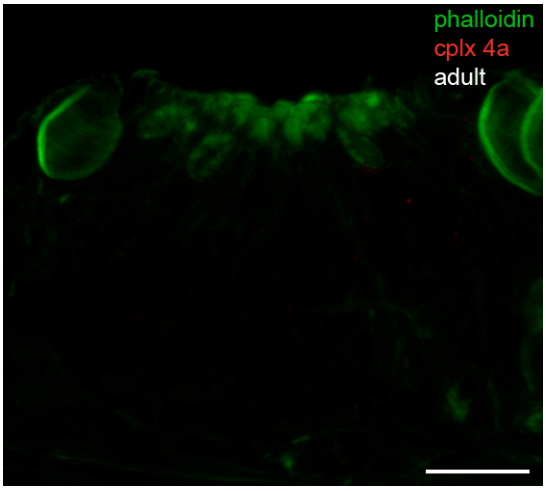

Figure 3-12. Adult zebrafish neuromasts lack complexin 4a. This confocal micrograph shows a coronal section through an adult zebrafish cranial neuromast labeled with phalloidin (green) and anti-complexin 4a (red). Complexin 4a is not expressed in either the apical or basolateral domain of adult neuromast hair cells. Scale bar= 10 μm.

Discussion

In this study, we isolated five zebrafish orthologs in the complexin 3/4 subfamily with several evolutionarily conserved features, and examined their expression with polyclonal antibodies that we and other investigators (Reim et al., 2005) have characterized. cDNA cloning, phylogenetic and syntenic analyses defined a new subfamily of SNARE complex regulators composed of complexin 3 and complexin 4. Examination of complexin 3/4 expression in the adult zebrafish nervous system reveals that members of this subfamily are enriched in many ribbon-containing sensory neurons. As in rodents, complexin 3/4 localizes to zebrafish retinal photoreceptor and bipolar cell presynaptic terminals. We have also extended previous studies by identifying complexin 3/4 in zebrafish pineal photoreceptor terminals. Zebrafish photoreceptors

lack appreciable complexin 3/4 immunoreactivity in their outer segments, including the periciliary ridge. Furthermore, we confirm a recent report showing that adult rodent hair cells lack complexin 3 and complexin 4. While adult zebrafish hair cell terminals also lack complexin 3/4, one or more members of this subfamily may cluster among zebrafish hair cell apical stereocilia. Finally, we propose that complexin 4a is a major isoform in zebrafish visual system ribbbon terminals. Taken together, these findings suggest that members of the complexin 3/4 subfamily are differentially targeted and may have multiple roles in ribbon-containing sensory neurons, which will be discussed further in Chapters 4-7 of this dissertation.

Characterization of zebrafish orthologs defines the complexin 3/4 subfamily in vertebrates

Many mammalian genes have two zebrafish orthologs due to an apparent genome duplication event in ray-finned fish (Amores et al., 1998; Postlethwait et al., 1998). For example, the mammalian SNAP-25 gene has two orthologs in zebrafish (Risinger et al., 1998). Phylogenetic analysis of the complexin 3/4 subfamily reveals the presence of two complexin 3 orthologs and three complexin 4 orthologs in zebrafish. While zebrafish complexins 3a and 3b share 85% amino acid identity, zebrafish complexins 4a and 4b share 76% amino acid identity. Since the fifth zebrafish ortholog has higher amino acid identity with zebrafish complexin 4 paralogs (57-59%) compared with zebrafish complexin 3 paralogs (50-53%), we have named this divergent isoform complexin 4c. Potential medaka (ENSORLP00000022544) and xenopus (ENSXETP00000014005) orthologs with high homology to zebrafish complexin 4c are located in the ENSEMBL database, which provides evidence for several *cplx* gene duplication events in the evolutionary history of teleosts and amphibians.

Vertebrate complexins 3 and 4 exhibit several conserved proteomic and genomic features that differentiate this subfamily from complexins 1 and 2. For example, a motif that defines vertebrate complexins 3 and 4 is the carboxy-terminal CAAX moiety (where C=cysteine, A=aliphatic, X=serine, threonine, or cysteine), which can undergo post-translational modifications that lead to the addition of a prenyl anchor and reversible attachment to membranes (Reim et al., 2005). Targeting to membranes has important functional consequences for complexin 4 (Reim et al., 2005), and may also be accomplished through myristoylation since nearly all vertebrate complexins 3 and 4 (but not vertebrate complexins 1 and 2) have multiple myristoylation motifs (data not shown).

All vertebrate full-length members of the complexin 3/4 subfamily are encoded by three exons, including an invariant exon containing 88 nucleotides that encodes part of the putative core alpha helix that binds to an assembled SNARE complex (Reim et al., 2005). Highest amino acid homology between vertebrate complexins occurs within this core alpha helix. Complexin 1 binding is thought to stabilize the SNARE complex (Chen et al., 2002) in a fusion-ready state, preventing completion of fusion via an accessory alpha-helix (Xue et al., 2007; Giraudo et al., 2009; Maximov et al., 2009) until calcium enters the presynaptic terminal and binds to synaptotagmin 1 (Giraudo et al., 2006; Schaub et al., 2006; Tang et al., 2006). Complexin 3/4 subfamily members share substantial amino acid identity in the accessory alpha-helix (56%-100% when comparing mouse, human and zebrafish orthologs), but this sequence is not conserved with complexin 1/2 subfamily members (~25%). The amino terminus of complexin 1 has been shown to be necessary for exocytosis (Xue et al., 2007), but this region also diverges with complexin 3/4 subfamily members (~25% amino acid identity). The functional consequences of these differences remain to be determined.

Members of the complexin 3/4 subfamily are enriched in many ribbon-containing sensory neurons

Few proteins involved in the synaptic vesicle cycle are known to be expressed selectively in ribbon presynaptic terminals (reviewed in Schmitz, 2009; Zanazzi and Matthews, 2009). Therefore, the identification of ribbon-specific isoforms of these synaptic regulators is of special interest. We have extended a previous study describing expression of complexin 3/4 in retinal ribbon terminals (Reim et al., 2005) by showing that members of this subfamily are also enriched in the ribbon terminals of the photosensitive zebrafish pineal organ. It will be of interest to determine whether complexin 3 and complexin 4 are found in mammalian pinealocytes, which contain other components of the ribbon exocytotic machinery (Spiwoks-Becker et al., 2008; Zanazzi and Matthews, 2009) even though these cells are not directly photosensitive in the adult (for review, see Vollrath, 1981). In potential support, a survey of mammalian EST databases reveals the presence of complexin 3 (CD741334.1) and complexin 4 (CB748805.1 and CB801796.1) ESTs. Taken together, these results indicate that complexin 3/4 isoforms, such as complexin 4a in zebrafish, are markers for several types of visual system ribbon terminals.

While complexin 3/4 localizes to the axons and presynaptic terminals of ribbon-

containing sensory neurons in the zebrafish visual system, members of this subfamily are absent from the corresponding basolateral domains of zebrafish hair cells. Rather, complexin 3/4 immunoreactivity appears on their apical surfaces. The area around the hair cell cuticular plate contains large quantities of vesicles that traffic between the cytoplasm and plasma membrane (Kachar et al., 1997). Co-localization with the binding of phalloidin to F-actin above the cuticular plate suggests that complexin 3/4 is a component of stereocilia rather than vesicles near the apical plasma membrane. Immunoelectron microscopy will be necessary to determine the precise localization of zebrafish complexin 3/4 in the stereocilia. During the course of this study, Strenzke et al. (2009) utilized RT-PCR and immunocytochemistry with the two anti-complexin rabbit polyclonal antibodies to conclude that complexin 3/4 is not expressed in rodent inner ear hair cells. Our preliminary experiments confirm that complexin 3 is not expressed in hair cells of the adult mouse utricle (data not shown). Additional experiments are needed to examine the expression of complexin 3/4 in hair cells of the adult zebrafish inner ear since we focused on neuromast hair cells, and to determine the specific complexin isoform(s) expressed in adult hair cells.

Emerging evidence suggests that different ribbon synapses have quite unique properties to support their distinctive tasks (reviewed in Matthews and Fuchs, 2010). This is certainly true for visual system versus octavolateral system ribbon terminals, and our results add another specialization for visual system terminals. Even within a sensory system, different ribbon-containing cell types appear to selectively express different molecules (reviewed in Zanazzi and Matthews, 2009). For example, zebrafish cones, but not rods, express synaptojanin 1 (Holzhausen et al., 2009), which has multiple functions in the synaptic vesicle cycle (reviewed in Zanazzi and Matthews, 2007). Complexin 4a also appears restricted to cone terminals in the OPL (this study). Given that the zebrafish is cone-dominant, especially during early development, it will be important to examine the targeting and functions of this isoform during embryogenesis and in the larval stage. This will be done in the next three chapters.

Chapter 4

Differential targeting of complexins 3 and 4 in ribbon-containing sensory neurons during zebrafish development

Introduction

Over the past half century, substantial progress has been made in elucidating the assembly of the transduction apparatus in both photoreceptors (reviewed in Kennedy and Malicki, 2009) and hair cells (reviewed in Nayak et al., 2007). The developing photoreceptor elaborates, from an inner segment centriole, an apical cilium whose outer tip balloons and invaginates several times to form the outer segment disks (Nilsson, 1964; Olney, 1968). Intense trafficking of proteins such as opsin occurs through the connecting cilium (Defoe and Besharse, 1985) to support the frequent remodelling of the outer segment (Young, 1967). In hair cells, short microvilli on the apical surface begin to surround a centrally located kinocilium, which then migrates to the periphery and induces the elongation of adjacent microvilli (see, for example, Mbiene and Sans, 1986). The microvilli become anchored in the cuticular plate, and proteinaceous links form between the microvilli, which may be transiently expressed during development in mammals (Goodyear et al., 2005). Vesicle trafficking immediately below the cuticular plate may support the stereocilia (Kachar et al., 1997; Safieddine et al., 2002).

Ultrastructural studies of ribbon development in retinal photoreceptors (Meller, 1968; Olney, 1968), hair cells (Sobkowicz et al., 1986), and pinealocytes (King and Dougherty, 1980) suggest that ribbons (floating, spherical, and surrounded by vesicles) are found first in the perinuclear cytoplasm. As development proceeds, ribbons appear to migrate basally in photoreceptor axons toward the presynaptic terminals (Olney, 1968). Ribbon cytomatrix proteins, such as RIBEYE, are found in migrating non-membranous densities, termed precursor spheres (Regus-Leidig et al., 2009; Regus-Leidig et al., 2010), which may correspond to migrating ribbons. In the presynaptic terminal, a ribbon attaches to the plasma membrane via an arciform density (Ladman, 1958) and has enlarged with maturation, likely due to multiple RIBEYE homophilic and heterophilic interactions (Magupalli et al., 2008). Besides ribbons, several groups have examined the accumulation of synaptic vesicle proteins in the developing rodent retina, revealing clustering in the outer plexiform layer (OPL) and inner plexiform layer (IPL) before synapse maturation (Greenlee et al., 1996; Dhingra et al., 1997; Greenlee et al.,

2001; von Kriegstein and Schmitz, 2003). Since the examined synaptic vesicle proteins are found at both conventional and ribbon synapses, the targeting of ribbon terminal-specific synaptic vesicle proteins is poorly understood.

To begin to delineate the targeting of the exocytotic machinery specifically in ribbon-containing neurons, we examined the expression of complexins 3 and 4 in the zebrafish visual and octavolateral systems during the first week of development. Utilizing the polyclonal antibody that recognizes all five zebrafish orthologs, we demonstrate that these proteins are rapidly targeted to presynaptic terminals in the retina and pineal organ concomitantly with RIBEYE b. In embryonic hair cells of the inner ear and lateral line, however, complexin 3/4 immunoreactivity clusters on their apical surfaces, among their stereocilia, rather than along the basolateral plasma membrane with RIBEYE b. While a complexin 4a-specific antibody and riboprobe selectively label visual system ribbon-containing neurons, neuromasts and the inner ear contain complexin 4b. These results provide evidence for the concurrent transport and/or assembly of multiple components of the active zone in developing ribbon terminals. In addition, these results suggest differential targeting and functions of complexin 3/4 members in visual versus octavolateral system ribbon-containing neurons during development.

Results

Complexin 3/4 is expressed in visual system ribbon presynaptic terminals in the zebrafish larvae

The pan-complexin 3/4 antibody was used to examine the expression of this subfamily in the embryonic and larval zebrafish nervous system. Sensory systems develop rapidly in zebrafish such that visual and octavolateral responses can be robustly elicited by five days post-fertilization (dpf) (Brockerhoff et al., 1995; Nicolson et al., 1998). Therefore, 5 dpf larval sections were stained with the pan-complexin 3/4 antibody and the zpr 1/FRet 43 monoclonal antibody. As in adult zebrafish, complexin 3/4 is most highly expressed in the retina in larval zebrafish (Figure 4-1A). Striking complexin 3/4 immunoreactivity can be observed throughout the retinal outer plexiform layer (OPL) and inner plexiform layer (IPL) (Figure 4-1A). Complexin 3/4 co-localizes with zpr 1/FRet 43 in terminals of double cone photoreceptors, but is not restricted to these terminals in the OPL (Figure 4-1B). In addition, some complexin 3/4 immunoreactivity can be observed in photoreceptor outer segments and in the outer nuclear layer

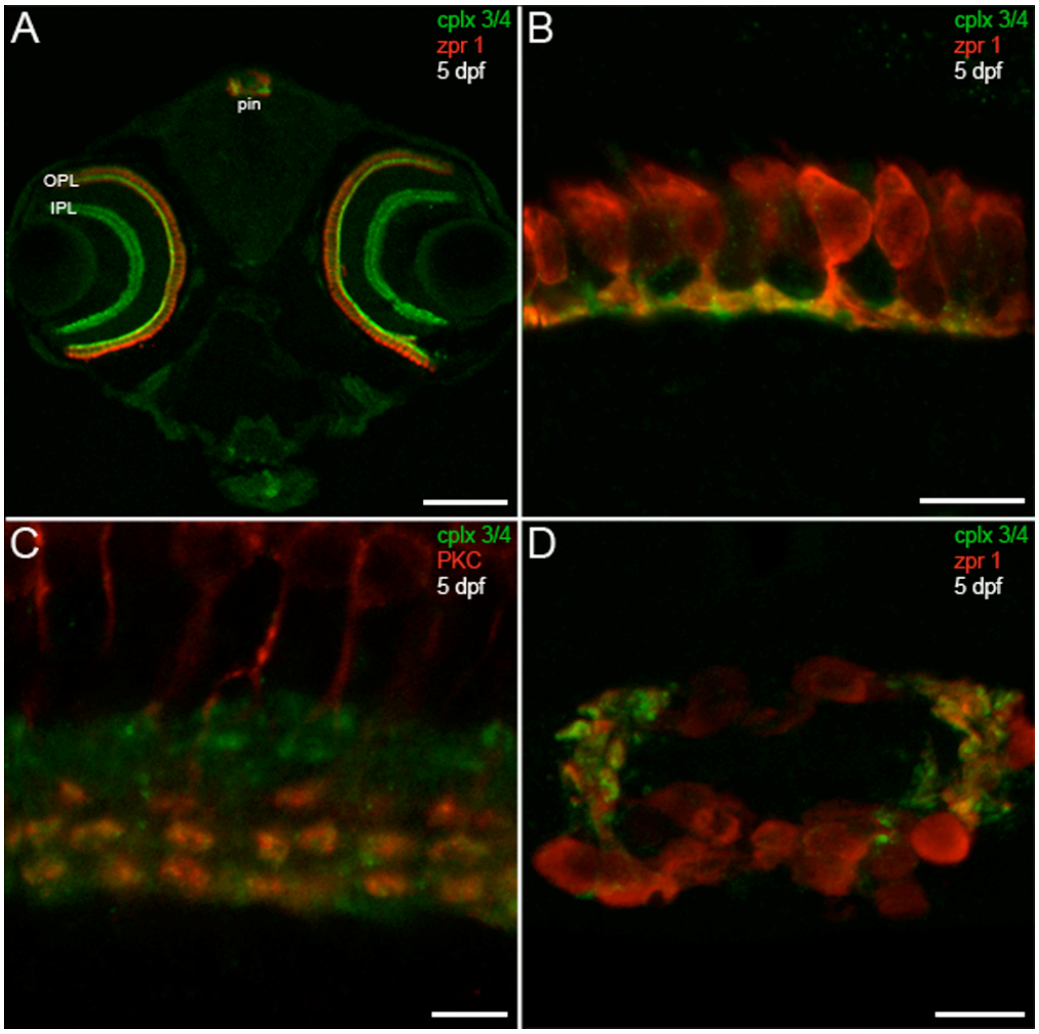

Figure 4-1. Predilection of complexin 3/4 for ribbon presynaptic terminals in the larval zebrafish visual system. A. A confocal projection of a 5-dpf zebrafish transverse section stained with the pan-complexin 3/4 antibody (green) and the zpr 1/FRet 43 antibody (red), which labels double cone photoreceptors, reveals complexin 3/4 immunoreactivity throughout the retinal plexiform layers (OPL, IPL) and in the pineal organ (pin). B. A high-magnification confocal projection of double cone photoreceptors (red) in the retinal OPL labeled with the complexin 3/4 antibody (green) shows that some of the complexin 3/4 immunoreactivity in the larval zebrafish OPL is found in double cone terminals. C. Double-labeling with anti-protein kinase C (red) reveals overlap of complexin 3/4 (green) in ON bipolar cell terminals in the retinal IPL. D. A confocal projection of a transverse section through the pineal organ reveals zpr 1/FRet 43-positive photoreceptors (red) and complexin 3/4 (green) in processes and terminals at the lateral border. Sections incubated with secondary antibodies alone exhibit background immunofluorescence in the retina and pineal (data not shown). Scale bars: 125 μm (A); 10 μm (B, D); 5 μm (C). Reproduced from Zanazzi and Matthews (2010) with permission from BioMed Central.

(Figure 4-1B). In the IPL, complexin 3/4 appears in both sublamina a and sublamina b, overlapping with protein kinase C in ON bipolar cell terminals (Figure 4-1C).

In the larval zebrafish pineal organ, ribbon-containing photoreceptors send short axons ventrolaterally to terminate on projection neurons (Masai et al., 1997; Allwardt and Dowling, 2001). Complexin 3/4 concentrates in zpr 1/FRet 43-positive processes and terminals at the lateral border of the pineal organ (Figure 4-1D). Additional complexin 3/4 immunoreactivity can be observed in zpr 1/FRet 43-negative processes in the pineal neuropil (Figure 4-1D), which is a plexus that contains processes from several types of photoreceptors (reviewed in Ekström and Meissl, 1997). Taken together, these results indicate that complexin 3/4 delineates many ribbon-containing sensory neurons in the larval zebrafish visual system.

Concomitant targeting of complexin 3/4 and RIBEYE b to photoreceptor terminals during zebrafish embryogenesis

To begin to characterize the targeting of the exocytotic machinery to ribbon terminals, we examined the spatiotemporal expression profiles of complexin 3/4 and RIBEYE b relative to zpr 1/FRet 43 during photoreceptor development. In teleosts, photoreceptors differentiate in the pineal organ before differentiating in the retina. In zebrafish, most pineal progenitors exit the cell cycle between 18-20.5 hpf (Cau et al., 2008). Therefore, embryonic zebrafish were fixed at several developmental time points starting at 24 hpf. No complexin 3/4 or zpr 1/FRet 43 immunoreactivity was apparent in the pineal organ at 24 hpf (data not shown). At 29 hpf, small numbers of zpr 1/FRet 43-positive photoreceptors with short axons can be observed (Figure 4-2A, red). Very low levels of complexin 3/4 are found in zpr 1/FRet 43-positive pineal photoreceptors, and the immunoreactivity localizes to the developing neuropil (Figure 4-2A, green, arrows). To examine the targeting of other components of the exocytotic machinery, we utilized a polyclonal antibody directed against RIBEYE b (Obholzer et al., 2008). At 29 hpf, RIBEYE b is also found at very low levels in zpr 1/FRet 43-positive pineal photoreceptor terminals (Figure 4-2B, arrow). By 36 hpf, the neuropil at the lateral border of the pineal has become well-developed, with processes emanating from dorsomedial zpr 1/FRet 43-positive and zpr 1/FRet 43-negative photoreceptor somata. Complexin 3/4 expression has been upregulated in processes and terminals, some of which co-localizes with zpr 1/FRet 43 (Figure 4-2C). RIBEYE b puncta are found in photoreceptor axons and their terminals (Figure 4-2D).

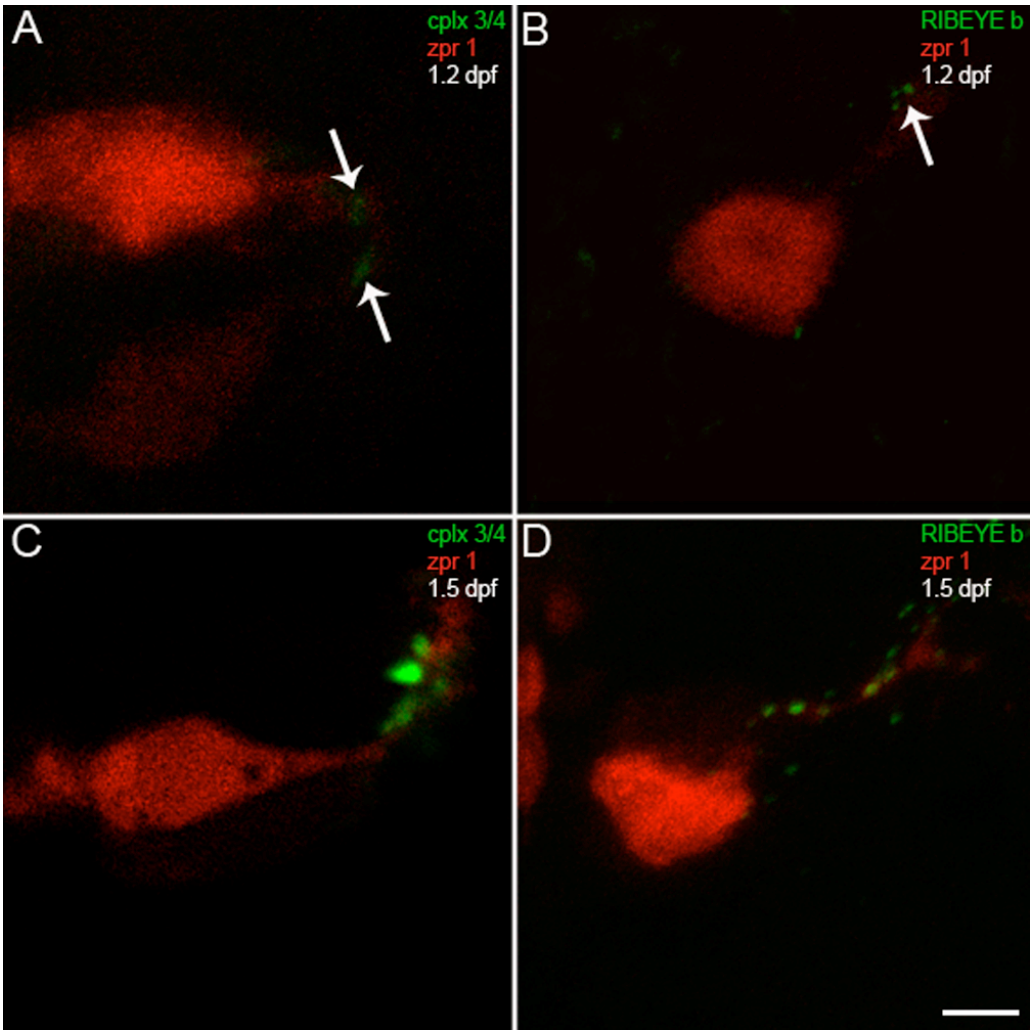

Figure 4-2. Complexin 3/4 concentrates in pineal photoreceptor terminals concomitant with RIBEYE b. A. A high-magnification confocal projection of zpr 1/FRet 43-positive pineal double cone photoreceptors (red) double-stained for complexin 3/4 (green) at 29 hpf shows low levels of complexin in photoreceptor terminals (arrows). Ventral is toward the top and lateral is toward the right. B. A section from a different embryo at 29 hpf double-stained with anti-zpr 1/FRet 43-positive (red) and anti-RIBEYE b (green) shows three small RIBEYE puncta in a pineal photoreceptor terminal (arrow). C. By 36 hpf, complexin 3/4 (green) is highly expressed in neuropil at the lateral border of the pineal organ, in both zpr 1/FRet 43-positive (red) and zpr 1/FRet 43-negative photoreceptor axons and terminals. D. Several RIBEYE b puncta (green) are present in pineal photoreceptor axons and terminals at 36 hpf. Scale bar= 5 μm. Reproduced from Zanazzi and Matthews (2010) with permission from BioMed Central.

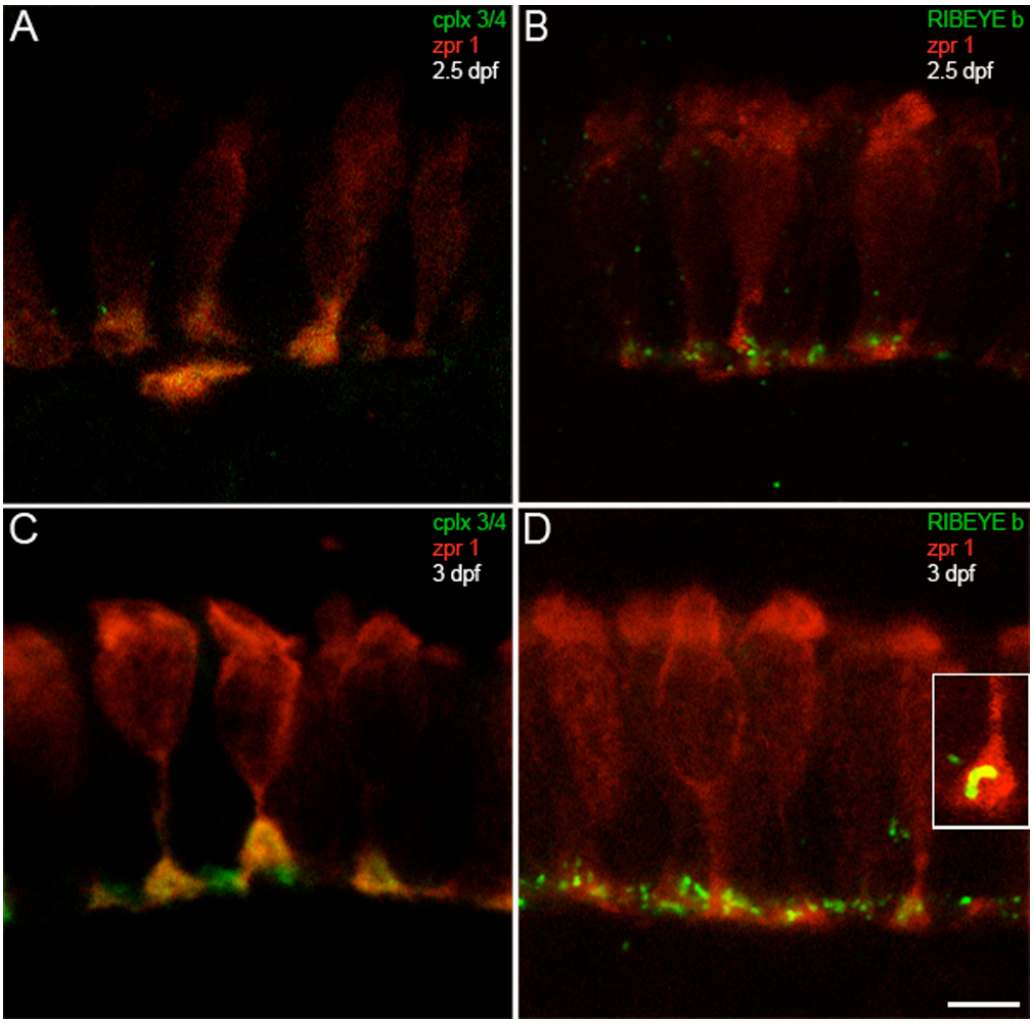

Figure 4-3. Complexin 3/4 concentrates in retinal photoreceptor terminals concomitant with RIBEYE b. A. The zpr 1/FRet 43 monoclonal antibody (red) and the pan-complexin 3/4 polyclonal (green) were also used to localize these complexins in developing retinal photoreceptors. At 60 hpf, retinal photoreceptors are most prominent in the ventronasal patch, where complexin 3/4 immunoreactivity appears in some photoreceptor terminals. B. RIBEYE b (green) has also started to cluster in photoreceptor terminals (red) in the outer plexiform layer at 60 hpf. C. At 72 hpf, complexin 3/4 (red) is highly expressed in zpr 1/FRet 43-positive (red) and zpr 1/FRet 43-negative photoreceptor terminals in the ventronasal patch. D. Pleiomorphic RIBEYE b (green) expression is found at 72 hpf in zpr 1/FRet 43-positive (red) and zpr 1/FRet 43-negative photoreceptor terminals in the ventronasal patch. The inset shows a zpr 1/FRet 43-positive terminal containing curvilinear RIBEYE b immunoreactivity that may correspond to a ribbon. Scale bar= 5 μm. Reproduced from Zanazzi and Matthews (2010) with permission from BioMed Central.

We next examined complexin 3/4 expression in the developing retina. At 48 hpf, zebrafish photoreceptors are exiting the cell cycle (Nawrocki, 1985), and small numbers of zpr 1/FRet 43-positive photoreceptors can be observed in the retinal ventronasal patch at 50 hpf (Raymond et al., 1995). At 48 hpf, we did not observe zpr 1/FRet 43 in the retina (data not shown). By 60 hpf, zpr 1/FRet 43-positive photoreceptors are found in the ventronasal patch, where they express complexin 3/4 (Figure 4-3A) and RIBEYE b (Figure 4-3B) in their terminals. By 3 dpf, complexin 3/4 (Figure 4-3C, green) and RIBEYE b (Figure 4-3D, green) have become concentrated in photoreceptor terminals throughout the retina. In some terminals, RIBEYE b has clustered into curvilinear structures (Figure 4-3D, inset) that most likely correspond to ribbons (tom Dieck et al., 2005). Taken together, these results suggest that complexin 3/4 and RIBEYE b appear concomitantly in retinal and pineal photoreceptors and are rapidly targeted to their axons and terminals.

Complexin 3/4 immunoreactivity on the apical surfaces of inner ear and lateral line hair cells in larval zebrafish

To determine whether members of the complexin 3/4 subfamily are also expressed in larval zebrafish sensory hair cells, we compared the distribution of complexin 3/4 immunoreactivity with that of fluorophore-tagged phalloidin, which labels actin-rich stereociliary bundles. In the larval zebrafish inner ear, striking complexin 3/4 immunoreactivity appears among the stereociliary bundles, but not in the basolateral domains, of macular hair cells (Figure 4-4A, arrowheads). Complexin 3/4 also localizes to stereociliary bundles in hair cells of the anterior, lateral and posterior cristae (data not shown). At higher magnification, it becomes evident that complexin 3/4 immunoreactivity concentrates at the base of the stereociliary bundle (Figure 4-4B). Double-labeling with anti-zn 1, a monoclonal antibody that recognizes a cytoplasmic antigen found in subpopulations of hair cells (Kornblum et al., 1990; Bang et al., 2001), confirms that complexin 3/4 localizes to the apical surface of the hair cell (Figure 4-4C). Substantial accumulation of complexin 3/4 immunoreactivity was also observed on the apical surfaces of hair cells in the neuromasts of the cranial (Figure 4-4D) and trunk lateral lines (data not shown). In summary, these results confirm that members of the complexin 3/4 subfamily are enriched in distinct subcellular domains of many sensory neurons that contain ribbons.

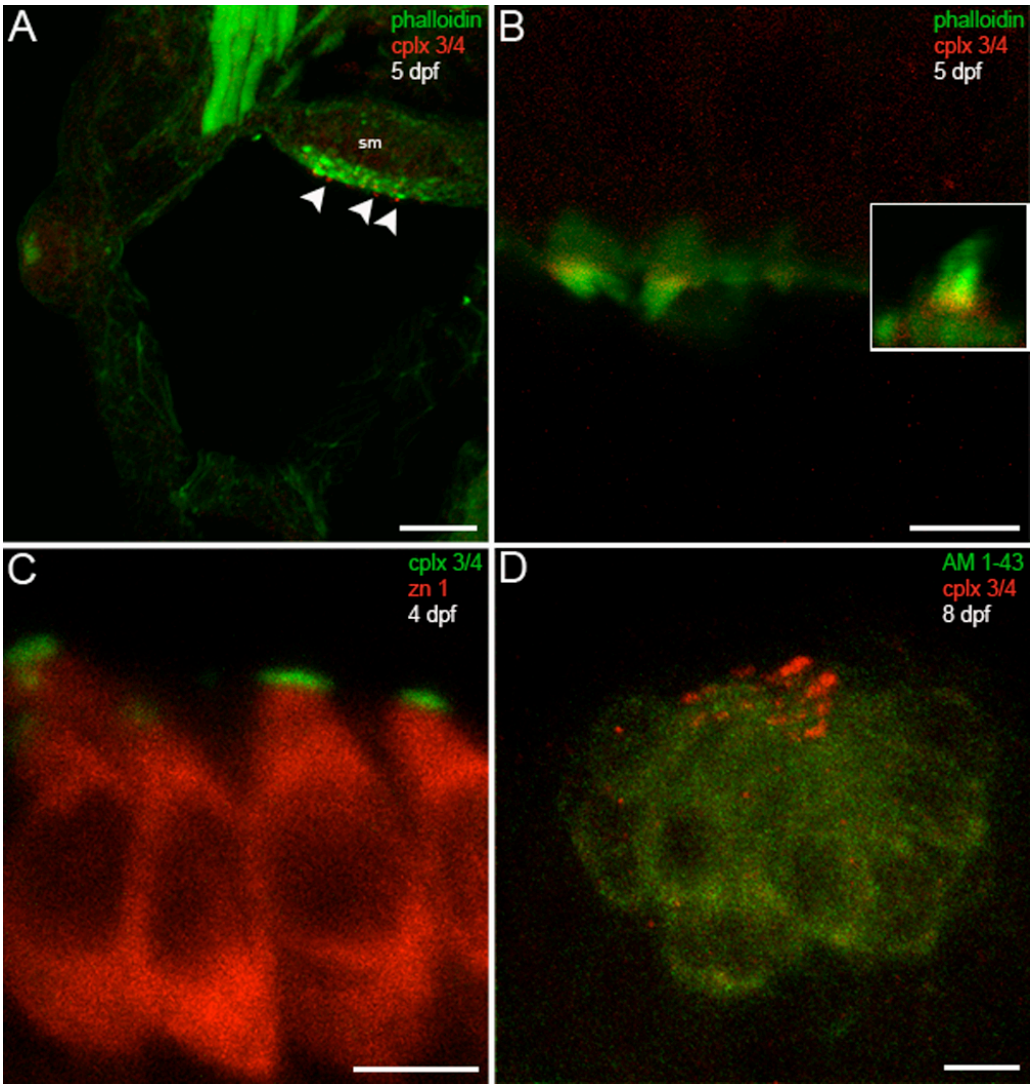

Figure 4-4. Hair cells in the larval zebrafish inner ear and lateral line exhibit complexin 3/4 immunoreactivity on their apical surfaces. A. A confocal projection of a 5 dpf zebrafish transverse section through the otic vesicle reveals complexin 3/4 immunoreactivity (red) on the apical surfaces of inner ear hair cells in the saccular macula (sm) (arrowheads) labeled with phalloidin (green). B. A high-magnification view shows complexin 3/4 immunoreactivity (red) at the base of stereocilia labelled by phalloidin above the actin-rich cuticular plate. The inset contains an enlargement of a hair bundle. C. Complexin 3/4 immunoreactivity (green) directly abuts zn 1 cytoplasmic immunoreactivity (red) on the apical surfaces of inner ear hair cells. D. To examine neuromast hair cells, larval zebrafish were incubated with AM1-43 (green), fixed, sectioned sagittally, and labeled with anti-complexin 3/4 (red). Complexin 3/4 is also present on the apical surfaces of neuromast hair cells. Neuromast and inner ear sections incubated with secondary antibodies alone exhibited background immunofluorescence (data not shown). Scale bars= 25 μm (A), 5 μm (B, C, D). Reproduced from Zanazzi and Matthews (2010) with permission from BioMed Central.

Rapid clustering of complexin 3/4 immunoreactivity on the apical surfaces of inner ear and lateral line hair cells in embryonic zebrafish

Hair cells in the zebrafish inner ear (Haddon and Lewis, 1996; Riley et al., 1997) and lateral lines (Lopez-Schier and Hudspeth, 2006) differentiate rapidly, with formation of stereocilia soon after exit from the cell cycle. The first hair cells to differentiate, called tether cells, exist in two pairs that project stereocilia and kinocilia into the otic vesicle by 24 hpf (Haddon and Lewis, 1996; Riley et al., 1997). We have observed putative tether cells with complexin 3/4 immunoreactivity solely among their stereocilia at 24 hpf (data not shown). At 36 hpf, few hair cells in the anterior and posterior maculae have stereocilia, but those that do typically have complexin 3/4 immunoreactivity primarily on their apical surfaces (Figure 4-5A, red, arrowheads) and RIBEYE b puncta on their basolateral surfaces (Figure 4-5B, red). The latter finding is consistent with a recent report showing RIBEYE b at the base of inner ear hair cells at 27 hpf (Tanimoto et al., 2009). By 48 hpf, several macular hair cells have acquired actin-rich stereocilia with complexin 3/4 (Figure 4-5C, arrowheads) and have upregulated RIBEYE b (Figure 4-5D, red).

In the zebrafish lateral lines, the otic neuromast differentiates first at 34 hpf (Raible and Kruse, 2000). At 36 hpf, phalloidin labels otic neuromast hair cell stereocilia with faint complexin 3/4 immunoreactivity (Figure 4-6A, arrowheads). By this time, RIBEYE b has already concentrated in large puncta at the base, and in smaller cytoplasmic puncta, in a couple of hair cells in the neuromast (Figure 4-6B, red). By 48 hpf, complexin 3/4 (Figure 4-6C, red, arrowheads) and RIBEYE b (Figure 4-6D, red) have been upregulated in more hair cells in the otic neuromast. Ultrastructural evidence of mature ribbons in zebrafish neuromast hair cells at 2 dpf has previously been reported (Lopez-Schier and Hudspeth, 2006). Taken together, these results suggest that complexin 3/4 and RIBEYE b immunoreactivities are targeted rapidly to different compartments in zebrafish inner ear and lateral line hair cells.

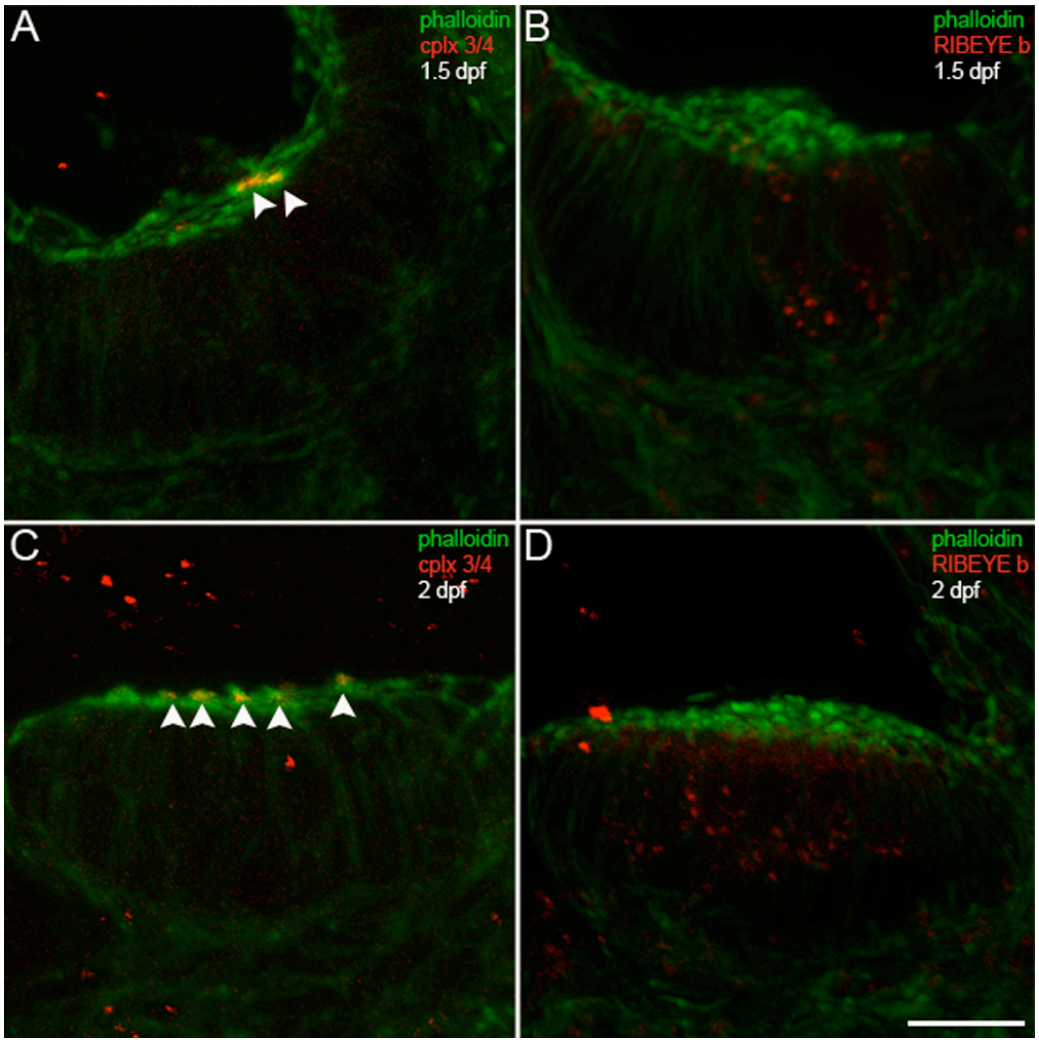

Figure 4-5. Complexin 3/4 does not co-localize with RIBEYE b in embryonic inner ear hair cells. A. This panel contains a high-magnification confocal projection through the posterior macula in the zebrafish inner ear at 36 hpf. Using phalloidin (green) as a marker of developing hair cell stereocilia, one can observe a small number of hair cells with stereocilia. Complexin 3/4 (red) is already apparent among these stereocilia (arrowheads). B. Dual immunolabeling of RIBEYE b (red) and F-actin with phalloidin (green) in the anterior macula at 36 hpf. Note that RIBEYE b has clustered into large puncta on the basolateral membrane of hair cells with stereocilia. C. At 48 hpf, many more hair cells with stereocilia (green) can be observed in the anterior macula. Complexin 3/4 immunoreactivity (red) can be observed among these stereocilia (arrowheads). D. RIBEYE b (red) is upregulated in the cytoplasm of more hair cells in the anterior macula at 48 hpf. Scale bar= 10 μm. Reproduced from Zanazzi and Matthews (2010) with permission from BioMed Central.

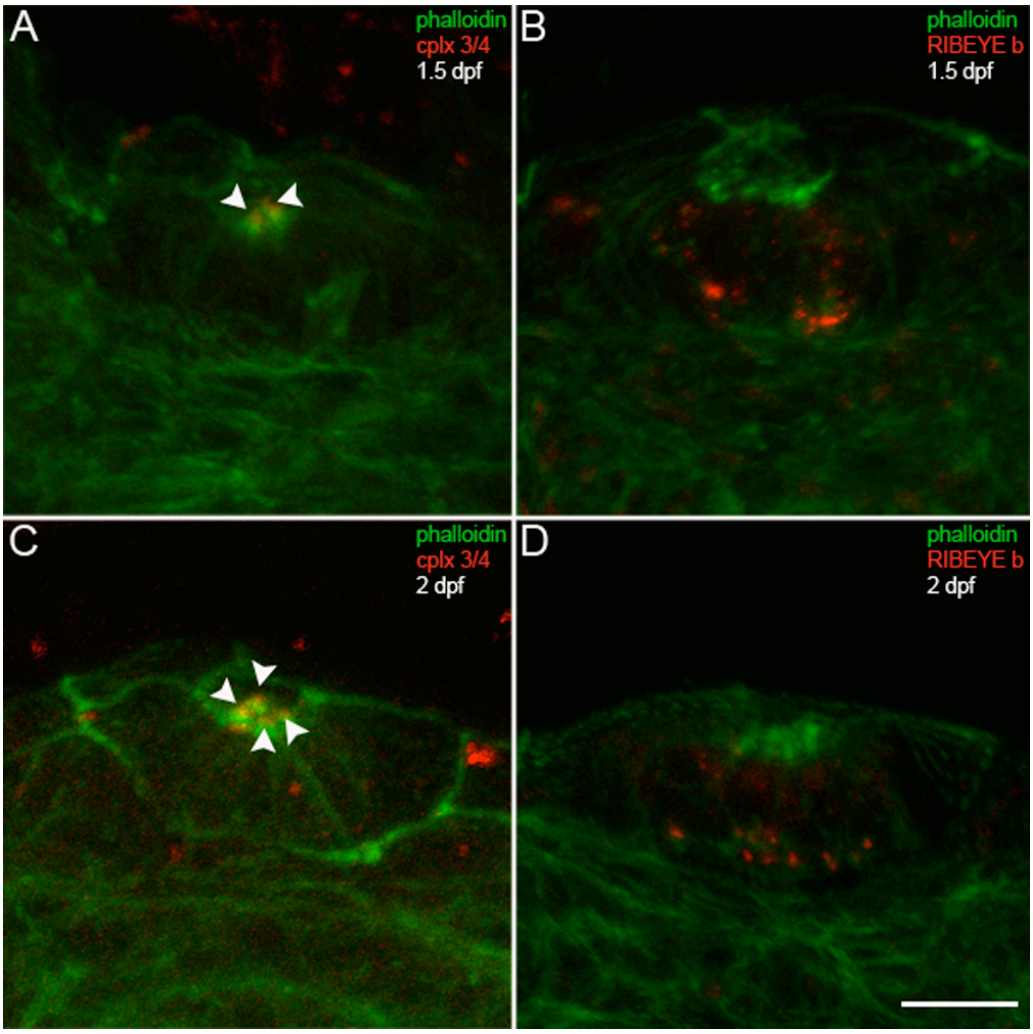

Figure 4-6. Complexin 3/4 does not co-localize with RIBEYE b in embryonic neuromast hair cells. A. 36 hpf embryonic zebrafish were sectioned transversely. Phalloidin (green) and anti-complexin 3/4 (red) were used to probe otic neuromasts. Note that complexin 3/4 is weakly expressed among neuromast hair cell stereocilia at this time (arrowheads). B. Large RIBEYE b puncta (red) can be observed at the base, and diffuse cytoplasmic immunoreactivity elsewhere, in a couple of neuromast hair cells at 36 hpf. C. Greater numbers of hair cells in an otic neuromast have stereocilia (green) at 48 hpf. These hair cells also have apical complexin 3/4 immunoreactivity (red, arrowheads). D. At 48 hpf, many hair cells in an otic neuromast have RIBEYE b immunoreactivity (red). Scale bar= 10 μm. Reproduced from Zanazzi and Matthews (2010) with permission from BioMed Central.

Complexin 4a specifically marks visual system ribbon presynaptic terminals during development

Staining of larval zebrafish sections with the complexin 4a antibody and anti-zpr 1/FRet 43 reveals abundant complexin 4a in the retinal plexiform layers and lateral borders of the pineal organ (Figure 4-7A). Complexin 4a is more restricted to retinal double cone (Figure 4-7B) and pineal photoreceptor (Figure 4-7D) terminals when compared to pan-complexin 3/4 immunoreactivity (Figure 4-1A, D). In the retinal IPL, complexin 4a is detectable in sublamina a and in PKC-positive presynaptic terminals in sublamina b (Figure 4-7C).

In contrast to the pan complexin 3/4 antibody, the complexin 4a antibody does not label hair cells in the inner ear or lateral line (Figure 4-8). Panel A shows a confocal projection of a larval zebrafish inner ear probed with phalloidin (green) and the complexin 4a antibody (red). Inner ear hair cells do not contain complexin 4a immunoreactivity (Figure 4-8A, arrowheads). Higher magnification of individual hair cells and their stereocilia confirms the absence of complexin 4a (Figure 4-8B). Inner ear sensory patches defined by the zn 1 monoclonal antibody lack complexin 4a (Figure 4-8C). Hair cells in neuromasts of the cranial (Figure 4-8D) and trunk (data not shown) lateral lines also lack complexin 4a. Taken together, these results indicate that complexin 4a is differentially expressed in ribbon-containing sensory neurons with a predilection for presynaptic terminals in the zebrafish visual system. In addition, hair cells contain one or more isoforms of the complexin 3/4 subfamily distinct from complexin 4a.

Differential distribution of complexin 3/4 isoforms in larval zebrafish

To determine the specific expression patterns of all complexin 3/4 isoforms, we performed whole mount in situ hybridization of 5 dpf larval zebrafish with paralog-specific riboprobes (Figure 4-9). Consistent with the immunocytochemistry experiments, all complexin 3/4 isoforms except for complexin 3b are robustly expressed in the larval zebrafish retina. An RNA dot blot with the complexin 3b antisense probe confirmed that the probe recognizes complexin 3b mRNA (Figure 4-10). Of note, complexin 4a localizes predominantly to the retina (Figure 4-9C). While complexin 4b is also highly expressed in the retina, it appears in neuromasts of the lateral line and in the inner ear (Figure 4-9D, arrowheads). Taken together, these results suggest subfunctionalization in the complexin 3/4 subfamily in zebrafish.

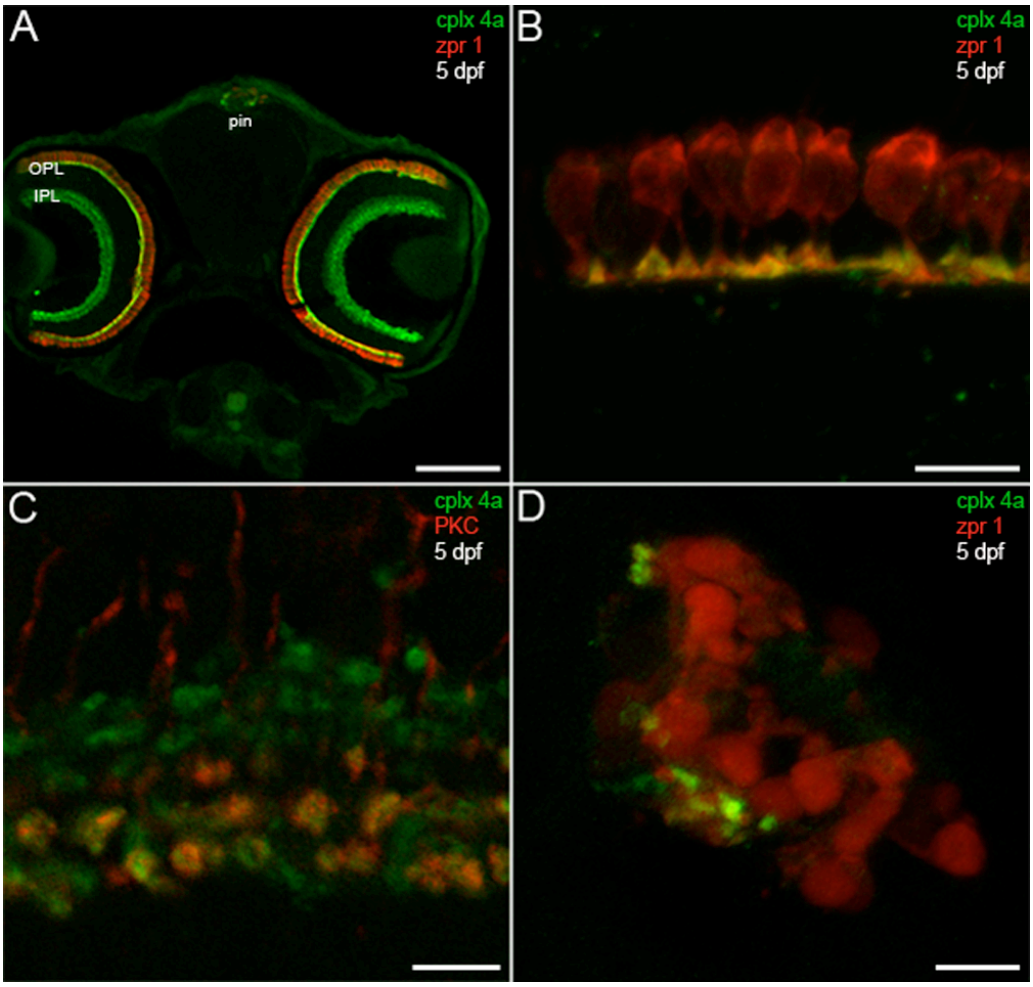

Figure 4-7. Complexin 4a marks larval visual system ribbon presynaptic terminals. A. A confocal micrograph of a 5 dpf zebrafish transverse section stained with the anti-complexin 4a antibody (green) and anti-zpr 1/FRet 43 (red). Note the similarity between the complexin 4a expression pattern and that of complexin 3/4 (Figure 1A) at low magnification in the retinal plexiform layers (OPL, IPL) and pineal organ (pin). B. At high magnification, complexin 4a appears to be restricted primarily to the terminals of double cone photoreceptors in the retinal outer plexiform layer. C. A confocal planar projection of the retinal inner plexiform layer shows overlap of complexin 4a (green) in PKC-positive (red) ON bipolar cell terminals in the IPL. D. A confocal planar projection of a 5 dpf zebrafish sagittal section through the pineal organ is shown. Zpr 1/FRet 43-positive photoreceptors (red) are oriented such that their outer segments are medial and their short axons and presynaptic terminals are lateral. Complexin 4a (green) specifically localizes to putative terminals. Sections incubated with secondary antibodies alone exhibited background immunofluorescence in the retina and pineal (data not shown). Scale bars= 125 μm (A), 10 μm (B, D), 5 μm (C). Reproduced from Zanazzi and Matthews (2010) with permission from BioMed Central.

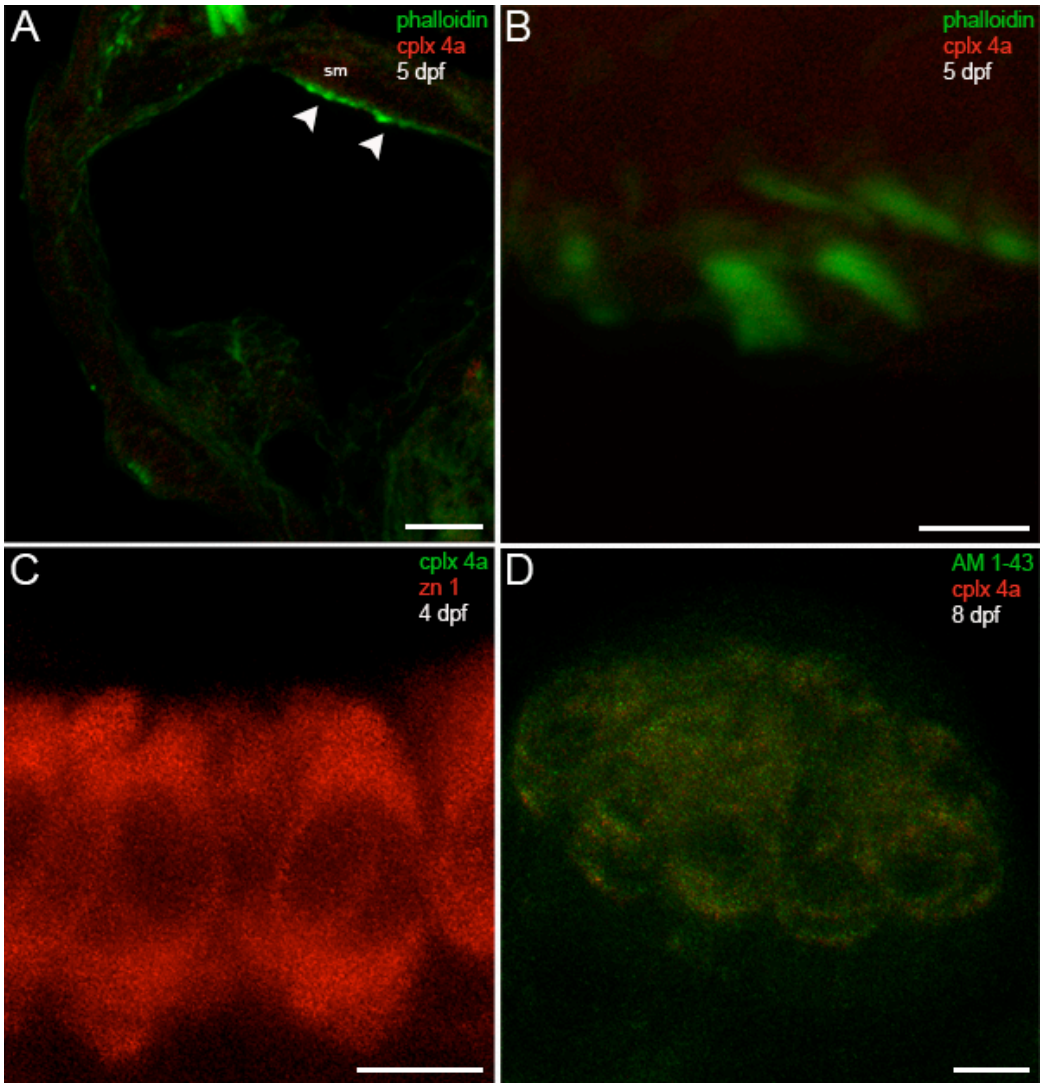

Figure 4-8. Complexin 4a is not expressed in hair cells of the larval zebrafish octavolateral system. A. A low-magnification confocal micrograph of a transverse section through the otic vesicle of a 5 dpf zebrafish shows saccular macula (sm) inner ear hair cell stereocilia stained with phalloidin (green) that lack complexin 4a (red, arrowheads). B. A high-magnification en face view of inner ear hair cells labelled with phalloidin (green) confirms the absence of complexin 4a (red) among their stereocilia. C. Inner ear hair cells labeled with anti-zn 1 (red) lack complexin 4a (green). D. A high-magnification confocal planar projection through a cranial neuromast labeled with AM1-43 (green) indicates that complexin 4a is also absent from these hair cells. Sections incubated with only secondary antibodies exhibit very low levels of diffuse immunofluorescence throughout the hair cells (data not shown). Scale bars= 25 μm (A), 5 μm (B, C, D). Reproduced from Zanazzi and Matthews (2010) with permission from BioMed Central.

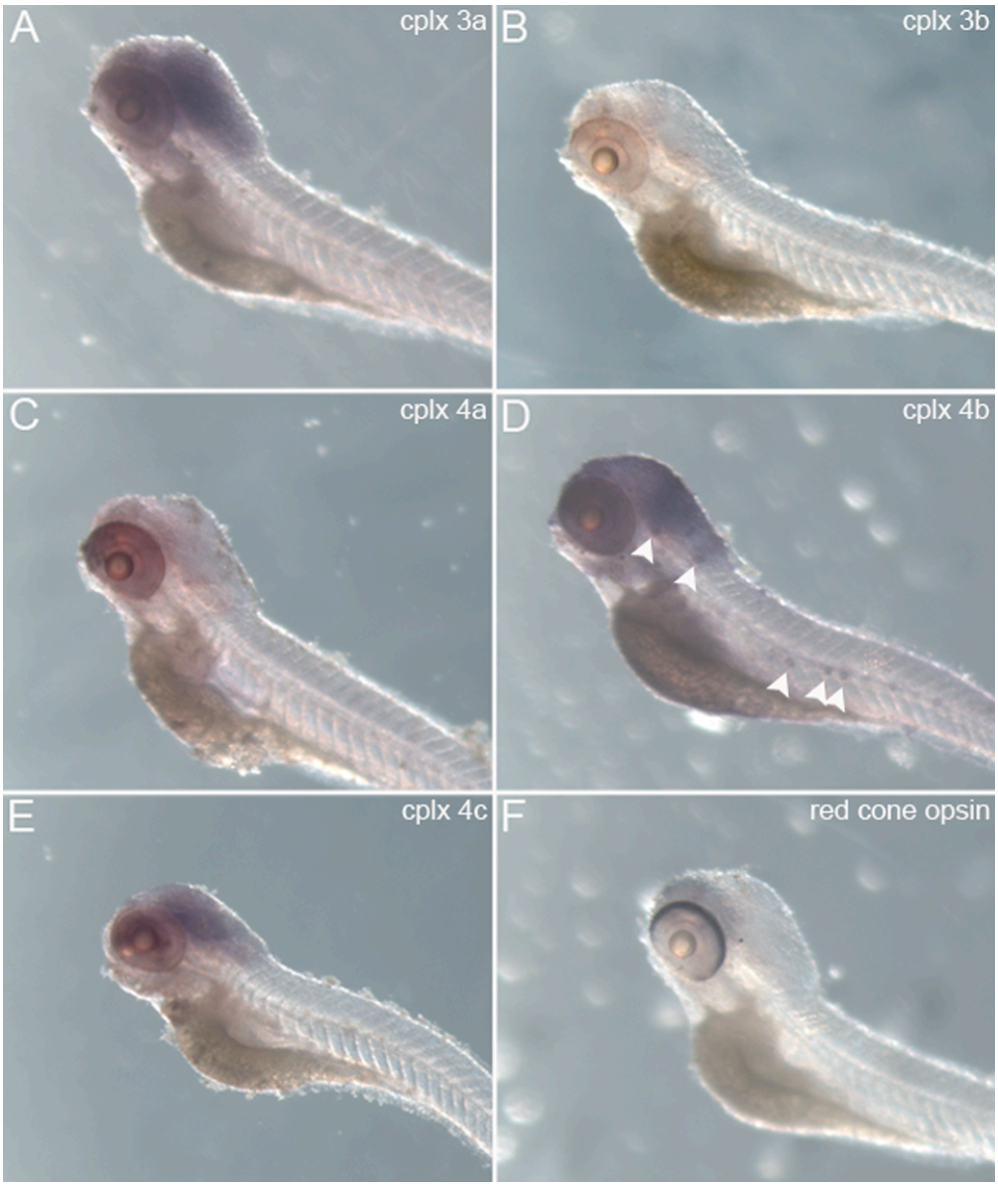

Figure 4-9. Distinct expression of complexin 3/4 isoforms in the larval zebrafish. Whole mount in situ hybridization of 5 dpf larval zebrafish was performed with digoxigenin-labeled RNA antisense probes directed against complexin 3a (A), complexin 3b (B), complexin 4a (C), complexin 4b (D), complexin 4c (E) and red cone opsin (F). Robust expression of all isoforms, except for complexin 3b, is observed in the retina. Complexin 4b is the only isoform found in neuromasts of the lateral lines and in the inner ear (arrowheads). In situ hybridization with the corresponding sense probes revealed little reaction product except for complexin 3a (data not shown). Reproduced from Zanazzi and Matthews (2010) with permission from BioMed Central.

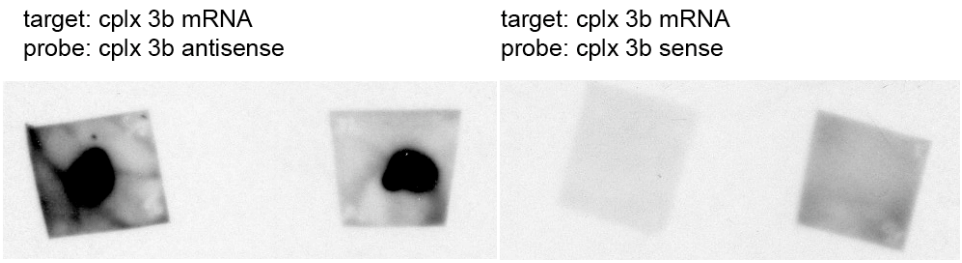

Figure 4-10. RNA dot blot confirms that the complexin 3b antisense probe hybridizes with its complementary target. 0.2 ng of full-length complexin (cplx) 3b mRNA was spotted on four pieces of nylon membrane, uv-crosslinked and incubatedwith 0.5 ng/μl of digoxigenin-labeled complexin 3b antisense (two left panels) or sense (two right panels) riboprobes. The antisense, but not the sense, riboprobe hybridized with the complexin 3b transcript.

Discussion

In this study, we have shown that members of the complexin 3/4 subfamily can have very different fates during the development of visual and octavolateral receptor cells in zebrafish. Complexin 3/4 is undetectable in the RIBEYE-containing basolateral domain of hair cells, whereas complexin 3/4 becomes highly concentrated in the RIBEYE-containing presynaptic terminals of photoreceptors. Conversely, striking complexin 3/4 immunoreactivity appears on the apical surfaces of hair cells, at the base of their stereocilia, while low levels of complexin 3/4 appear in the apical domain of photoreceptors. Finally, in situ hybridization with paralog-specific probes suggests that triplication of complexin 4 in zebrafish may have led to subfunctionalization. The targeting of complexin 3/4 is considered further below.

Targeting of the complexin 3/4 subfamily to different compartments in ribbon-containing sensory neurons

The plasma membranes of photoreceptors and hair cells, like prototypical epithelial cells, are polarized into apical and basolateral domains with distinct organelles. This polarity depends, in part, upon the precise targeting of plasma membrane proteins that contain specific signals recognized in the trans-Golgi network or in various endosomal compartments, leading to sorting into transport vesicles that traffick along microtubules to the apical or basolateral surfaces (reviewed in Mellman and Nelson, 2008; Weisz and Rodriguez-Boulan, 2009). In hair cells, for example, a large insert targets a plasma membrane calcium ATPase (PMCA) isoform to the apical stereociliary bundles, while a leucine-isoleucine motif in another site provides a targeting signal to the basolateral domain (Grati et al., 2006; Hill et al., 2006). Extrinsic synaptic vesicle

proteins may also have targeting signals (reviewed in Bonanomi et al., 2006), but they are not well-characterized. The targeting signals used by the complexins remain to be determined.

A compartmentalized vesicular trafficking system around the cuticular plate likely supports apical targeting of proteins in the hair cell (Kachar et al., 1997; Safieddine et al., 2002). Meanwhile, rhodopsin-bearing transport carriers mediate apical trafficking in photoreceptors (Deretic and Papermaster, 1991; Deretic et al., 2004). Comparatively little is known about the trafficking of active zone components, including synaptic vesicles, to presynaptic terminals in sensory receptor cells. Two recent papers have revealed that, in photoreceptors, ribbon-associated components travel down the axon in so-called ribbon precursor spheres (Regus-Leidig et al., 2009; Regus-Leidig et al., 2010). Our results are consistent with a model whereby complexin 3/4 members utilize these direct apical and basolateral routes of delivery during development. However, since the differentiation of the receptor cells occurs very rapidly in zebrafish, it is quite possible that indirect targeting, via mechanisms such as transcytosis, may occur. Real-time visualization of fluorescently tagged complexins may provide insights into their targeting. The addition of tannic acid, a fixative that disturbs vesicular trafficking, to the apical or basolateral domain of receptor cells in vitro, may help to delineate the route of delivery (Polishchuk et al., 2004).

Since RIBEYE b is not expressed in bipolar cells (Wan et al., 2005), we were unable to analyze the time course of complexin 3/4 accumulation in bipolar cell terminals relative to a ribbon marker. However, it was observed that complexin 3/4 appeared to be targeted directly to bipolar cell terminals very rapidly after its clustering in retinal photoreceptor terminals (data not shown). Live imaging of fluorescently tagged components of the exocytotic machinery, expressed under the control of retinal bipolar cell (Morgan et al., 2006; Schroeter et al., 2006) or other ribbon-containing neuron promoters (Holzhausen et al., 2009), may shed additional light on the mechanisms and signals that regulate their targeting.

Chapter 5

Roles for complexin 4a in zebrafish visual function

Introduction

During early vertebrate development, the pineal organ differentiates before the retina (reviewed in Vollrath, 1981; Ekström and Meissl, 1997). Indeed, neurons in the pineal are among the first to differentiate in the central nervous system (Wilson and Easter, 1991). Very little is known about the functional significance of the pineal during early development besides entrainment of the circadian oscillator (reviewed in Falcón et al., 2009) and background adaptation in response to ambient light levels (reviewed in Bagnara and Hadley, 1970). Anamniotes can rapidly adapt to backgrounds via centripetal and centrifugal translocation of pigment granules on microtubule tracks in neural crest–derived chromatophores (Figure 5-1), which include black melanophores, yellow xanthophores, red erythrophores, white leucophores and iridescent iridophores (reviewed in Fujii, 2000). Young amphibian larvae (Babak, 1910; Laurens, 1914; Bagnara, 1960) and teleost embryos (Shiraki et al., 2010) turn white in darkness as melanosomes aggregate in the perinuclear regions of the melanophores. Pinealectomy, but not enucleation, abolishes the paling response (Bagnara, 1960). It has long been known that pineal extracts blanche anamniotes (McCord and Allen, 1917), and melatonin aggregates embryonic and young larval melanosomes (Figure 5-1) (Bagnara, 1960). It has therefore been suggested that melatonin tonically released from the pineal at night directly causes lightening, whose physiological significance is unknown (Bagnara, 1964). In the light, embryos conversely darken (see, for example, Shiraki et al., 2010).

A developmental switch in the background adaptation response occurs typically around the time of hatching such that older anamniotes become dark in darkness and pale in light (reviewed in Parker, 1948). This response is primarily mediated by ocular photoreception (Babak, 1910; Laurens, 1914). In support of this pathway, many mutants with retinal defects have permanently dispersed melanosomes regardless of light levels (see, for example, Neuhauss et al., 1999). Light normally stimulates teleost larvae and adults to secrete melanin-concentrating hormone (MCH) from the posterior pituitary through a retino-hypothalamic projection (Figure 5-1). On the other hand, darkness stimulates the intermediate lobe of the pituitary to secrete

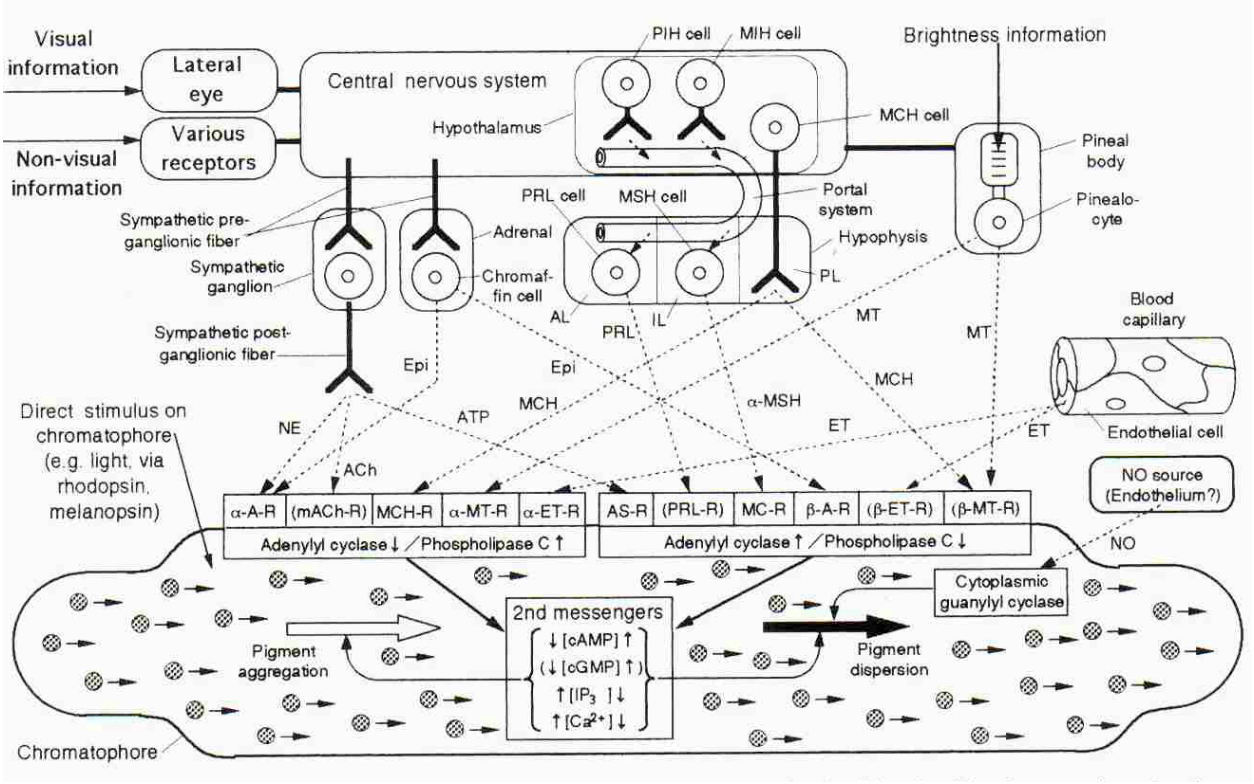

Figure 5-1. Regulation of chromatosomes in teleosts. Diagram showing the regulatory system for motile activities of melanophores and other light-absorbing chromatophores in teleosts. Explanations for abbreviations in the figure are arranged in order from left to right. α-A-R, α-adrenoceptor; NE, norepinephrine; mACh-R, muscarinic acetylcholine receptor; Ach, acetylcholine; MCH-R, MCH receptor; E, epinephrine; ATP, adenosine 5'-triphosphate; α-MT-R, α-MT receptor; PRL cell, prolactin-producing cell; MCH, melanin-concentrating hormone; α-ET-R, α-ET receptor; AL, anterior lobe of hypophysis; cAMP, cyclic adenosine 3', 5'-monophosphate; cGMP, cyclic guanosine 3', 5'-monophosphate; IP3, inositol-1,4,5-trisphosphate; PRL, prolactin; AS-R, adenosine receptor; MSH cell, MSH-producing cell; PIH cell, PRL-release inhibiting hormone-secreting cell; IL, intermediate lobe of hypophysis; PRL-R, PRL receptor; MIH cell, MSH-release inhibiting hormone; MC-R, melanocortin receptor; -MSH, α-melanophore-stimulating hormone; β-A-R, β-adrenoceptor; PL, posterior lobe of hypophysis; ET, endothelin; MT, melatonin; MCH cell, MCH-producing neuron in hypothalamus; β-ET-R, β-ET receptor; β-MT-R, β-melatonin receptor; NO, nitric oxide. Reproduced from Fujii (2000), with permission of Wiley.

melanophore-stimulating hormone (MSH), which disperses melanosomes (Figure 5-1). Besides hormones, chromatophores are regulated by the autonomic nervous system such that catecholamines aggregate melanosomes in teleost larvae and adults (reviewed in Fujii, 2000).

While photoreception in the pineal and retina has long been known to regulate background adaptation, many of the underlying molecular mechanisms are still obscure. We find that complexin 4a, which is expressed in the pineal and retinal neuropil, is required for embryonic and larval zebrafish background adaptation. In addition, larval complexin 4a morphants lack an optokinetic response. While many aspects of pineal and retinal photoreceptor presynaptic architecture appear normal, spherical floating ribbons are increased in complexin 4a morphants. Taken together, these results suggest that complexin 4a is necessary for vision in zebrafish.

Results

Knockdown of complexin 4a results in hypopigmentation and abnormal background adaptation in zebrafish embryos

To begin to examine the function of complexins in ribbon-containing neurons, we injected, into single-celled zebrafish embryos, 5-10 ng of a morpholino antisense oligonucleotide directed against the first ATG of complexin 4a. These morphants look morphologically similar, until 1.5 dpf, to embryos injected with 5-10 ng of a standard control morpholino directed against human beta globin (data not shown). Thereafter, the complexin 4a morphants begin to exhibit hypopigmentation, microphthalmia, and microcephaly when compared to controls (Figure 5-2). Pigmentation is specifically affected in the morphant integument, as retinal pigmentation appears grossly normal (Figure 5-2). Pericardial edema develops progressively, and the morphants die between 5.5-7 dpf (data not shown).

Nearly 300 hypopigmentation mutants were isolated in the first Tübingen screen (Kelsh et al., 1996). Some mutants, such as *colourless,* lack nearly all chromatophores (Kelsh et al., 1996; Kelsh et al., 2000) due to defects in migration, specification, and/or differentiation of neural crest cells into chromatophores. Therefore, we examined the anterior dorsal melanophore stripes between the eyes and the base of the head to determine whether the complexin 4a morphants exhibit reduced or abnormally distributed melanophores. Figure 5-3 reveals that the complexin 4a morphants contain normal numbers of melanophores that appear to migrate to their

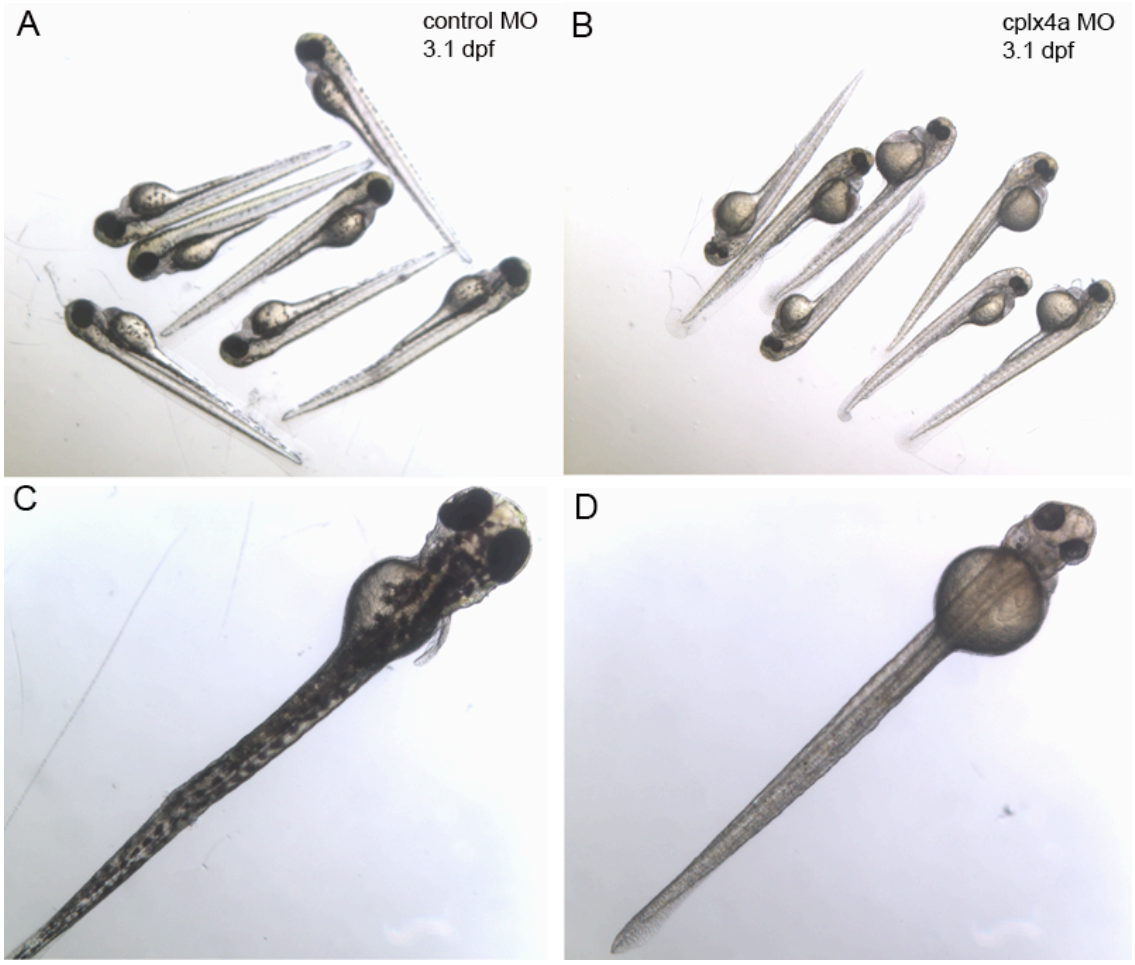

Figure 5-2. Knockdown of complexin 4a results in hypopigmentation, microcephaly and microphthalmia. Light micrographs of 3.1 dpf zebrafish injected at the one-cell stage with 5 ng of a morpholino antisense oligonucleotide targeting human beta-globin (A, C) or complexin 4a (B, D). While the complexin 4a morphants display normal overall body length, they exhibit microcephaly and microphthalmia. Melanin pigment levels in the dermis, but not the retina, are decreased in the complexin 4a morphants.

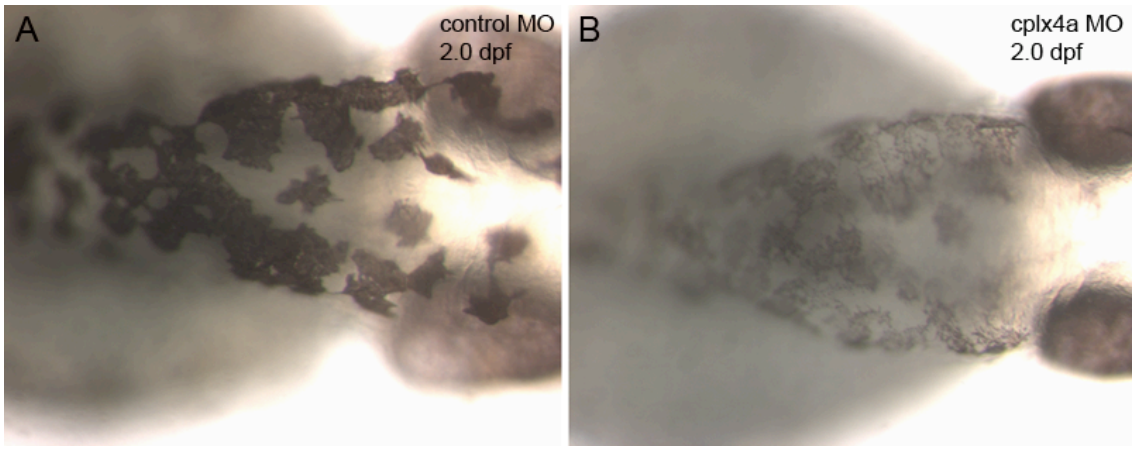

Figure 5-3. Neural crest-derived melanophores lack pigment in embryonic complexin 4a morphants. High-magnification micrographs reveal relatively normal numbers of antero-dorsal melanophores in the light-adapted complexin 4a morphants (B) compared to light-adapted controls (A). While eye melanophores have normal pigmentation, complexin 4a morphant integument melanophores lack pigment.

correct destinations; however, the melanophores exhibit a paucity of melanin. The complexin 4a morphants also contain normal numbers of melanophores, with decreased melanin, throughout the rest of the integument (data not shown).

Many extrinsic factors, such as ambient light levels, regulate the distribution and overall quantity of pigment-containing melanosomes within melanophores (reviewed in Yamaguchi and Hearing, 2009). Teleost embryos whiten during the night and darken during the day due in large part to melanosome aggregation and dispersal, respectively (reviewed in Fujii, 2000). To determine whether ambient light levels regulate complexin 4a morphant melanosomes, we examined control and complexin 4a morphant embryos before and after dark-adaptation (Figure 5-4). In the light, control morphant melanophores are dispersed, thereby covering much of the integument with pigment (Figure 5-4A). After dark adaptation, the embryo (especially the dorsal surface) whitens as melanosomes aggregate (Figure 5-4B). The residual melanosomes in the complexin 4a morphants, on the other hand, appear somewhat aggregated in the light (Figure 5-4C) and in darkness (Figure 5-4D). These results suggest that pineal visual function is impaired in the complexin 4a morphant embryos.

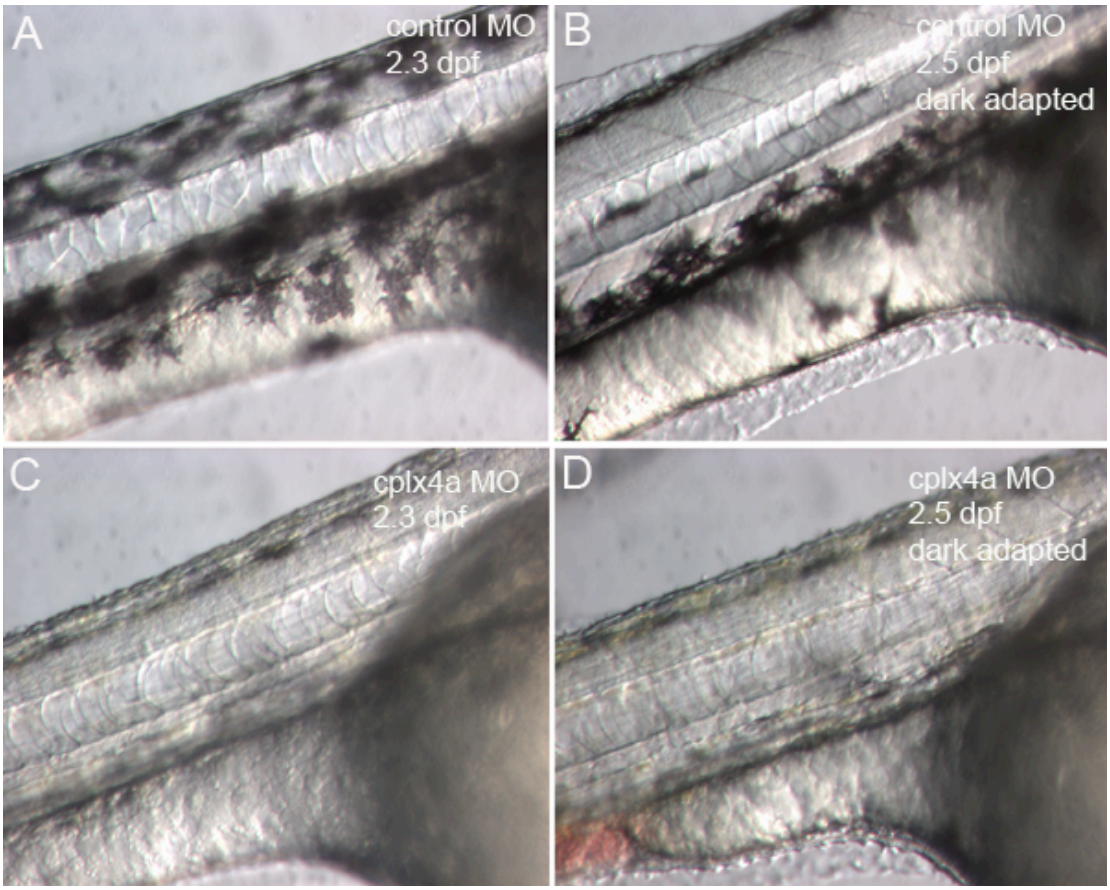

Figure 5-4. Embryonic complexin 4a morphants display abnormal melanosome trafficking in response to darkness. Light micrographs show dorsal views of light-adapted 2.3 dpf embryonic control morphant (A) and complexin 4a morphant (C) zebrafish. The same fish were then photographed after dark adaptation (B, D). In response to darkness, melanosomes concentrate within melanophores in control embryonic morphants, especially along their dorsal surface (B). In complexin 4a morphants, the melanophores appear to be in a "wildtype" dark-adapted state regardless of light (C) or dark (D) levels.

At this developmental age (2 dpf), the retina in the zebrafish embryo is not yet functional (for review, Fadool and Dowling, 2008). Indeed, retinal photoreceptors are just starting to exit the cell cycle at this time, and retinal bipolar cells have yet to differentiate. However, photoreceptors and effector neurons in the pineal organ differentiate between 1-2 dpf (Masai et al., 1997; Cau et al., 2008; our study, Chapter 4). Pinealectomy in teleost and amphibian embryos has indicated that the pineal mediates embryonic background adaptation (reviewed in Bagnara and Hadley, 1970; Fujii, 2000). Therefore, we first examined whether complexin 4a is expressed in the pineal organ during embryogenesis. Figure 5-5A shows that complexin 4a is expressed at high levels at 1.5 dpf in the ventrolateral neuropil of the pineal organ. Many double

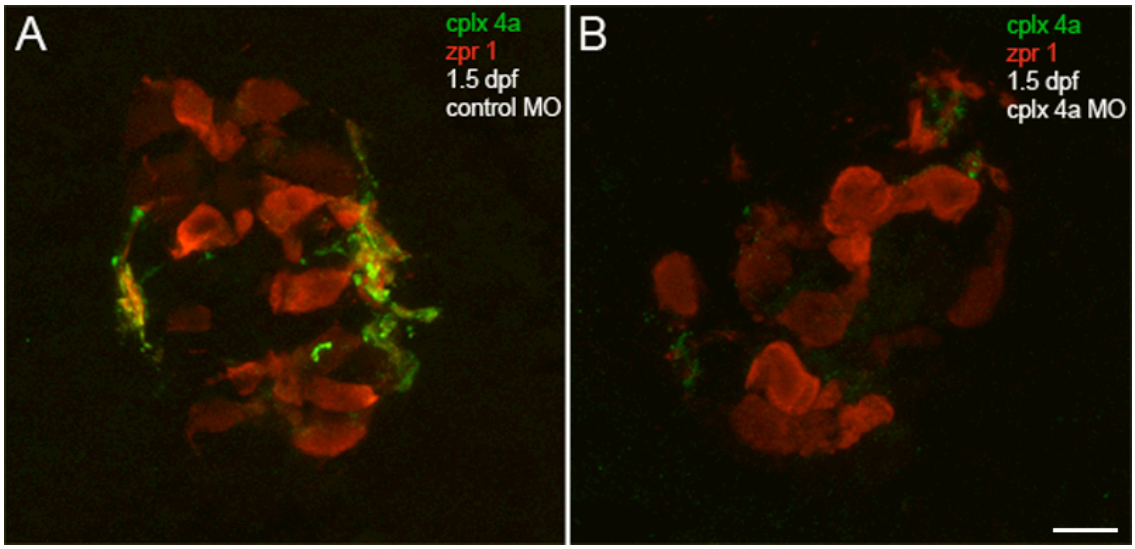

Figure 5-5. Immunocytochemistry confirms knockdown of complexin 4a in the embryonic zebrafish pineal. Control and complexin 4a morphants were fixed at 1.5 dpf, sectioned, and stained with anti-zpr 1/FRet 43 (in red) to label double cones and with anti-complexin 4a (in green). These confocal micrographs show dorsal views of the pineal organ in the control (A) and complexin 4a morphants (B). Complexin 4a expression is dramatically downregulated in the lateral neuropil of the complexin 4a morphants. Scale bar, 10 μm.

cone photoreceptors express complexin 4a in their terminals (Figure 5-5A). In the complexin 4a morphants, the pineal organ forms, but complexin 4a is dramatically downregulated in the neuropil (Figure 5-5B). At 1.5 dpf, complexin 4a protein is not expressed elsewhere in the wildtype zebrafish embryo (data not shown). Taken together, these results suggest that complexin 4a in the pineal organ is necessary for background adaptation.

To begin to determine the etiology of this defect, we examined by electron microscopy the ultrastructure of the pineal organ at 2 dpf in complexin 4a morphants and controls (Figure 5-6 and Figure 5-7). At this time point in zebrafish development, the pineal organ encompasses a major portion of the dorsal diencephalon (data not shown). In the dorsomedial part of the organ, several photoreceptor outer segments with well-formed disks were observed in the controls (Figure 5-6A) and complexin 4a morphants (Figure 5-6B). In some sections, one could observe a connecting cilium (9+0 microtubule arrangement) along with calycal processes (see, for example, Figure 5-6B). In the ventrolateral part of the organ, a dense, complex neuropil was present both in the controls (Figure 5-7A) and in the complexin 4a morphants (Figure 5-7B). Large photoreceptor pedicles, densely populated with synaptic vesicles, elaborated finger-like projections and made multiple synapses, some of which contained pleiomorphic ribbons attached

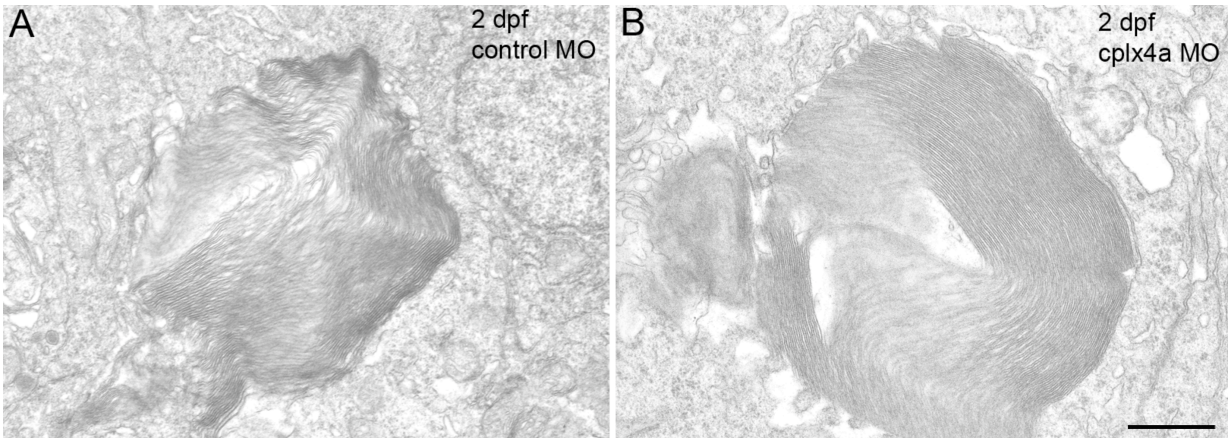

Figure 5-6. Ultrastructure of pineal photoreceptor outer segments in complexin 4a morphants and controls. Representative ultrathin transverse sections of 2 dpf control morphant (A) and complexin 4a morphant (B) pineal photoreceptor outer segments are shown. Normal pineal photoreceptor outer segments containing several disks, calycal processes, and a connecting cilium are seen in the complexin 4a morphant pineal (B). Scale bar, 500 nm.

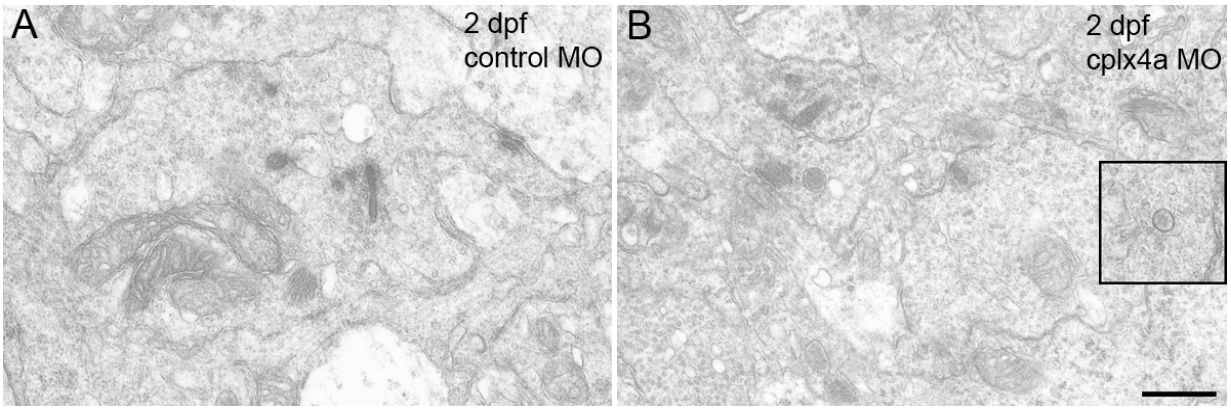

Figure 5-7. Ultrastructure of pineal photoreceptor ribbon presynaptic terminals in complexin 4a morphants and controls. Representative ultrathin transverse sections of 2 dpf control morphant (A) and complexin 4a morphant (B) pineal neuropil. In both cases, large photoreceptor presynaptic terminals make multiple synapses. Several ribbons are found in both samples, but spheres with an electron-dense center (B, inset) are found at higher levels in the complexin 4a morphant pineal neuropil. Scale bar, 500 nm.

to the plasma membrane (Figure 5-7A, B). Examination of several serial ultrathin sections that covered the entire extent of individual ribbons revealed no difference in ribbon dimensions between complexin 4a morphants and controls (data not shown). There is an increase, however, in floating ribbon spheres with electron-dense centers (McNulty, 1980) in the complexin 4a morphant photoreceptor terminals (Figure 5-7B inset).

Absent optokinetic responses and abnormal background adaptation in complexin 4a morphant larvae suggest impaired retinal function

During development, the other major site of complexin 4a expression is the retina (Chapter 4). A well-characterized behavioral assay for zebrafish that measures retinal visual function is the optokinetic response assay (reviewed in Brockerhoff, 2006). In this assay, larval zebrafish are immobilized in methylcellulose on a platform in the center of a rotating, opaque drum lined with black and white vertical stripes. The fish will follow the drum rotation up to a point, and then make a saccade to reset eye position. The number of saccades elicited from complexin 4a mutants at 4.25 dpf is significantly less than that obtained from control morpholino-injected fish (Figure 5-8), suggesting that the mutants are blind. It should be pointed out that the complexin 4a morphants do not exhibit spontaneous eye movements (i.e., in the absence of drum rotation), which control morphants exhibit at low levels over the course of a minute (data not shown). Therefore, the lack of an optokinetic response may be due to a sensory defect, a motor defect, or both.

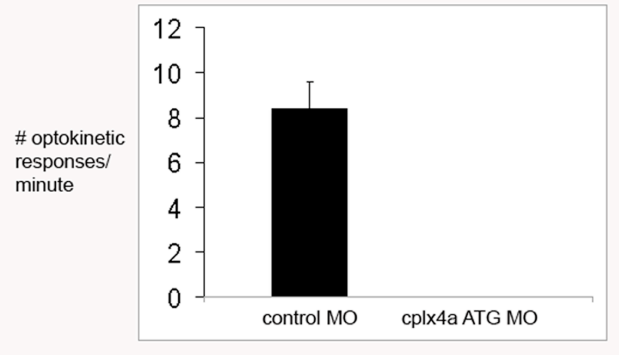

Figure 5-8. Complexin 4a morphants lack an optokinetic response. The mean values and SEM are shown for the number of optokinetic responses (OKR) per minute elicited from 4.25 dpf larvae. The number of OKR elicited from the cplx 4a morphants (MO) was significantly less than that obtained from control MO-injected larvae.

To determine whether the complexin 4a morphants have retinal sensory dysfunction, we examined the background adaptation response of larval morphants. A representative control (Figure 5-9A, C, E) and complexin 4a morphant (Figure 5-9B, D, F) are shown. In the control zebrafish larvae, melanosomes aggregate in the light, resulting in decreased black pigment coverage of the integument (Figure 5-9A). Overall, the fish appears lighter in the light. Indeed, one can readily observe clear areas surrounding aggregated pigment in light-adapted control

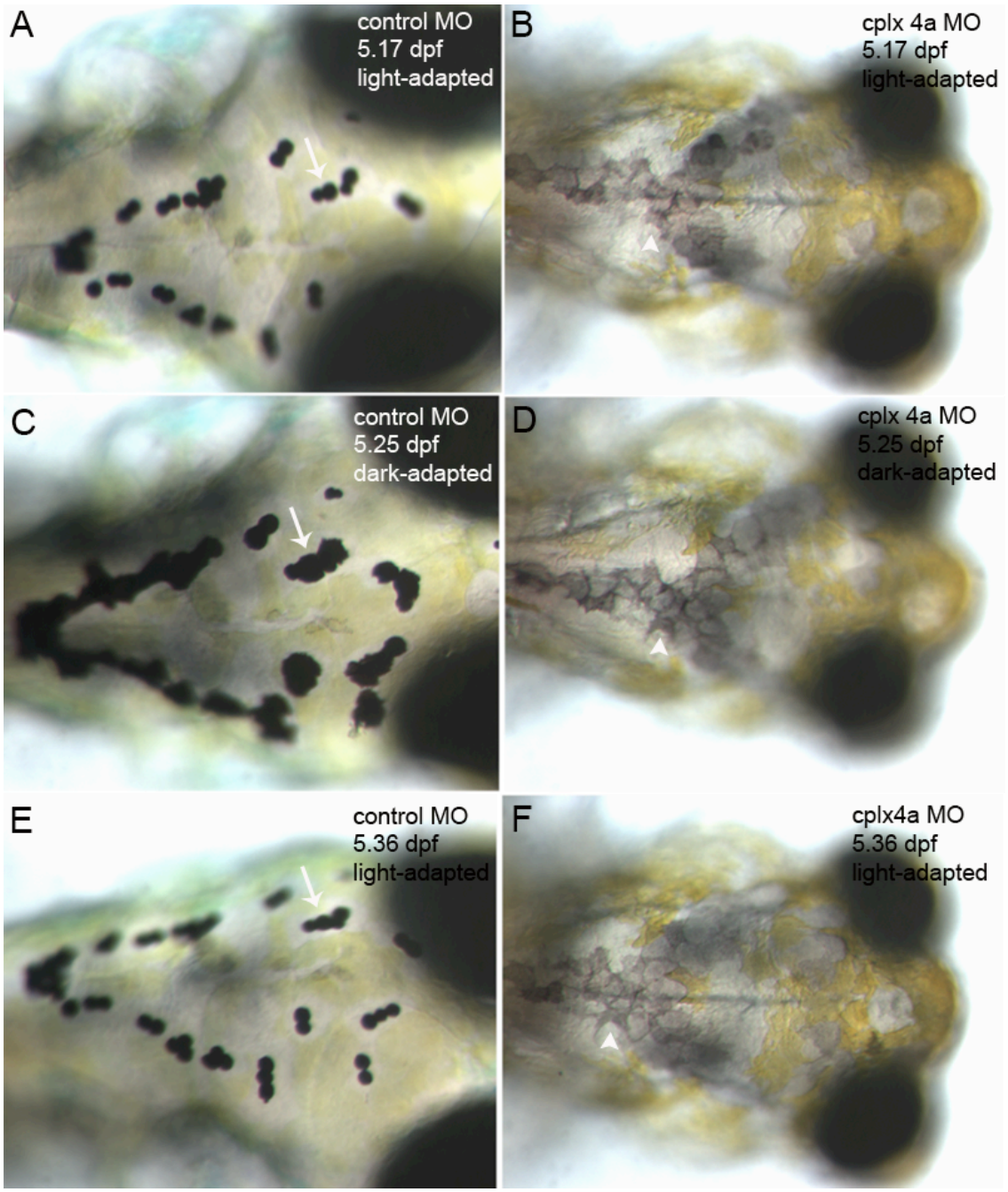

Figure 5-9. Abnormal melanophore light and dark responses in complexin 4a morphants. Light micrographs of antero-dorsal regions in live, non-anesthetized, larval zebrafish exhibiting background adaptation. Light-adapted control (A) and complexin 4a morphant (B) larvae were photographed, then dark-adapted for 1.5 hours (C, D), and then light-adapted for 1.75 hours (E, F). While control zebrafish larval melanophores aggregate pigment in the light (A, E), complexin 4a morphant pigment is dispersed (B, F). In the dark, both control zebrafish (C) and complexin 4a morphant (D) melanophores are dispersed. Arrows point to the same melanosome in the control fish, and arrowheads point to the same melanosome in the morphant fish.

larvae (Figure 5-9A, E). In light-adapted complexin 4a morphants, however, the pigment in melanophores is dispersed (Figure 5-9B). At high magnification, one can observe pigment outlining the dendritic melanophores (Figure 5-9B). After control larvae are dark-adapted, their pigment disperses (an arrow points to one melanophore) and covers a greater surface area, making the fish look dark overall (Figure 5-9C). In dark-adapted complexin 4a morphants, the melanophores appear unchanged (arrowhead points to one melanophore) (Figure 5-9D). Finally, light-adaptation of the control morphants again aggregates the melanosome, showing that melanosome trafficking is reversible and dynamic (Figure 5-9E). In the complexin 4a morphants, light-adaptation, does not change melanosome distribution (Figure 5-9F). These results suggest that complexin 4a morphants have a defect in retinal sensory function and/or an intrinsic defect in melanosome trafficking.

To determine whether the impaired background adaptation in the larval complexin 4a melanophores is due to an intrinsic trafficking defect, we examined whether their melanosomes can aggregate in response to epinephrine, a catecholamine that directly stimulates pigment aggregation in wildtype zebrafish (Sheets et al., 2007). Light-adapted control (Figure 5-10A) and complexin 4a morphant (Figure 5-10C) larvae were first photographed to document their aggregated and dispersed pigment, respectively. Then, these fish were incubated in 10^{-3}M epinephrine for 15 minutes and photographed. Epinephrine caused a slight additional aggregation of melanosomes in the controls (Figure 5-10B). Importantly, epinephrine induced a dramatic aggregation of melanosomes in the complexin 4a morphants (Figure 5-10D), revealing that the intrinsic trafficking machinery in these cells is normal. Together with the light and dark background adaptation experiments, these results suggest that larval complexin 4a morphants specifically do not respond to ambient light levels. The background adaptation and optokinetic response defects are consistent with retinal blindness in the complexin 4a morphants.

Therefore, we utilized immunocytochemistry to begin to examine the cellular and molecular architecture of the complexin 4a morphant retina. Consistent with microphthalmia, there are decreased numbers of zpr 1/FRet 43-positive double cone photoreceptors in larval complexin 4a morphants (Figure 5-11B, D) compared to controls (Figure 5-11A, C). Complexin 4a expression is also robustly decreased in both the OPL and IPL of the complexin 4a morphant retina at 4.3 dpf (Figure 5-11B). Staining with the pan-complexin 3/4 antibody reveals

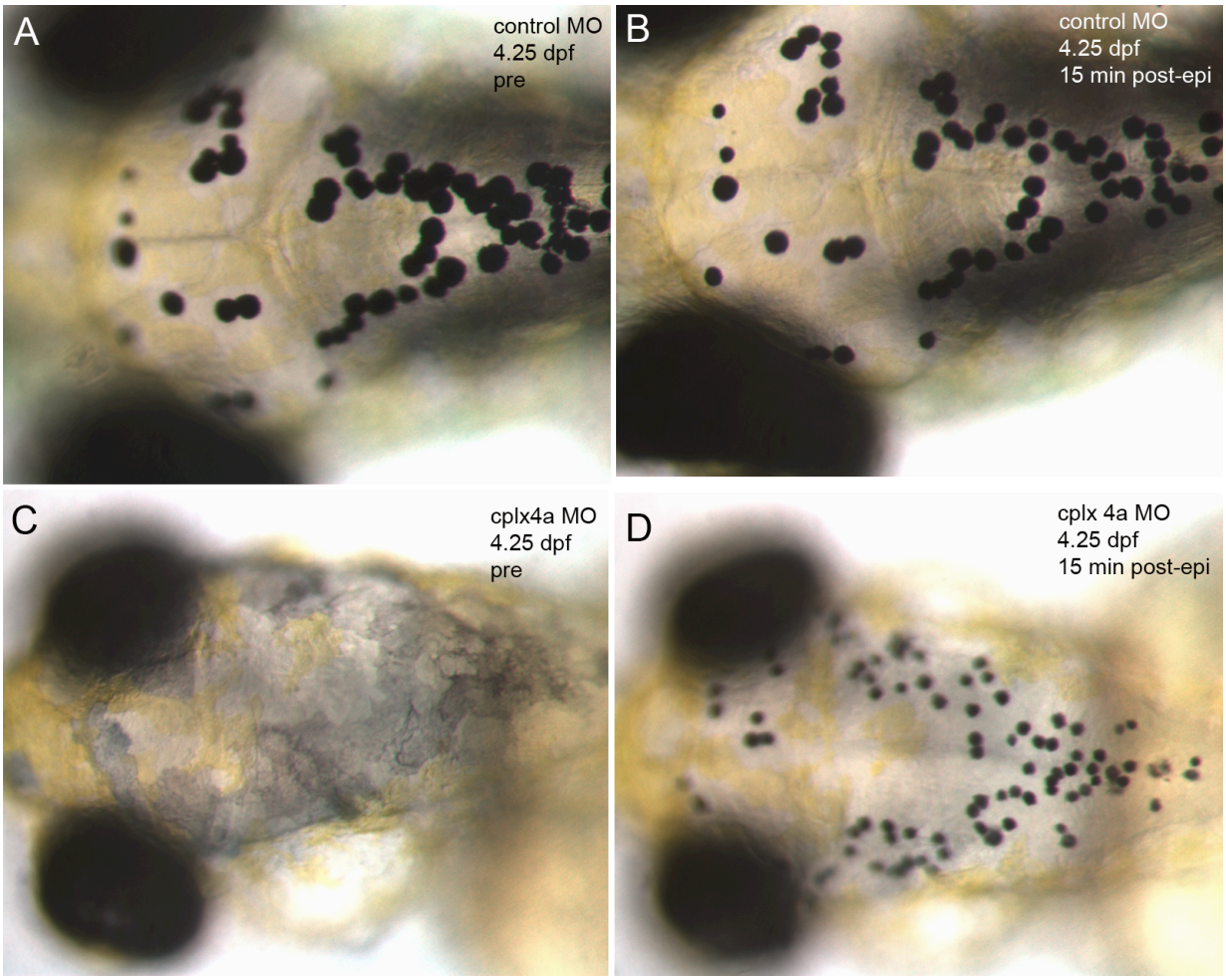

Figure 5-10. Epinephrine rescues the melanosome trafficking defect in complexin 4a morphants. Light micrographs of light-adapted control (A, B) and complexin 4a (C, D) morphant larvae immediately before (A, C) and 15 minutes after continuous treatment with 10^{-3} M epinephrine (B, D). In the presence of light, control morphants have aggregated melanosomes (A) that cluster slightly more in the presence of epinephrine (B). Light-adapted complexin 4a morphants have dispersed melanosomes (C) that can aggregate in the presence of epinephrine (D).

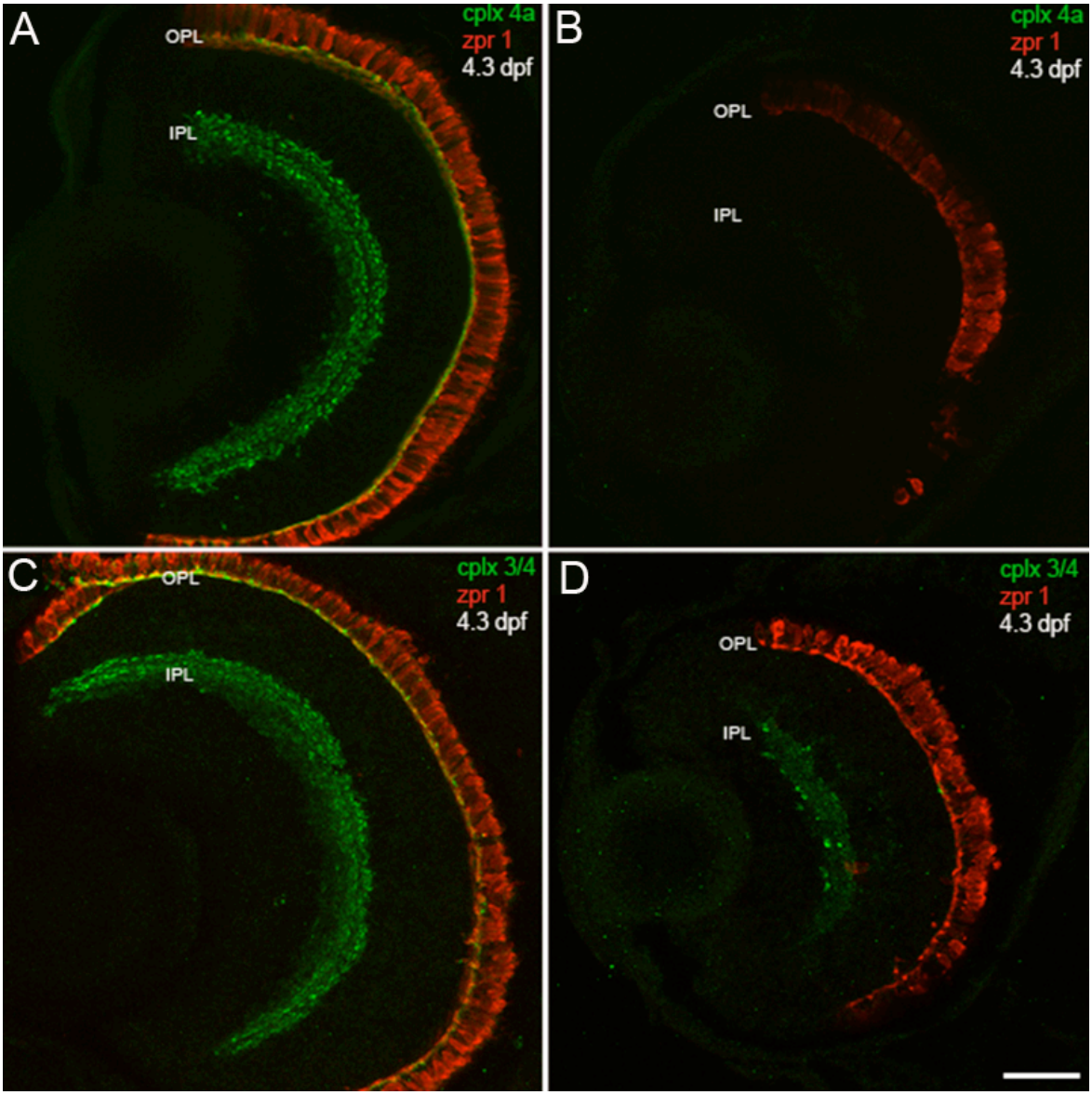

Figure 5-11. Knockdown of complexin 4a is maintained in the larval zebrafish retina. 4.3 dpf control (A, C) and complexin 4a morpholino-injected (B, D) larval zebrafish were sectioned transversely and stained with anti-zpr 1/FRet 43 (red) and either anti-complexin 4a (A, B) or anti-complexin 3/4 (C, D) (green). The complexin 4a translation-blocking morpholino dramatically decreases complexin 4a expression in the retinal outer plexiform layer (OPL) and inner plexiform layer (IPL) (B). Some complexin 3/4 immunoreactivity remains in the complexin 4a morphant retina (D). Scale bar, 30 μm. Modified from Zanazzi and Matthews (2010) with permission from BioMed Central.

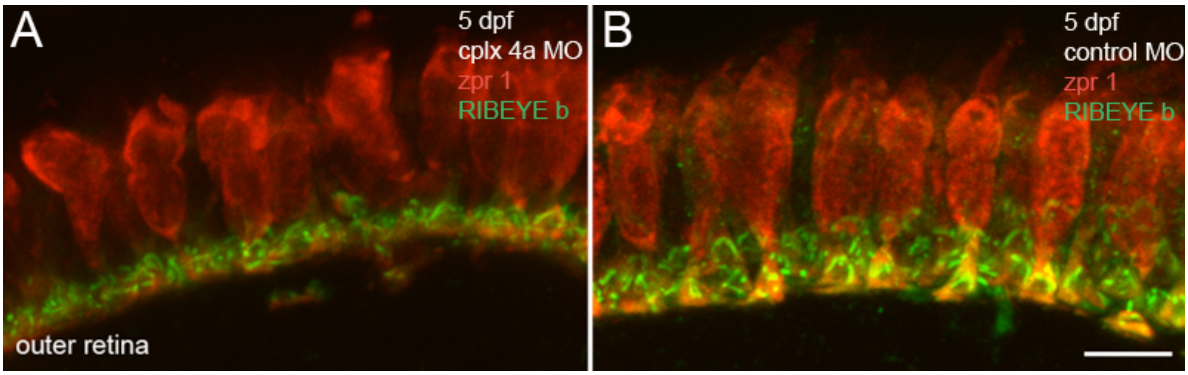

Figure 5-12. RIBEYE b expression in larval complexin 4a morphant retinal photoreceptors. These confocal micrographs of transverse sections of 5 dpf complexin 4a morphant (A) and control (B) larvae stained with anti-RIBEYE b (green) and anti-zpr 1/FRet 43 (red) show fewer RIBEYE b clusters in retinal photoreceptor presynaptic terminals in the complexin 4a morphants (A). Scale bar, 6 μm.

immunoreactivity primarily in the complexin 4a morphant IPL, especially in large terminals in sublamina b (Figure 5-11D). These results suggest that complexin 4a is a major complexin 3/4 isoform in visual system ribbon terminals. Consistent with the decreased number of photoreceptors in the complexin 4a morphants, there are fewer RIBEYE b curvilinear structures (that may correspond to ribbons) in the complexin 4a morphant retinal photoreceptors (Figure 5-12A) compared to controls (Figure 5-12B). Experiments examining the ultrastructure of complexin 4a morphant retinal photoreceptors and their responses to stimulus-induced depolarization are ongoing and will be discussed in Chapter 7.

Discussion

In this study, we address the roles of complexin 4a during zebrafish development. Loss of complexin 4a via knockdown with a translation-blocking morpholino antisense oligonucleotide results in hypopigmentation without affecting numbers or migration of neural crest cell-derived melanophores. Complexin 4a morphants do not undergo background adaptation during either their embryonic or larval stages, and lack an optokinetic response. Examination of visual system structure in the morphants reveals spherical, floating ribbons in pineal photoreceptor terminals and decreased numbers of retinal photoreceptors. Hence, complexin 4a plays a key role in pineal and retinal visual responses, as described below.

Mechanisms of background adaptation in embryonic and larval zebrafish

Fish and amphibians can profoundly and rapidly change their body color in response to light and circadian rhythms. These responses vary depending upon the age of the organism. Embryos lighten at night or in the presence of darkness due to the tonic release of its secreted hormone, melatonin, by photoreceptors (reviewed in Bagnara and Hadley, 1970). We have confirmed that zebrafish embryos whiten with dark adaptation due to melanosome aggregation. Complexin 4a morphants, however, do not exhibit this color change. Regardless of light levels, their melanosomes remain dispersed, which is their typical distribution in blinded states (Parker, 1948). Presumably, this dispersion is maintained by release of melanophore-stimulating hormone (MSH) from the pars intermedia of the pituitary. MSH plays a central role in the signaling pathways that regulate chromatosome trafficking (Figure 5-1). Preliminary experiments reveal that MSH expression is normal in the complexin 4a morphant pituitary (data not shown). The effects of MSH are counterbalanced in teleosts by a posterior pituitary hormone---melanin-concentrating hormone (MCH). A very recent paper has revealed that MCH is a downstream effector of the pineal in zebrafish background adaptation (Zhang et al., 2010). It is currently unclear whether the background adaptation defects in the complexin 4a morphant embryo are due to perturbation of MCH production or loss of melatonin production. Future studies should examine the effects of exogenous melatonin and/or MCH on complexin 4a morphants. It is possible that there are intrinsic defects in melanosome trafficking by the melanophores. Rescue experiments utilizing epinephrine had no effect on melanosome trafficking in wildtype, control morphant and complexin 4a morphant embryos (data not shown), which is consistent with work done in other wildtype organisms showing that there is a developmental switch in catecholamine sensitivity (reviewed in Parker, 1948).

There is a developmental switch in background adaptation that occurs in teleosts and amphibians, usually around the time of hatching or around the acquisition of eye movements (reviewed in Parker, 1948). Wildtype teleost and amphibian larvae and adults will adapt to light by aggregating their melanosomes, thereby lightening their integument. When wildtype anamniotes are placed in the dark, they will disperse their melanophores, thereby darkening their integument. This behavioral response is an indicator of normal retinal phototransduction and synaptic transmission. In the complexin 4a morphant larvae, residual melanosomes are dispersed regardless of light conditions but can aggregate in response to exogenous epinephrine. From

these experiments, we conclude that the complexin 4a morphant larvae fail to respond to ambient light levels due to defective retinal function.

Possible role of complexins and ribbon-associated signaling in visual responses

Many studies have shown that ribbons are upregulated at night (and downregulated during the day) in pineal photoreceptors (for review, see Vollrath, 1981). This rhythm correlates strongly with the circadian production of melatonin that is most pronounced at night. Given that pineal photoreceptors make ribbon synapses onto other pineal photoreceptors (see Vollrath, 1981), exocytosis from pineal photoreceptor ribbon presynaptic terminals may normally lead to the tonic production of melatonin and aggregated melanosomes (leading to blanching in darkness). Conversely, light may inhibit glutamate release and subsequent melatonin production. Since the complexin 4a morphant exhibits melanosomes that are "locked" in a dark-adapted state, our data are consistent with a role for complexin 4a as a brake for glutamate release in the light that is normally lifted in darkness. To determine whether exocytosis in photoreceptors is dysregulated in complexin 4a morphants, we have generated transgenic zebrafish that express a reporter of synaptic vesicle trafficking (see Chapter 7).

At night, while synaptic ribbons are upregulated in the pineal, they are downregulated in retinal photoreceptors (see, for example, Vollrath and Spiwoks-Becker, 1996). This downregulation of ribbon-associated signaling leads to dramatic deficiencies in vision at night for zebrafish larvae (Emran et al., 2010). Given these opposite circadian changes in retinal ribbon synaptic transmission (when compared to the pineal), it is intriguing that the retina and pineal mediate opposite effects on background adaptation. This may be due to the temporal activation (day versus night) of ribbon signaling in the two organs. We hypothesize that retinal photoreceptor ribbon-associated signaling leads to aggregated melanosomes and blanching of the anamniote. These results are consistent with our finding that complexin 4a in retinal ribbon presynaptic terminals is necessary for background adaptation. Our results are also consistent with the recent report that the complexin 3/4 double knockout mouse has decreased b-wave amplitudes, and increased implicit times, on an electroretinogram. Defective OPL synaptic transmission in the knockout is accompanied by increased floating spherical ribbons and slightly decreased levels of RIBEYE (Reim et al., 2009). In sum, these results indicate an evolutionarily required role for members of the complexin 3/4 subfamily in visual system signal transmission.

Chapter 6

Multiple roles for complexin 3a during zebrafish development

Introduction

Multiple molecular mechanisms regulate the dorsoventral patterning of the vertebrate body axis during early development (reviewed in Schier and Talbot, 2005; Lupo et al., 2006). Growth factors and transcription factors are expressed in specific spatial domains, and their activities are integrated to specify either a ventral fate or a dorsal fate for that domain. Signaling by bone morphogenetic proteins (BMPs) and Wnts are critical for specifying ventral cell fate. On the opposite side, the Spemann-Mangold organizer secretes several factors such as chordin, noggin and follistatin that inhibit ventralizing signals to produce the default dorsal fate (reviewed in Schier and Talbot, 2005; Lupo et al., 2006). The identification of several zebrafish mutants with expanded dorsal (Mullins et al., 1996) or ventral (Hammerschmidt et al., 1996) domains has contributed greatly to our understanding of the signaling pathways that underlie early dorsoventral patterning. Dorsalized mutants, depending upon the strength of the phenotype, have expanded anterior somites and a large notochord at the expense of tail formation (Mullins et al., 1996).

The developing eye field is also patterned along a dorsoventral axis by a distinct combination of growth factors and transcription factors (Figure 6-1) (reviewed in McLaughlin et al., 2003; Lupo et al., 2006). A recent study revealed that a secreted growth factor called radar specifies retinal dorsal fate, possibly through downstream BMP and T-box transcription factor activities (Gosse and Baier, 2009). To specify the ventral retina, sonic hedgehog acts through the ventral anterior homeobox (vax) proteins (Kim and Lemke, 2006). Vax 1 and vax 2 play critical roles in ventralizing the eye (Bertuzzi et al., 1999; Mui et al., 2002; Mui et al., 2005). In particular, vax 1 and vax 2 promote the differentiation of the ventral optic stalk progenitors into optic nerve astrocytes. In the absence of both transcription factors, these progenitors differentiate into dorsal neural retina (Mui et al., 2005).

In this study, we found that complexin 3a is structurally homologous to the vax family of transcription factors and may have roles in dorsoventral patterning. Injection into zebrafish embryos of a splice-blocking antisense morpholino oligonucleotide specific for complexin 3a

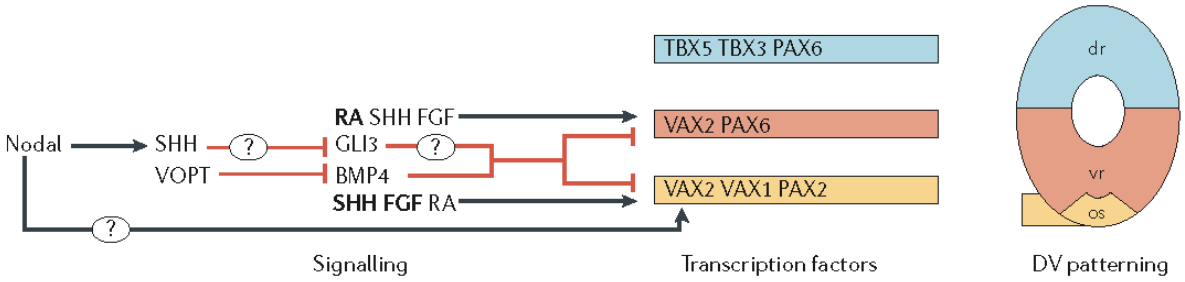

Figure 6-1. Molecular mechanisms underlying dorsoventral patterning in the developing eye. The eye vesicle is subdivided into three main regions—the optic stalk (os), the ventral retina (vr) and the dorsal retina (dr)— each of which expresses a distinct combination of transcription factors. Specification of vr and os requires inhibition of BMP signals by ventroptin (VOPT, chordin-like 1). SHH is required to specify both the vr and os, but whether it acts by inhibiting formation of the repressor form of GLI3 is not known (indicated by the question marks). Nodal signals act upstream of SHH and might also have a direct role in os specification. High RA (bold) and low SHH and FGF levels are involved in vr specification, whereas low RA and high SHH and FGF (bold) levels are involved in os specification. TBX3/5, T-box 3/5; VAX1/2, ventral anterior homeobox-containing gene 1/2. Modified from Lupo et al. (2006) with permission from Macmillan Publishers Ltd.

results in a dorsalized-like phenotype. This morpholino allowed for the production of a truncated complexin 3a that retained its SNARE-binding domain. The complexin 3a morphants have additional defects in eye development including microphthalmia, retinal differentiation and lamination. While overexpression of full-length complexin 3a also dorsalizes zebrafish embryos, overexpression of complexin 4a has no effect on dorsoventral patterning. Taken together, these results suggest that complexin 3a levels may regulate dorsoventral patterning during early zebrafish development.

Results

Modulation of complexin 3a levels dorsalizes zebrafish embryos and impairs visual behavior

To begin to determine the functions of other complexin 3/4 subfamily members, we designed a morpholino antisense oligonucleotide that targets the splice acceptor site between the second intron and third exon of complexin 3a pre mRNA (Figure 6-2A). Through steric blocking, this morpholino should inhibit nuclear processing of the complexin 3a pre mRNA such that intron 2 is not spliced out of the mature transcript. The presence of a stop codon in the second intron should lead to the production of a complexin 3a mRNA that lacks exon 3. It should

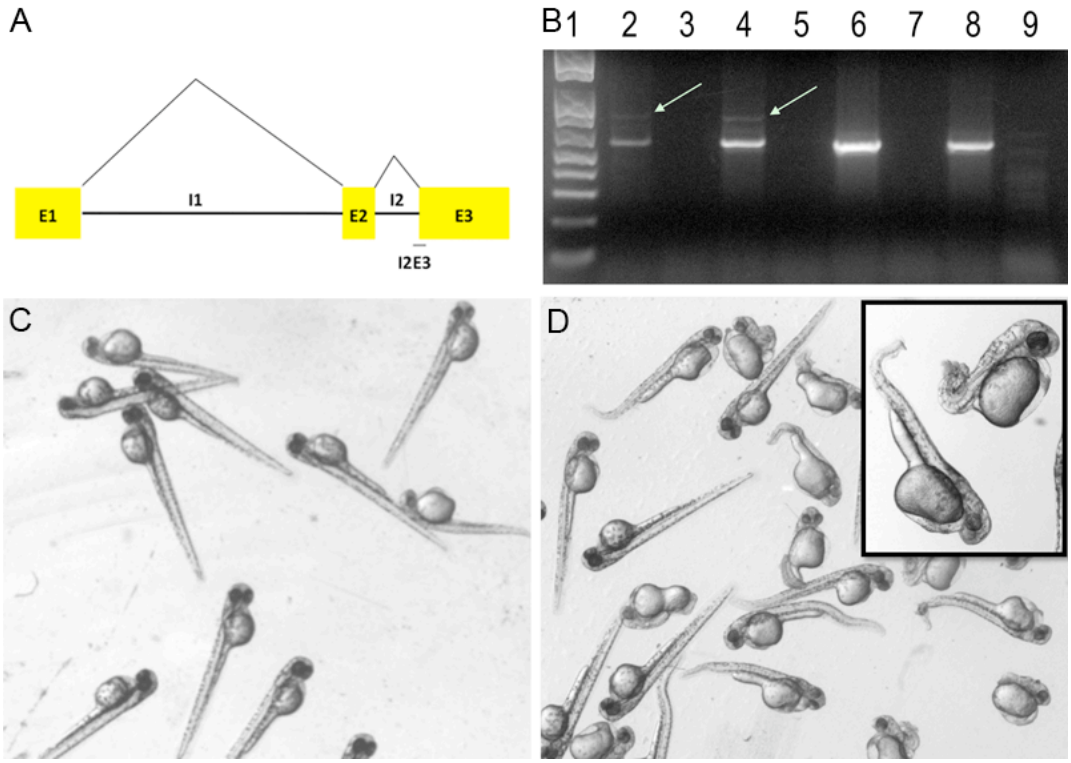

Figure 6-2. A splice-blocking morpholino directed against complexin 3a dorsalizes zebrafish. A. Morpholino (MO) antisense oligonucleotide specific for the junction of intron (I) 2 and exon (E) 3 in complexin 3a. This MO prevents intron 2 from being spliced out, leading to the insertion of a stop codon that truncates the protein after exon 2. B. RT-PCR analysis of complexin 3a mRNA in I2E3 MO-injected (lanes 2-5), control MO-injected (lanes 6-7), and wildtype 4.5 dpf larvae (lanes 8-9). Lanes 2, 4, 6, and 8 contain PCR products from RT cDNA, while lanes 3, 5, 7, and 9 contain products from non-RT cDNA. The I2E3 MO leads to the production of an abnormally large transcript (arrows) that contains intron 2 (data not shown). C., D. Light micrographs of control MO-injected and I2E3 MO-injected embryos, respectively, at 2.2 dpf. The complexin 3a morphants display a dorsalized phenotype that varies in its phenotypic strength (inset).

be noted that exon 2, which encodes the SNARE-binding domain, should remain in the mutant complexin 3a mRNA. This strategy was undertaken given the lack of a complexin 3a-specific antibody to assay the effectiveness of a translation-blocking morpholino. Furthermore, this splice junction was targeted as it allowed for reliable assay of transcript alteration with RT-PCR analysis.

Injection of the splice-blocking antisense morpholino oligonucleotide specific for complexin 3a into zebrafish embryos results in mutants with dorsalized-like phenotypes (Mullins et al., 1996) that vary in their phenotypic strengths (Figure 6-2D). Compared to the controls (Figure 6-2C), there is an expansion in dorsally-derived structures and a reduction in ventrally-derived structures in some of the complexin 3a morphants (Figure 6-2D). For example, the

notochord is larger in the complexin 3a morphants while the ventrally-derived tail is curly and nearly absent (see Figure 6-2D, inset). Dorsoventral pattern formation in the morphants is already abnormal at 1 dpf (data not shown). By RT-PCR analysis, we confirmed that the morphants contained a complexin 3a transcript with an intron (Figure 6-2B) that included a stop codon, leading presumably to a truncated protein. PCR product without the insertion of intron 2 was predicted to be 423 nucleotides in length, while the insertion of intron 2 would result in a product of 519 nucleotides. The larger transcript was gel-purified, sequenced, and found to encode a transcript with the intron and stop codon (data not shown).

Similar to the complexin 4a morphants (Chapter 5), the complexin 3a larval morphants exhibit microphthalmia. Unlike the complexin 4a morphants, which exhibit normal retinal lamination and differentiation, the complexin 3a morphant retina displays gross defects in retinal patterning and differentiation (Figure 6-3B). These retinas are characterized by patchy zpr 1/FRet 43 that sometimes extends radially into the inner retina. Similarly, PKC immunoreactivity is also not well-laminated (Figure 6-3B) compared to controls (Figure 6-3A). Not surprisingly, these morphants lack an optokinetic response at 4.5 dpf (Figure 6-3C).

Injection of 50 pg full-length complexin 3a mRNA into one-celled zebrafish embryos also results in dorsalization that is apparent during embryogenesis (Figure 6-4B). This effect is dose-dependent as injection of 150 pg of complexin 3a leads to more severe dorsalized phenotypes (data not shown). Injection of either 50 pg of lacZ mRNA (Figure 6-4A) or 50 pg of complexin 4a mRNA (Figure 6-5B) has no effect on dorsoventral patterning. Taken together, these results suggest that perturbation of complexin 3a levels specifically leads to defects in patterning of the zebrafish embryo.

Injection of a complexin 3b morpholino antisense oligonucleotide does not perturb zebrafish development or affect visual behavior

Given the early developmental effects of complexin 3a perturbation, we also analyzed the effects of a morpholino antisense oligonucleotide directed against the first ATG of complexin 3b. Injection of this morpholino has no effect on zebrafish morphology up to 5 dpf (data not shown). Furthermore, complexin 3b morphants have a normal optokinetic response at 4.5 dpf (Table 6-1). These results are consistent with low, if any, expression of complexin 3b in zebrafish larvae (see Chapter 4).

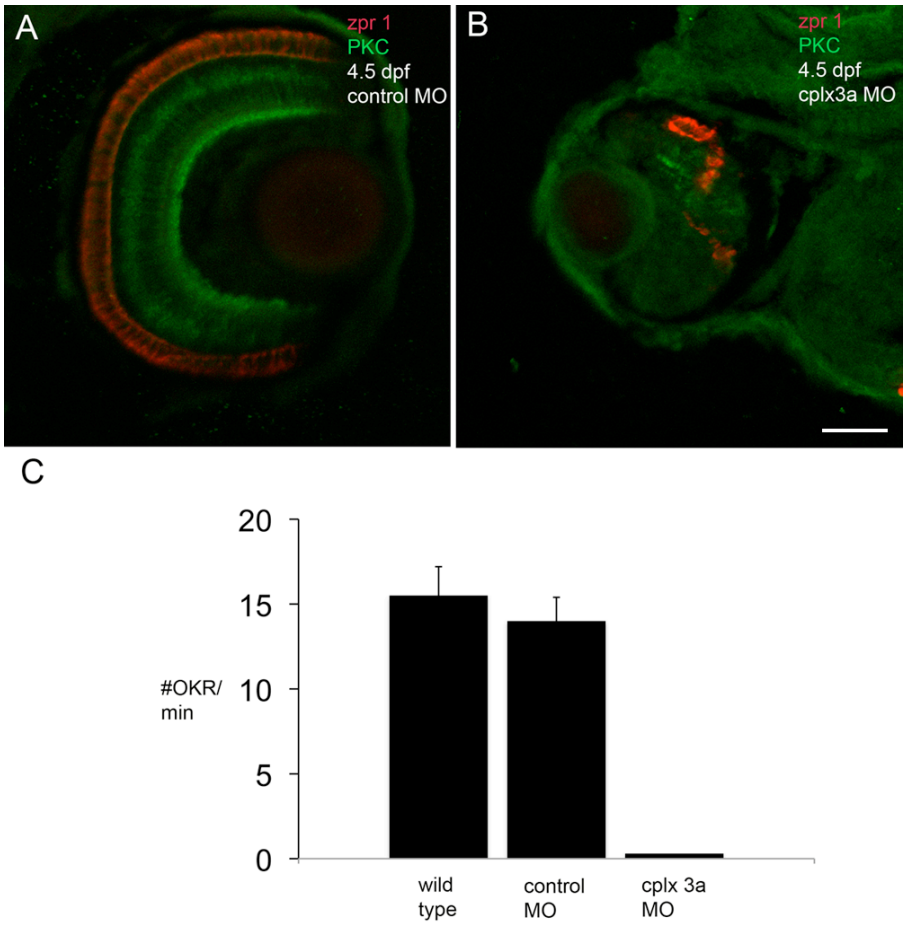

Figure 6-3. Complexin 3a morphants lack an optokinetic response and display multiple eye abnormalities. 4.5 dpf control MO-injected (panel A) and complexin 3a MO-injected (panel B) larval zebrafish eyes were sectioned coronally and stained with anti-zpr 1 (red) and anti-PKC (green). These confocal projections reveal microphthalmia, decreased numbers of photoreceptors and bipolar cells, and abnormal retinal lamination in the complexin 3a morphants. Scale bar, 50 μm. Panel C shows the mean values and SEM for the number of optokinetic responses (OKR) per minute elicited from 4.5 dpf larvae (n=10 for each group of larvae). The number of OKR elicited from the complexin 3a morphants was significantly less than that obtained from wildtype or control MO-injected larvae (Student's t-test, $p \leq 0.005$). Scale bar, 50 μm.

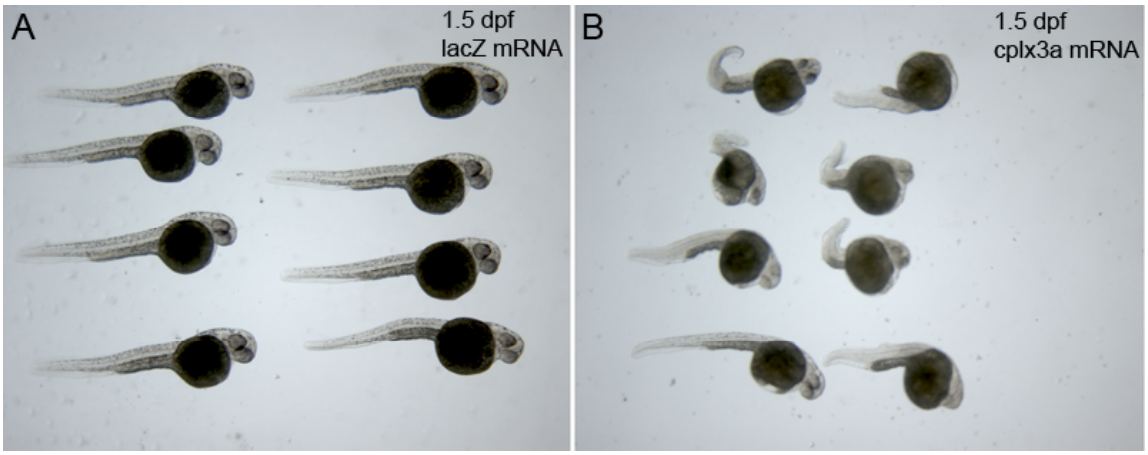

Figure 6-4. Overexpression of full-length complexin 3a mRNA promotes dorsalization. 50 pg of either lacZ mRNA (A) or complexin 3a mRNA (B) was pressure-injected into single-celled zebrafish embryos, and embryos were then maintained for 36 hours at 28.5°C. These brightfield micrographs show that many complexin 3a overexpressors have a dorsalized phenotype (B).

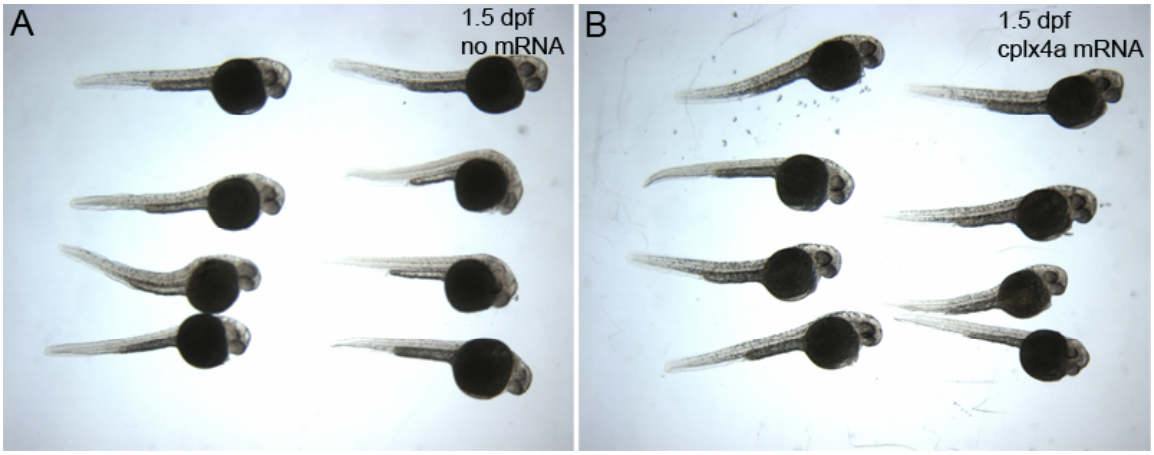

Figure 6-5. Overexpression of full-length complexin 4a mRNA does not affect dorsoventral patterning. 50 pg of complexin 4a mRNA (B) was pressure-injected into single-celled zebrafish embryos, and embryos were then maintained for 36 hours at 28.5°C. These brightfield micrographs show that the complexin 4a overexpressors appear very similar to embryos that were not injected (A).

4.5 dpf zebrafish	**# OKR/min**
wildtype	12 +/- 1.1
Control MO (7.5 ng)	12 +/- 0.8
Cplx 3b MO (7.5 ng)	11 +/- 2.4

Table 6-1. Microinjection of an antisense morpholino targeting the first ATG of complexin 3b does not perturb optokinetic responses.

Complexin 3a and 3b are members of the ventral anterior homeobox family

During the course of these studies, ENSEMBL classified complexin 3 orthologs, but not complexin 4 orthologs, in the ventral anterior homeobox 1 (vax1) family of transcription factors (http://www.ensembl.org/Danio_rerio/familyview? family=ENSF00000001861). Alignment of the zebrafish complexin 3a and 3b proteins with zebrafish vax 1 reveals highest identity over the vax 1 homeodomain, which covers the complexin 3 SNARE-binding domain (Figure 6-6). Re-analysis of this region in complexin 3 proteins with several algorithms revealed that it falls short in being classified as a homeodomain (data not shown). It remains to be determined whether this domain in complexin 3 can function as a homeodomain to affect dorsoventral patterning.

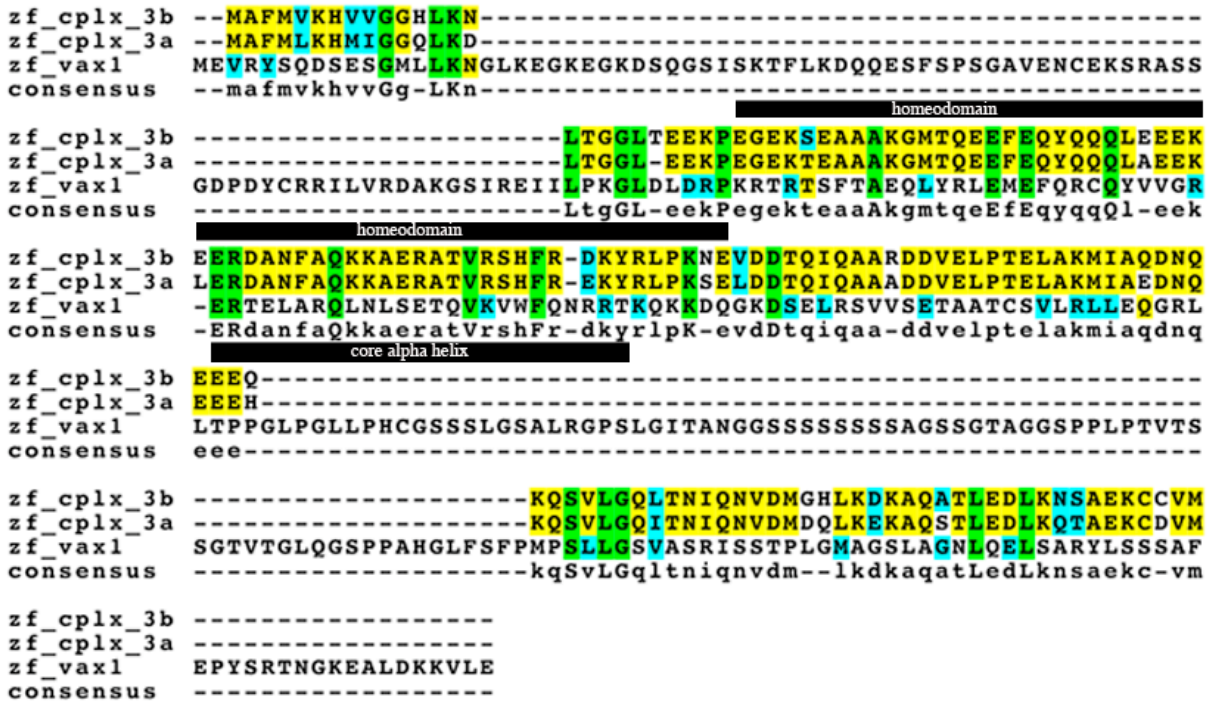

Figure 6-6. CLUSTALW alignment of zebrafish complexin 3a, 3b and vax1 proteins. The green shaded regions highlight amino acids that are conserved in zebrafish complexin 3a, 3b and vax1. The yellow shaded regions denote amino acids conserved between complexin 3a and 3b only. Conserved amino acid substitutions are shown in aqua blue. The position of the vax 1 homeodomain is marked above the aligned sequences, and the complexin core alpha helix is marked below the aligned sequences. Note that the core alpha helix is located within the homeodomain. Cplx, complexin; vax, ventral anterior homeobox; zf, zebrafish.

Discussion

In this study, we examined the functions of the complexin 3 paralogs during zebrafish development. Injection of a splice-blocking antisense morpholino oligonucleotide specific for complexin 3a has pleiotropic effects during zebrafish development. Dorsoventral pattern formation in the morphants is abnormal at 24 hpf, and this abnormality persists during embryogenesis. Overexpression of complexin 3a mRNA, but not overexpression of complexin 4a, also leads to dorsoventral patterning defects during embryogenesis. The complexin 3a morphant larvae display several visual system abnormalities, including microphthalmia and abnormal retinal differentiation and lamination, which likely contribute to the lack an optokinetic response at 4.5 dpf. Whether these effects on eye development are related to dorsoventral patterning defects is currently unclear. However, the retinal lamination defects seen in the complexin 3a morphants are not strictly defects in dorsoventral patterning. Both the ventral optic nerve and the dorsal retina are still present in these morphants (data not shown), while in vax1/2 double knockouts, the eye is dorsalized such that the optic nerve differentiates into retinal tissue (Mui et al., 2005).

Complexins may be multifunctional proteins

In addition to their well-studied role as regulators of synaptic vesicle fusion, we have provided evidence in this chapter for additional roles for the complexins during development of the zebrafish embryo. The mechanisms by which complexin 3a may regulate cell fate during development are unknown. A first step to address these questions may be to determine whether several newly identified domains in complexin 3a are functional. Does the bipartite nuclear localization signal allow for complexin 3a to shuttle into the nucleus during development? If so, does complexin 3a bind to DNA, possibly through its homeodomain-like region? Finally, does the complexin 3a PAZ domain (Lingel et al., 2003; Song et al., 2003; Yan et al., 2003) bind to RNA and promote post-transcriptional gene silencing in the cytoplasm? Elucidation of the functional roles of these domains may shed light on the possible functions of complexin 3a during development.

Dual roles for components of the ribbon exocytotic machinery are not without precedent. Indeed, RIBEYE/CtBP2 is a bifunctional gene whose protein products function in ribbon formation and transcriptional corepression (reviewed in Piatigorsky, 2001). CtBP2 regulates

differentiation in several cell types due to its control of transcription (reviewed in Piatigorsky, 2001). In zebrafish retinal bipolar cells, RIBEYE a regulates a late step in differentiation, although it is currently unclear whether this is a secondary defect due to impaired synaptic transmission (Wan et al., 2005). SNAP-25 is required for rodent photoreceptor differentiation (Greenlee et al., 2002) and the development of several neuronal cell types (Johansson et al., 2008), but it is also unknown whether these are direct effects on transcription. Given that SNAREs are expressed during the earliest stages of development (reviewed in Hepp and Langley, 2001), it will be important to determine whether SNARE complex proteins and their regulators have direct roles in the determination of cell fate.

Chapter 7
Conclusions and Future Directions

Vertebrate sensory receptor cells transduce and transmit a broad range of information, with high fidelity over a prolonged period of time, via specialized organelles that are polarized to distinct subdomains. In the apical part of receptor cells, exquisitely sensitive, modified cilia and microvilli detect photons and pressure waves, respectively, and convert these signals into graded changes in membrane potential. The basolateral presynaptic terminals contain proteinaceous ribbons that modify their release of synaptic vesicles in response to these graded changes. The molecular mechanisms that underlie the development and functions of these organelles are incompletely understood. This dissertation focused on the development and functions of some molecular and subcellular specializations that support the transduction and transmission of sensory signals in ribbon-containing neurons. In particular, we analyzed the expression and functions of a novel subfamily of SNARE complex regulators, composed of complexin 3 and complexin 4, during development and in the adult zebrafish.

At conventional synapses, complexins appear to stabilize the SNARE complex in a fusion-ready state before calcium enters the presynaptic terminal and binds to synaptotagmin. Therefore, the identification of ribbon-specific isoforms of these synaptic regulators is of special interest. By searching the ENSEMBL and GenBank databases, we identified and subsequently cloned five zebrafish orthologs that show 50-75% amino acid identity with mammalian complexins 3 and 4. Phylogenetic analysis revealed two complexin 3 paralogs and three complexin 4 paralogs. Utilizing a polyclonal antibody that recognizes all five isoforms, we demonstrated that these proteins are enriched in ribbon-containing sensory neurons during development and in the adult zebrafish. In particular, complexin 3/4 overlaps with zpr 1 in terminals of double cone photoreceptors in the retinal outer plexiform layer and in the pineal neuropil. Complexin 3/4 overlaps with protein kinase C in ON bipolar cell terminals in the inner plexiform layer. In hair cells of the inner ear and lateral line, however, complexin 3/4 is not expressed in their ribbon terminals. Rather, complexin 3/4 localizes to their apical compartment, at the base of their stereocilia. Utilizing a polyclonal antibody specific for complexin 4a, we find that this isoform is the predominant isoform in visual system ribbon terminals. Moreover, this isoform is not expressed in hair cells. Whole mount in situ hybridization with paralog-specific

riboprobes reveals that complexin 4b is the primary isoform expressed in zebrafish hair cells, suggesting that complexin 4 is triplicated with system-specific functions.

Knockdown and overexpression approaches reveal that complexins have multiple roles during zebrafish development. Modulation of complexin 3a levels affects dorsoventral patterning and eye development, while complexin 3b has no detectable function during early development. These proteins are homologous to members of the vax1 family of transcription factors. Knockdown of complexin 4a impairs background adaptation during embryogenesis and larval development, with minor changes in pineal and retinal photoreceptor presynaptic architecture. A defect in the optokinetic response of complexin 4a morphants confirms that complexin 4a is required for vision. We are currently investigating whether complexin 3/4 regulates synaptic vesicle exocytosis in photoreceptors and bipolar cells, as described below.

Future directions

Is there a decrease in evoked exocytosis in complexin 4a morphant pineal complex and retinal ribbon-containing neurons?

We have generated transgenic zebrafish that express a fluorescent reporter of exocytosis, called sypHy (Granseth et al., 2006; Zhu et al., 2009), in ribbon-containing neurons. This reporter consists of synaptophysin fused to a pH-sensitive GFP (pHluorin). We have generated six lines of transgenic zebrafish. Three lines of fish express synaptophysin tagged to either one, two, or four pHluorin molecules (subsequently called 1x, 2x, or 4x sypHy) under the control of a heat shock promoter (hsp 70), and the other three lines of fish express 1x, 2x, or 4x sypHy under the control of an mGluR6 promoter to drive expression in retinal ON bipolar cells. Heat shock of embryonic (Figure 7-1A), larval (data not shown), or adult (Figure 7-1D) hsp70-sypHy transgenic zebrafish for one hour at 37°C induces an increase in fluorescence from the eye over the ensuing 24 hours. In particular, retinal cones (but not bipolar cells) (Figure 7-1B, C, E, F) express robust levels of sypHy that is appropriately targeted to their presynaptic terminals. While hsp70-sypHy transgenic zebrafish are inducible and express very little sypHy constitutively (Figure 7-1A, top panel), mGluR6-sypHy transgenic zebrafish constitutively express sypHy in the eye (Figure 7-2A) starting at 3.5 dpf. Larval mGluR6-sypHy transgenic zebrafish exhibit punctate sypHy expression in the distal inner plexiform layer (Figure 7-2D) in putative large ON bipolar cell terminals (Figure 7-2E).

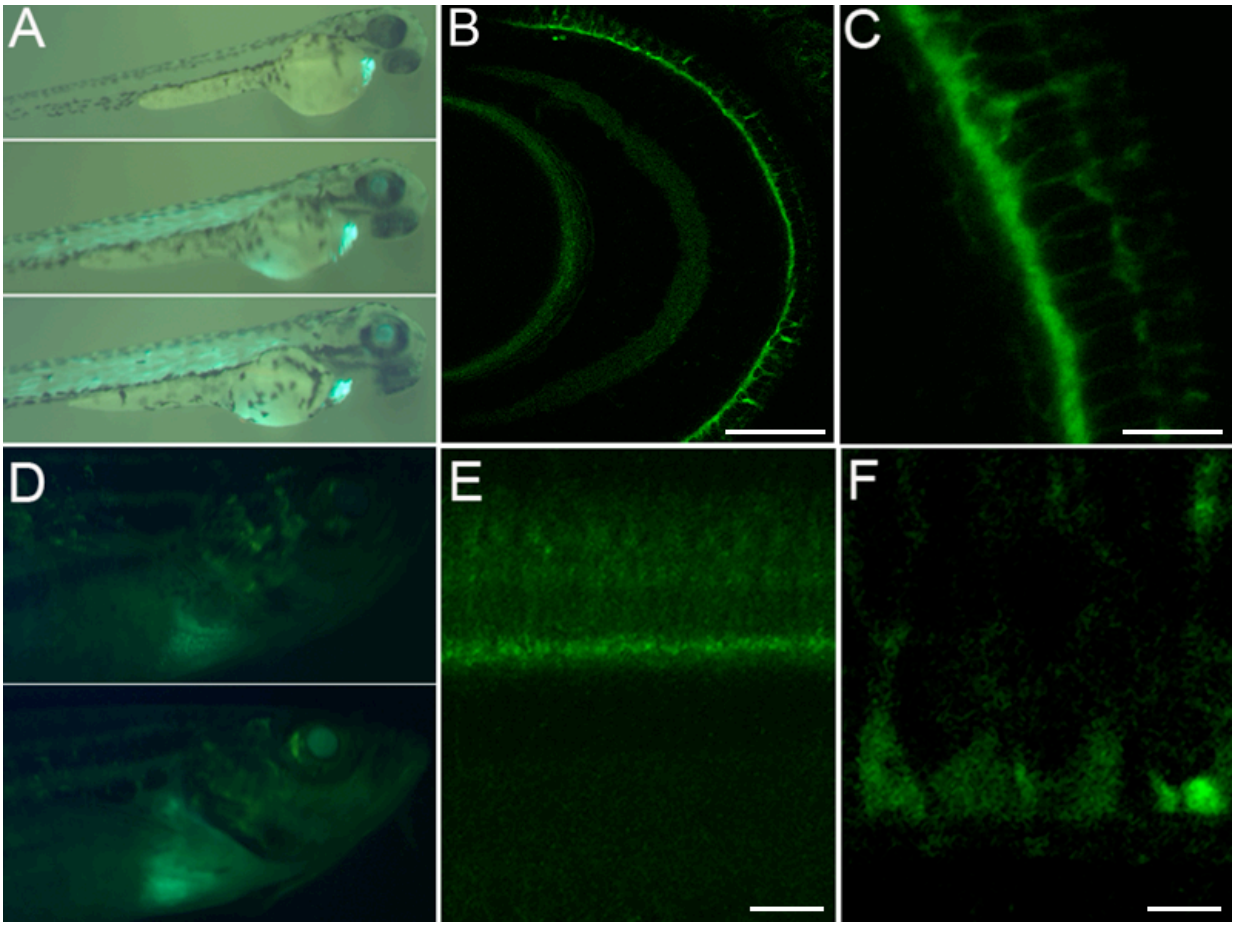

Figure 7-1. Generation of transgenic zebrafish that express sypHy in retinal photoreceptor terminals. A. A 2 dpf hsp70-1x sypHy transgenic zebrafish immediately before heat shock (upper panel) and at 4 (middle panel) and 10 hours post-heat shock (lower panel). Note the green fluorescence in the eye, muscle and yolk sac that increases progressively over the course of 10 hours. The green fluorescence in the heart is due to a minicassette, consisting of EGFP fused to the cardiac myosin light chain 2 promoter, which acts as an independent fluorescent transgenesis marker. B. Confocal projection through a frozen section of a 5 dpf transgenic zebrafish retina 4.5 hours after heat shock. SypHy expression localizes to the outer plexiform layer (OPL), but not the inner plexiform layer (IPL) or somatic layers of the larval retina. C. Higher magnification reveals that sypHy localizes primarily to presumptive cone terminals in the OPL. D. Epifluorescence micrographs of a 9 mpf, non-heat shocked transgenic zebrafish (upper panel) and a transgenic 8 hours after heat shock (lower panel). E. Confocal projection of a retinal frozen section of a heat shocked adult transgenic zebrafish.SypHy continues to be expressed in the OPL, but not the IPL, of the zebrafish retina. F. Higher magnification reveals that sypHy localizes to presumptive adult cone terminals (arrows). Scale bars, 50 μm (B), 10 μm (C), 25 μm (E), 5 μm (F).

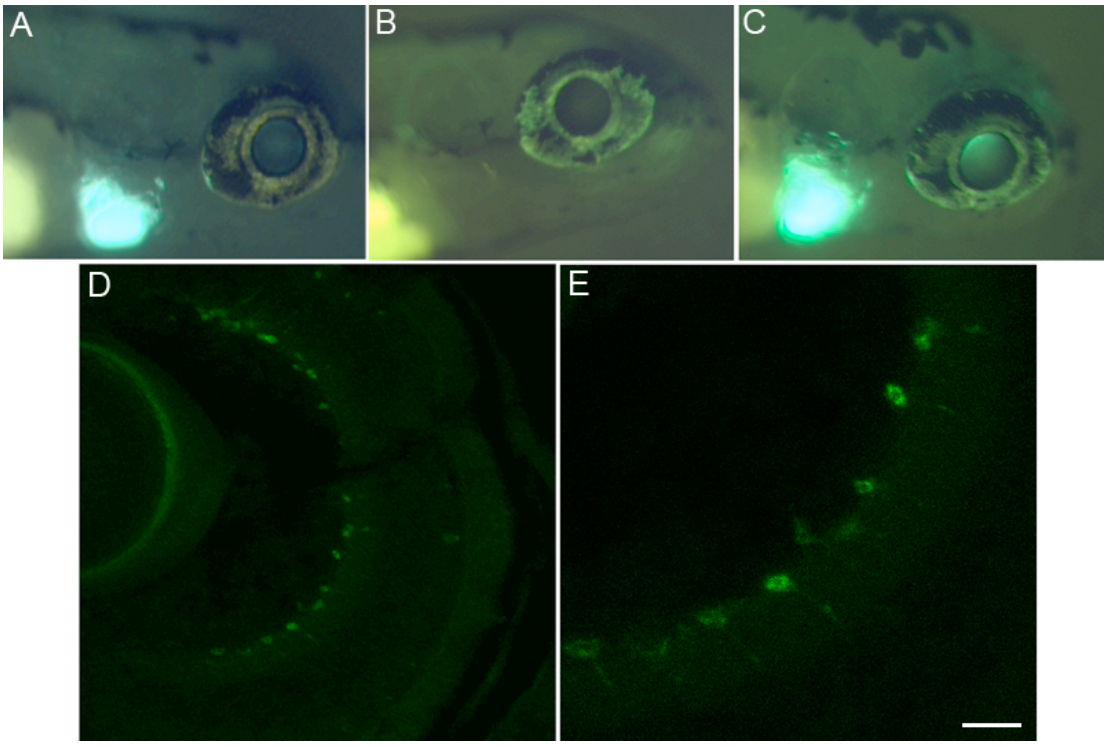

Figure 7-2. SypHy is targeted to putative ON bipolar cell terminals in mGluR6 transgenic zebrafish. A. 8 dpf transgenic zebrafish expressing 1x sypHy under the control of the mGluR6 promoter. The green fluorescence in the heart is due to the minicassette consisting of EGFP fused to the cardiac myosin light chain 2 promoter, which acts as an independent fluorescent transgenesis marker. B. 7 dpf wildtype zebrafish larva. C. 8 dpf transgenic zebrafish expressing EGFP under the control of the mGluR6 promoter. Note the higher level of expression in the eye of this fish compared to the mGluR6-1x sypHy fish. D. 4 dpf mGluR6-1x sypHy fish were fixed, frozen, sectioned, immersed in PBS pH 7.4 and imaged. This panel shows a confocal projection through the eye of one transgenic. Expression is primarily found in the IPL, with much lower expression within somata in the ONL. E. Labeled synaptic terminals located at the inner edge of the IPL are synaptic terminals of Mb1 bipolar cells. Scale bar, 25 μm (D), 10 μm (E).

Besides retinal photoreceptors, the hsp70 promoter drives sypHy expression in other organs, including the pineal (Figure 7-3A), inner ear (Figure 7-3B), and lateral line (Figure 7-3C). To address whether complexin 4a impairs evoked exocytosis, one can therefore inject the complexin 4a morpholino into single-celled sypHy transgenics and stimulate the morphant ribbon-containing neurons with high potassium during embryogenesis or in the young larvae. Since complexin 4a is not expressed in the inner ear or lateral line hair cells (Chapter 2, Chapter 3), these cells provide internal controls to examine whether knockdown of complexin 4a impairs evoked exocytosis. Initial attempts to isolate healthy retinal photoreceptors and bipolar cells by enzymatic digestion from 4-5 dpf larval transgenic zebrafish proved unsuccessful. Further

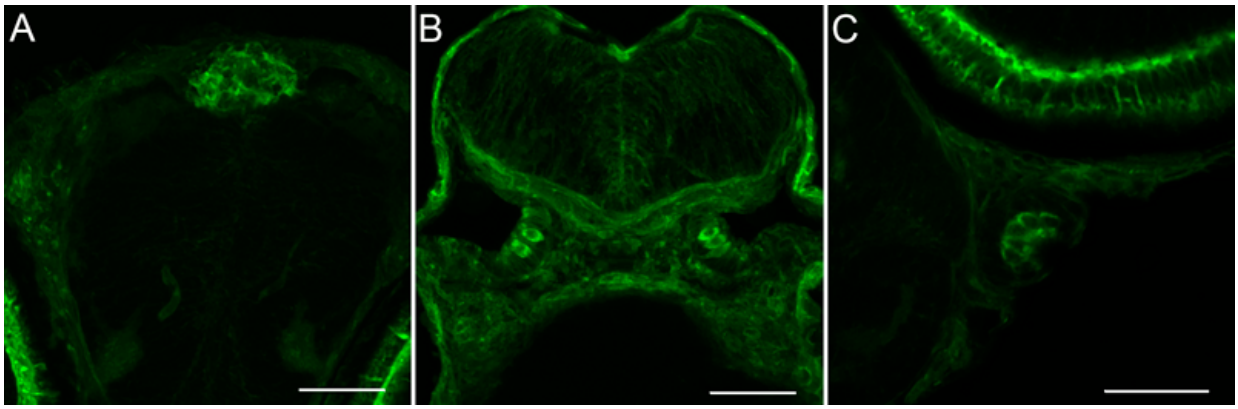

Figure 7-3. The hsp70 promoter drives sypHy expression in pineal photoreceptors and hair cells. Besides retinal photoreceptors, this promoter drives strong expression of sypHy in the larval (5 dpf) pineal (A) as well as in larval hair cells of the inner ear (B) and lateral line (C). Scale bars, 50 μm (A, B), 40 μm (C).

modification of the pronase digestion protocol may prove useful. We also attempted to stimulate the pineal organ of live transgenic morphants, but sypHy fluorescence on the skin and/or muscle (see Figure 7-1A) obscures the fluorescence from the pineal. An additional alternative preparation could be the use of retinal slices from morphant transgenic larvae.

Does a peptide from the complexin 3 SNARE-binding domain localize to ribbons and affect exocytosis?

One approach to examine complexin 3/4 function in adults may be to dialyze a complexin peptide directly into ribbon-containing neurons. This approach has recently been used for syntaxin 3b in goldfish bipolar cells (Curtis et al., 2010). Tokumaru et al. (2001) identified a peptide, called SBD-2 (SNARE-binding domain-2), which blocks the interaction between squid complexin and syntaxin. This peptide (EEMRQTIRDKYGLKK, amino acids 63-77 in squid complexin) inhibits evoked exocytosis when microinjected into the squid giant synapse. Half-maximal inhibition occurs at a peptide concentration of 1-2 mM. Since mouse rod bipolar cells only express complexin 3 (Reim et al., 2005; this study), we chose to synthesize a fluorescent mouse complexin 3 peptide that can be dialyzed into mouse rod bipolar cells. The amino acid sequence homologous to squid SBD-2 in mouse complexin 3 is ATLRSHFRDKYRLPK (amino acids 70-84 in mouse complexin 3). This complexin 3 peptide may be considered a dominant-negative since it does not include the amino terminus of the complexin protein, which has been shown to be necessary for exocytosis (Xue et al., 2007).

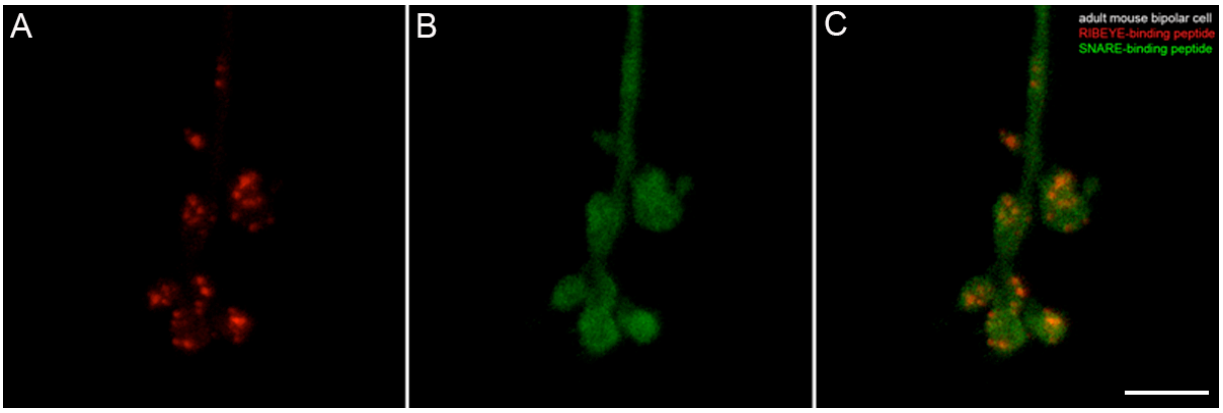

Figure 7-4. Live adult mouse retinal bipolar cell terminals dialyzed with RIBEYE-binding peptide and mouse complexin 3 peptide. Dissociated adult mouse retinal bipolar cell somata were patch-clamped, dialyzed with 30 μM RIBEYE-binding peptide (red) and 1 mM complexin 3 peptide (SNARE-binding peptide, green), and the presynaptic terminals were imaged approximately 1-2 minutes after break-in. Panel A shows RIBEYE-binding peptide puncta and panel B shows complexin 3 peptide in the distal axon and presynaptic terminals of a representative mouse bipolar cell. Panel C shows an overlay of these two confocal micrographs, which are projections of a series of z-axis optical sections through the terminals. Scale bar, 5 μm.

After live adult mouse retinal rod bipolar cells were patch-clamped and dialyzed with the complexin 3 peptide (along with a fluorescent RIBEYE-binding peptide), ribbons were readily labeled (Figure 7-4A) while the fluorescent complexin 3 peptide appears to be primarily diffuse throughout the bipolar cell axon and terminals (Figure 7-4B). In fixed adult mouse retinal rod bipolar cells, ribbons were labeled with an anti-CtBP2 antibody (Figure 7-5A, B, red) while the complexin 3 peptide appeared primarily diffuse (Figure 7-5A, B, green). However, profile plots of presynaptic terminals suggest some colocalization of the RIBEYE-binding peptide (red) and complexin 3 peptide (green) (Figure 7-6). Given the high concentration of complexin 3 peptide used in these studies (1 mM), it is likely that lower concentrations will show a more restricted distribution. Future studies should be performed to determine the Kd of the complexin 3 peptide, and to determine whether the peptide affects exocytosis in mouse bipolar cells. Since there are only 1-2 amino acid differences between the mouse complexin 3 peptide and the homologous zebrafish complexin 3 peptides, the mouse complexin 3 peptide may also be used to investigate exocytosis in zebrafish bipolar cells, some of which have large presynaptic terminals (~8 μm, personal observations).

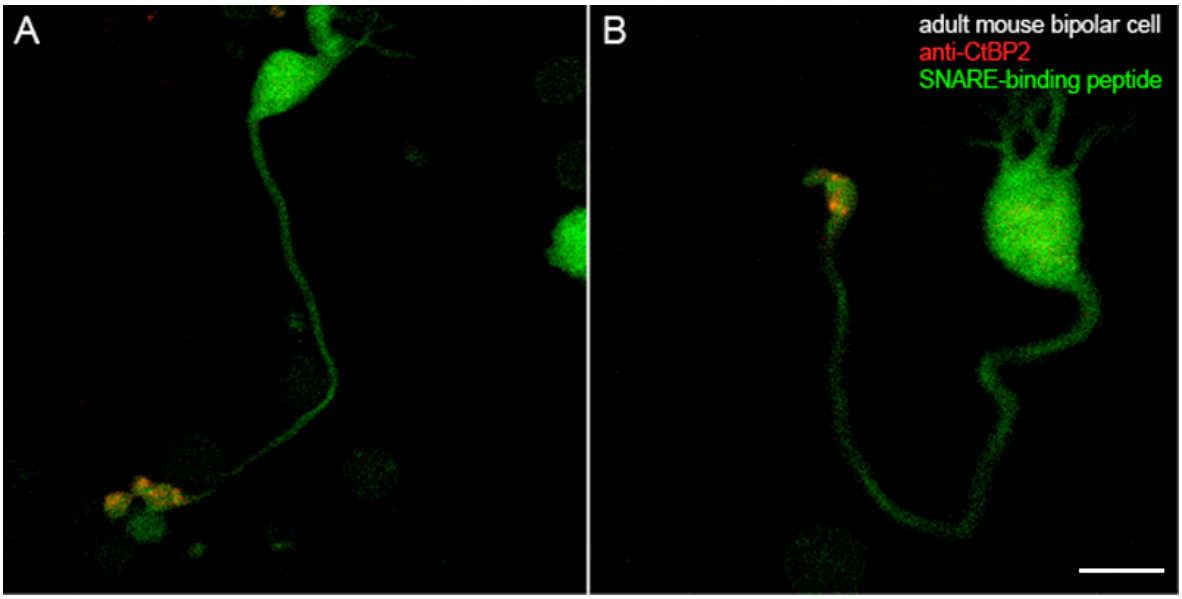

Figure 7-5. Fixed adult mouse retinal bipolar cells labeled with anti-CtBP2 and mouse complexin 3 peptide. Dissociated adult mouse retinal bipolar cells were plated onto glass coverslips, fixed, permeabilized with methanol, and incubated with anti-CtBP2 and the complexin 3 peptide (SNARE-binding peptide). Panels A and B show confocal micrographs of z-axis projections through two representative mouse bipolar cells loaded with anti-CtBP2 (red) and the complexin 3 peptide (green). While CtBP2/RIBEYE primarily clusters in presynaptic terminals, the complexin 3 peptide labels the mouse bipolar cell. Scale bar, 10 μm.

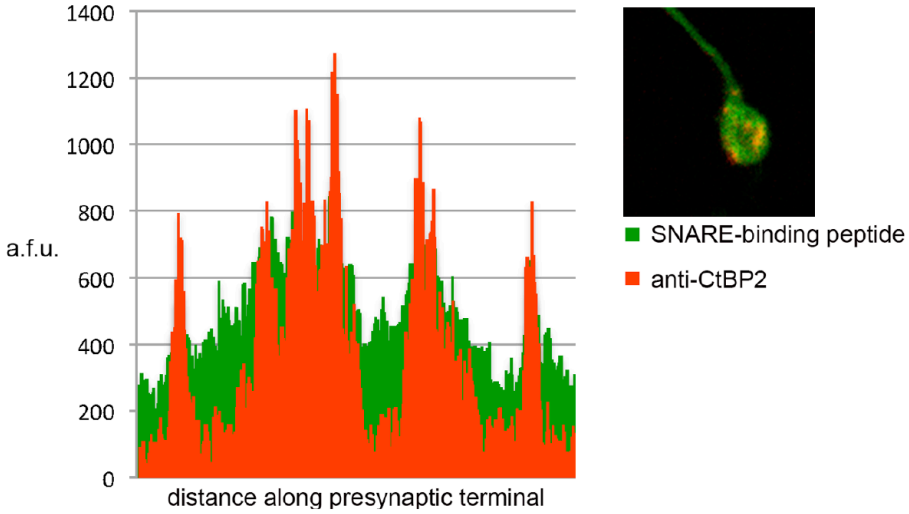

Figure 7-6. Profile plot of complexin 3 peptide and anti-CtBP2 fluorescence intensities across an adult mouse retinal bipolar cell presynaptic terminal. Dissociated adult mouse retinal bipolar cells were plated onto glass coverslips, fixed, permeabilized with methanol, and incubated with anti-CtBP2 and the complexin 3 peptide (SNARE-binding peptide). The inset shows a confocal projection containing a series of z-stacks through an entire presynaptic terminal labeled with anti-CtBP2 (red) and complexin 3 peptide (green). Fluorescence intensity profiles, for anti-CtBP2 (red trace) and complexin 3 peptide (green trace) across this presynaptic terminal, show co-localization. a.f.u., arbitrary fluorescence units.

Additional future directions

Examination of the expression and functions of the complexin 3/4 subfamily of SNARE regulators uncovered several novel findings and several results consistent with recent work performed on this subfamily in mammals (Reim et al., 2005; Reim et al., 2005; Strenzke et al., 2009). The novel finding of a role for complexin 3a during development could be followed by a study of complexin 3a mRNA and/or protein expression during early development. If complexin 3a expression is primarily dorsal in the developing otic vesicle, for example, this result would strengthen the hypothesis that complexin 3a is involved in dorsoventral patterning. The possibility exists that assembled SNARE complexes, rather than complexin 3a, have a dorsoventral gradient. Therefore, the complexin 3a SBD may be used as a probe during early development to visualize these complexes.

The finding that complexin 4a is required for visual system function depended on the use of an antisense morpholino oligonucleotide that blocked complexin 4a translation. It will be important to determine whether injection of full-length complexin 4a mRNA in the morphants rescues the defects in visual responses. As an alternative to the rescue experiments, we have performed preliminary experiments with a second morpholino. Injection of a morpholino antisense oligonucleotide directed against the 5'UTR did not affect visual responses or produce a phenotype (data not shown). It has not yet been determined if this morpholino can knock down complexin 4a expression, especially since it is not directed against the first ATG.

Finally, it will be worthwhile to examine more precisely the expression and functions of complexin 4b in hair cells. Several new antibodies against mammalian complexin 3/4 have recently become commercially available. These antibodies could be screened with our HEK cells that individually express complexin 3/4 family members. In addition, knockdown of complexin 4b or knockout with zinc finger nucleases could be used to perturb its expression. Several behavioral screens could be used to determine whether complexin 4b affects hair cell function in the inner ear and lateral line (Nicolson et al., 1998).

Bibliography

Abbas L, Whitfield TT (2010) The zebrafish inner ear. In: Zebrafish (Perry SF, Ekker M, Farrell AP, Brauner CJ, eds) San Diego: Academic Press.

Adato A, Lefèvre G, Delprat B, Michel V, Michalski N, Chardenoux S, Weil D, El-Amraoui A, Petit C (2005) Usherin, the defective protein in Usher syndrome type IIA, is likely to be a component of interstereocilia ankle links in the inner ear sensory cells. Hum Mol Genet 14:3921-3932.

Ahmed ZM, Goodyear R, Riazuddin S, Lagziel A, Legan PK, Behra M, Burgess SM, Lilley KS, Wilcox ER, Riazuddin S, Griffith AJ, Frolenkov GI, Belyantseva IA, Richardson GP, Friedman TB (2006) The tip-link antigen, a protein associated with the transduction complex of sensory hair cells, is protocadherin-15. J Neurosci 26:7022-7034.

Alexandre D, Ghysen A (1999) Somatotopy of the lateral line projection in larval zebrafish. Proc Natl Acad Sci U S A 96:7558-7562.

Allwardt BA, Lall AB, Brockerhoff SE, Dowling JE (2001) Synapse formation is arrested in retinal photoreceptors of the zebrafish nrc mutant. J Neurosci 21:2330-2342.

Allwardt BA, Dowling JE (2001) The pineal gland in wild-type and two zebrafish mutants with retinal defects. J Neurocytol 30:493-501.

Amores A, Force A, Yan YL, Joly L, Amemiya C, Fritz A, Ho RK, Langeland J, Prince V, Wang YL, Westerfield M, Ekker M, Postlethwait JH (1998) Zebrafish hox clusters and vertebrate genome evolution. Science 282:1711-1714.

An SJ, Grabner CP, Zenisek D (2010) Real-time visualization of complexin during single exocytic events. Nat Neurosci 13:577-583.

Babak E (1910) Zur Chromatischen Hautfunktion Der Amphibien, Pflugers Arch 131: 87-118.

Bagnara JT (1960) Pineal regulation of the body lightening reaction in amphibian larvae. Science 132:1481-1483.

Bagnara JT (1964) Independent actions of pineal and hypophysis in the regulation of chromatophores of anuran larvae. Gen Comp Endocrinol 123:299-303.

Bagnara JT, Hadley ME (1970) Endocrinology of the amphibian pineal. Am Zool 10:201-216.

Bang PI, Sewell WF, Malicki JJ (2001) Morphology and cell type heterogeneities of the inner ear epithelia in adult and juvenile zebrafish (Danio rerio). J Comp Neurol 438:173-190.

Baylor DA, Matthews G, Nunn BJ (1984) Location and function of voltage-sensitive

conductances in retinal rods of the salamander, Ambystoma tigrinum. J Physiol 354:203-223.

Belyantseva IA, Boger ET, Naz S, Frolenkov GI, Sellers JR, Ahmed ZM, Griffith AJ, Friedman TB (2005) Myosin-XVa is required for tip localization of whirlin and differential elongation of hair-cell stereocilia. Nat Cell Biol 7:148-156.

Berntson AK, Morgans CW (2003) Distribution of the presynaptic calcium sensors, synaptotagmin I/II and synaptotagmin III, in the goldfish and rodent retinas. J Vis 3:274-280.

Beurg M, Fettiplace R, Nam JH, Ricci AJ (2009) Localization of inner hair cell mechanotransducer channels using high-speed calcium imaging. Nat Neurosci 12:553-558.

Beutner D, Voets T, Neher E, Moser T (2001) Calcium dependence of exocytosis and endocytosis at the cochlear inner hair cell afferent synapse. Neuron 29:681-690.

Blaxter JHS, Fuiman LA (1989) Function of the free neuromasts of marine teleost larvae. In: The Mechanosensory Lateral Line. Neurobiology and Evolution (Coombs S, Görner P, Münz, H) New York: Springer-Verlag.

Bleckmann H, Topp G (1981) Surface wave sensitivity of the lateral line system of the topminnow Aplocheilus lineatus. Naturwissenschaften 68: 624-625.

Bolz H, von Brederlow B, Ramírez A, Bryda EC, Kutsche K, Nothwang HG, Seeliger M, del C-Salcedó Cabrera M, Vila MC, Molina OP, Gal A, Kubisch C (2001) Mutation of CDH23, encoding a new member of the cadherin gene family, causes Usher syndrome type 1D. Nat Genet 27:108-112.

Bonanomi D, Benfenati F, Valtorta F (2006) Protein sorting in the synaptic vesicle life cycle. Prog Neurobiol 80:177-217.

Bowen ME, Weninger K, Ernst J, Chu S, Brunger AT (2005) Single-molecule studies of synaptotagmin and complexin binding to the SNARE complex. Biophys J 89:690-702.

Bracher A, Kadlec J, Betz H, Weissenhorn W (2002) X-ray structure of a neuronal complexin-SNARE complex from squid. J Biol Chem 277:26517-26523.

Brockerhoff SE (2006) Measuring the optokinetic response of zebrafish larvae. Nat Protoc 1:2448-2451.

Brose N. 2008. For better or for worse: Complexins regulate SNARE function and vesicle fusion. Traffic 9:1403-1413.

Brown SD, Hardisty-Hughes RE, Mburu P (2008) Quiet as a mouse: dissecting the molecular and genetic basis of hearing. Nat Rev Genet 9:277-290.

Bunt AH (1971) Enzymatic digestion of synaptic ribbons in amphibian retinal photoreceptors. Brain Res 25:571-577.

Burns ME, Baylor DA (2001) Activation, deactivation, and adaptation in vertebrate photoreceptor cells. Annu Rev Neurosci 24:779-805.

Cajal SR (1892) The Structure of the Retina. (Thorpe SA, Glickstein M, transl), Springfield: Thomas 1972.

Carr CM, Munson M (2007) Tag team action at the synapse. EMBO Rep 8:834-838.

Cau E, Quillien A, Blader P (2008) Notch resolves mixed neural identities in the zebrafish epiphysis. Development 135:2391-2401.

Chen S, Diamond JS (2002) Synaptically released glutamate activates extrasynaptic NMDA receptors on cells in the ganglion cell layer of rat retina. J Neurosci 22:2165-2173.

Chen X, Tomchick DR, Kovrigin E, Arac D, Machius M, Südhof TC, Rizo J (2002) Three-dimensional structure of the complexin/SNARE complex. Neuron 33:397-409.

Chicka MC, Chapman ER (2009) Concurrent binding of complexin and synaptotagmin to liposome-embedded SNARE complexes. Biochemistry 48:657-659.

Choi SY, Borghuis BG, Rea R, Levitan ES, Sterling P, Kramer RH (2005) Encoding light intensity by the cone photoreceptor synapse. Neuron 48:555-562.

Claas B, Münz H (1981) Projection of lateral line afferents in a teleost's brain. Neurosci Lett 23:287-290.

Coggins MR, Grabner CP, Almers W, Zenisek D (2007) Stimulated exocytosis of endosomes in goldfish retinal bipolar neurons. J Physiol 584:853-865.

Copenhagen DR, Jahr CE (1989) Release of endogenous excitatory amino acids from turtle photoreceptors. Nature 341:536-539.

Corey DP, García-Añoveros J, Holt JR, Kwan KY, Lin SY, Vollrath MA, Amalfitano A, Cheung EL, Derfler BH, Duggan A, Géléoc GS, Gray PA, Hoffman MP, Rehm HL, Tamasauskas D, Zhang DS (2004) TRPA1 is a candidate for the mechanosensitive transduction channel of vertebrate hair cells. Nature 432:723-730.

Corti A (1851) Recherches sur l'organe de Corti de l'ouïe des mammifères. Z wiss Zool 3:1-106.

Curtis LB, Doneske B, Liu X, Thaller C, McNew JA, Janz R (2008) Syntaxin 3b is a t-SNARE specific for ribbon synapses of the retina. J Comp Neurol 510:550-559.

Curtis L, Datta P, Liu X, Bogdanova N, Heidelberger R, Janz R (2010) Syntaxin 3B is essential for the exocytosis of synaptic vesicles in ribbon synapses of the retina. Neurosci 166:832-841.

Defoe DM, Besharse JC (1985) Membrane assembly in retinal photoreceptors. II. Immunocytochemical analysis of freeze-fractured rod photoreceptor membranes using anti-opsin antibodies. J Neurosci 5:1023-1034.

Delprat B, Michel V, Goodyear R, Yamasaki Y, Michalski N, El-Amraoui A, Perfettini I, Legrain P, Richardson G, Hardelin JP, Petit C (2005) Myosin XVa and whirlin, two deafness gene products required for hair bundle growth, are located at the stereocilia tips and interact directly. Hum Mol Genet 14:401-410.

Denizot J-P, Bensouilah M, Roesler R, Schugardt C, Kirschbaum F (2007) Larval electroreceptors in the epidermis of mormyrid fish: II. the promormyromast. J Comp Neurol 501:801-823.

Deretic D, Papermaster DS (1991) Polarized sorting of rhodopsin on post-Golgi membranes in frog retinal photoreceptor cells. J Cell Biol 113:1281-1293.

Deretic D, Traverso V, Parkins N, Jackson F, Rodriguez de Turco EB, Ransom N (2004) Phosphoinositides, ezrin/moesin, and rac1 regulate fusion of rhodopsin transport carriers in retinal photoreceptors. Mol Biol Cell 15:359-370.

De Robertis E, Franchi CM (1956) Electron microscope observations on synaptic vesicles in synapses of the retinal rods and cones. J Biophys Biochem Cytol 2:307-318.

DeVries SH, Schwartz EA (1999) Kainate receptors mediate synaptic transmission between cones and 'Off' bipolar cells in a mammalian retina. Nature 397:157-160.

Dhingra NK, Ramamohan Y, Raju TR (1997) Developmental expression of synaptophysin, synapsin I and syntaxin in the rat retina. Brain Res Dev Brain Res 102:267-273.

Dick O, tom Dieck S, Altrock WD, Ammermuller J, Weiler R, Garner CC, Gundelfinger ED, Brandstätter JH (2003) The presynaptic active zone protein bassoon is essential for photoreceptor ribbon synapse formation in the retina. Neuron 37:775-786.

Dijkgraaf S (1963) The functioning and significance of the lateral-line organs. Biol Rev Camb Philos Soc 38:51-105.

Dowling JE, Boycott BB (1966) Organization of the primate retina: electron microscopy. Proc R Soc Lond B Biol Sci 166:80-111.

Dowling JE (1987) The Retina: an approachable part of the brain. Cambridge: The Belknap Press, Harvard University Press.

Dror AA, Avraham KB (2009) Hearing loss: mechanisms revealed by genetics and cell biology. Annu Rev Genet 43:411-437.

Eatock RA, Lysakowski A (2006) Mammalian vestibular hair cells. In: Vertebrate Hair Cells (Eatock RA, Fay RR, Popper AN, eds) New York:Springer.

Edmonds BW, Gregory FD, Schweizer FE (2004) Evidence that fast exocytosis can be predominantly mediated by vesicles not docked at active zones in frog saccular hair cells. J Physiol 560:439-450.

Ekström P (1984) Central neural connections of the pineal organ and retina in the teleost Gasterosteus aculeatus L. J Comp Neurol 226:321-335.

Ekström P, Meissl H (1997) The pineal organ of teleost fishes. Rev Fish Biol Fisheries 7:199-284.

el-Amraoui A, Sahly I, Picaud S, Sahel J, Abitbol M, Petit C (1996) Human Usher 1B/mouse shaker-1: the retinal phenotype discrepancy explained by the presence/absence of myosin VIIA in the photoreceptor cells. Hum Mol Genet 5:1171-1178.

Emran F, Rihel J, Adolph AR, Dowling JE (2010) Zebrafish larvae lose vision at night. Proc Natl Acad Sci USA107:6034-6039.

Ernest S, Rauch GJ, Haffter P, Geisler R, Petit C, Nicolson T (2000) Mariner is defective in myosin VIIA: a zebrafish model for human hereditary deafness. Hum Mol Genet 9:2189-2196.

Fadool JM (2003) Development of a rod photoreceptor mosaic revealed in transgenic zebrafish. Dev Biol 258:277-290.

Fadool JM, Dowling JE (2008) Zebrafish: a model system for the study of eye genetics. Prog Retin Eye Res 27:89-110.

Falcón J, Besseau L, Boeuf G (2006) Molecular and cellular regulation of pineal organ responses. Fish Physiol 25:243-306.

Falcón J, Besseau L, Fuentès M, Sauzet S, Magnanou E, Boeuf G. Structural and functional evolution of the pineal melatonin system in vertebrates (2009) Ann NY Acad Sci 1163:101-111.

Famiglietti EV Jr, Kaneko A, Tachibana M (1977) Neuronal architecture of on and off pathways to ganglion cells in carp retina. Science 198:1267-1269.

Fay RR (1984) The goldfish ear codes the axis of acoustic particle motion in three dimensions. Science 225:951-954.

Fernandez I, Araç D, Ubach J, Gerber SH, Shin O, Gao Y, Anderson RG, Südhof TC, Rizo J (2001) Three-dimensional structure of the synaptotagmin 1 C2B-domain: synaptotagmin 1 as a phospholipid binding machine. Neuron 32:1057-1069.

Fetcho JR, O'Malley DM (1995) Visualization of active neural circuitry in the spinal cord of intact zebrafish. J Neurophysiol 73:399-406.

Fettiplace R, Hackney CM (2006) The sensory and motor roles of auditory hair cells. Nat Rev Neurosci 7:19-29.

Field GD, Chichilnisky EJ (2007) Information processing in the primate retina: circuitry and coding. Annu Rev Neurosci 30:1-30.

Flock A, Wersall J (1962) A study of the orientation of the sensory hairs of the receptor cells in the lateral line organ of fish, with special reference to the function of the receptors. J Cell Biol 15:19-27.

Fuchs P.A. and T. Parsons (2006). Synaptic physiology of hair cells. In Springer Handbook of Auditory Research. Vol. 27:Sensory Hair Cells (Eatock RA, Fay RR, Popper AN, eds) New York:Springer.

Fujii R (2000) The regulation of motile activity in fish chromatophores. Pigment Cell Res 13:300-319.

Furukawa T (1981) Effects of efferent stimulation on the saccule of goldfish. J Physiol 315:203-215.

Geleoc GSG, Holt JR (2009) Hair Cells: Sensory Transduction. In: Encyclopedia of Neurosciences (Squire LR, ed) San Diego:Academic Press.

Gilbert SP (2001) High-performance fungal motors. Nature 414:597-598.

Gillespie PG, Müller U (2009) Mechanotransduction by hair cells: models, molecules, and mechanisms. Cell 139:33-44.

Giraudo CG, Eng WS, Melia TJ, Rothman JE (2006) A clamping mechanism involved in SNARE-dependent exocytosis. Science 313:676-680.

Giraudo CG, Garcia-Diaz A, Eng WS, Yamamoto A, Melia TJ, Rothman JE (2008) Distinct domains of complexins bind SNARE complexes and clamp fusion in vitro. J Biol Chem 283:21211-21219.

Giraudo CG, Garcia-Diaz A, Eng WS, Chen Y, Hendrickson WA, Melia TJ, Rothman JE (2009) Alternative zippering as an on-off switch for SNARE-mediated fusion. Science 323:512-516.

Glowatzki E, Fuchs PA (2002) Transmitter release at the hair cell ribbon synapse. Nat Neurosci 5:147-154.

Gorner P (1963) Untersuchungen zur Morphologie und Elektrophysiologie des Seitenlinienorgans vom Krallenfrosch (*Xenopus laevis* Daudin). Z Vergl Physiol 47:316-338.

Goodyear RJ, Marcotti W, Kros CJ, Richardson GP (2005) Development and properties of stereociliary link types in hair cells of the mouse cochlea. J Comp Neurol 485:75-85.

Gosse NJ, Baier H (2009) An essential role for Radar (Gdf6a) in inducing dorsal fate in the zebrafish retina. Proc Natl Acad Sci U S A 106:2236-2241.

Granseth B, Odermatt B, Royle SJ, Lagnado L (2006) Clathrin-mediated endocytosis is the dominant mechanism of vesicle retrieval at hippocampal synapses. Neuron 51:773-786.

Grant GB, Dowling JE (1995) A glutamate-activated chloride current in cone-driven ON bipolar cells of the white perch retina. J Neurosci 15:3852-3862.

Grati M, Aggarwal N, Strehler EE, Wenthold RJ (2006) Molecular determinants for differential membrane trafficking of PMCA1 and PMCA2 in mammalian hair cells. J Cell Sci 119:2995-3007.

Gray EG, Pease HL (1971) On understanding the organisation of the retinal receptor synapses. Brain Res 35:1-15.

Greenlee MH, Roosevelt CB, Sakaguchi DS (2001) Differential localization of SNARE complex proteins SNAP-25, syntaxin, and VAMP during development of the mammalian retina. J Comp Neurol 430:306-320.

Greenlee MH, Wilson MC, Sakaguchi DS (2002) Expression of SNAP-25 during mammalian retinal development: thinking outside the synapse. Semin Cell Dev Biol 13:99-106.

Guan R, Dai H, Rizo J (2008) Binding of the Munc13-1 MUN domain to membrane-anchored SNARE complexes. Biochemistry 47:1474-1481.

Haddon C, Lewis J (1996) Early ear development in the embryo of the zebrafish, Danio rerio. J Comp Neurol 365:113-128.

Hammerschmidt M, Pelegri F, Mullins MC, Kane DA, van Eeden FJ, Granato M, Brand M, Furutani-Seiki M, Haffter P, Heisenberg CP, Jiang YJ, Kelsh RN, Odenthal J, Warga RM, Nüsslein-Volhard C (1996) dino and mercedes, two genes regulating dorsal development in the zebrafish embryo. Development 123:95-102.

Hassan ES (1989) Hydrodynamic imaging of the surroundings by the lateral line of the blind cave fish Anoptichthys jordani. In: The Mechanosensory Lateral Line: Neurobiology and Evolution (Coombs S, Görner P, Münz H, eds) New York: Springer-Verlag.

Heidelberger R, Heinemann C, Neher E, Matthews G (1994) Calcium dependence of the rate of exocytosis in a synaptic terminal. Nature 371:513-515.

Heidelberger R (1998) Adenosine triphosphate and the late steps in calcium-dependent exocytosis at a ribbon synapse. J Gen Physiol 111:225-241.

Heidelberger R, Sterling P, Matthews G (2002) Roles of ATP in depletion and replenishment of the releasable pool of synaptic vesicles. J Neurophysiol 88:98-106.

Heidelberger R, Wang MM, Sherry DM (2003) Differential distribution of synaptotagmin immunoreactivity among synapses in the goldfish, salamander, and mouse retina. Vis Neurosci 20:37-49.

Heidelberger R, Thoreson WB, Witkovsky P (2005) Synaptic transmission at retinal ribbon synapses. Prog Retin Eye Res 24:682-720.

Hepp R, Langley K (2001) SNAREs during development. Cell Tissue Res 305:247-253.

Heuser J, Lennon AM (1973) Morphological evidence for exocytosis of acetylcholine during formation of synaptosomes from Torpedo electric organ. J Physiol 233:39P-41P.

Hilfiker S, Pieribone VA, Czernik AJ, Kao HT, Augustine GJ, Greengard P (1999) Synapsins as regulators of neurotransmitter release. Philos Trans R Soc Lond B Biol Sci 354:269-279.

Hill JK, Williams DE, Lemasurier M, Dumont RA, Strehler EE, Gillespie PG (2006) Splice-site A choice targets plasmamembrane Ca2+-ATPase isoform 2 to hair bundles. J Neurosci 26:6172–6180.

Hirano AA, Brandstätter JH, Brecha NC (2005) Cellular distribution and subcellular localization of molecular components of vesicular transmitter release in horizontal cells of rabbit retina. J Comp Neurol 488:70-81.

Hodge R (1998) Preparation of RNA dot-blots. Methods Mol Biol 86:73-75.

Hoekstra D, Janssen J (1985) Non-visual feeding behaviour of the mottled sculpin, *Cottus bairdi* in Lake Michigan. Env Biol Fish 12:111–117.

Holt M, Cooke A, Neef A, Lagnado L (2004) High mobility of vesicles supports continuous exocytosis at a ribbon synapse. Curr Biol 14:173-183.

Hu K, Carroll J, Rickman C, Davletov B (2002) Action of complexin on SNARE complex. J Biol Chem 277:41652-41656.

Hudspeth AJ (1989) How the ear's works work. Nature 341:397-404.

Huntwork S, Littleton JT (2007) A complexin fusion clamp regulates spontaneous neurotransmitter release and synaptic growth. Nat Neurosci 10:1235-1237.

Ishida AT, Stell WK, Lightfoot DO (1980) Rod and cone inputs to bipolar cells in goldfish retina. J Comp Neurol 191:315-335.

Ishizuka T, Saisu H, Odani S, Abe T (1995) Synaphin: a protein associated with the docking/fusion complex in presynaptic terminals. Biochem Biophys Res Commun 213:1107-1114.

Itakura M, Misawa H, Sekiguchi M, Takahashi S, Takahashi M (1999) Transfection analysis of functional roles of complexin I and II in the exocytosis of two different types of secretory vesicles. Biochem Biophys Res Commun 265:691-696.

Johansson JU, Ericsson J, Janson J, Beraki S, Stanić D, Mandic SA, Wikström MA, Hökfelt T, Ogren SO, Rozell B, Berggren PO, Bark C (2008) An ancient duplication of exon 5 in the Snap25 gene is required for complex neuronal development/function. PLoS Genet 4(11):e1000278.

Kachar B, Battaglia A, Fex J (1997) Compartmentalized vesicular traffic around the hair cell cuticular plate. Hear Res 107:102-112.

Kaneko A (1970) Physiological and morphological identification of horizontal, bipolar and amacrine cells in goldfish retina. J Physiol 207:623-633.

Kappers JA (1960) The development, topographical relations and innervation of the epiphysis cerebri in the albino rat. Z Zellforsch Mikrosk Anat 52:163-215.

Kazmierczak P, Sakaguchi H, Tokita J, Wilson-Kubalek EM, Milligan RA, Müller U, Kachar B (2007) Cadherin 23 and protocadherin 15 interact to form tip-link filaments in sensory hair cells. Nature 449:87-91.

Kelsh RN, Brand M, Jiang YJ, Heisenberg CP, Lin S, Haffter P, Odenthal J, Mullins MC, van Eeden FJ, Furutani-Seiki M, Granato M, Hammerschmidt M, Kane DA, Warga RM, Beuchle D, Vogelsang L, Nüsslein-Volhard C (1996) Zebrafish pigmentation mutations and the processes of neural crest development. Development 123:369-389.

Kelsh RN, Eisen JS (2000) The zebrafish colourless gene regulates development of non-ectomesenchymal neural crest derivatives. Development 127:515-525.

Kennedy B, Malicki J (2009) What drives cell morphogenesis: a look inside the vertebrate photoreceptor. Dev Dyn 238:2115-2138.

Khimich D, Pujol R, tom Dieck S, Egner A, Gundelfinger ED, Moser T (2005) Hair cell synaptic ribbons are essential for synchronous auditory signalling. Nature 434:889-894.

Kikkawa Y, Mburu P, Morse S, Kominami R, Townsend S, Brown SD (2005) Mutant analysis reveals whirlin as a dynamic organizer in the growing hair cell stereocilium. Hum Mol Genet 14:391-400.

Kim JW, Lemke G (2006) Hedgehog-regulated localization of Vax2 controls eye development. Genes Dev 20:2833-2847.

Kimmel CB, Ballard WW, Kimmel SR, Ullmann B, Schilling TF (1995) Stages of embryonic development of the zebrafish. Dev Dyn 203:253-310.

King TS, Dougherty WJ (1980) Neonatal development of circadian rhythm in "synaptic" ribbon numbers in the rat pinealocyte. Am J Anat 157:335-343.

Korf HW, Wagner U (1980) Evidence for a nervous connection between the brain and the pineal organ in the guinea pig. Cell Tissue Res 209:505-510.

Kornblum HI, Corwin JT, Trevarrow B (1990) Selective labeling of sensory hair cells and neurons in auditory, vestibular, and lateral line systems by a monoclonal antibody. J Comp Neurol 301:162-170.

Ladman AJ (1958) The fine structure of the rod-bipolar cell synapse in the retina of the albino rat. J Biophys Biochem Cytol 4:459-466.

Lagnado L, Gomis A, Job C (1996) Continuous vesicle cycling in the synaptic terminal of retinal bipolar cells. Neuron 17:957-967.

Larison KD, Bremiller R (1990) Early onset of phenotype and cell patterning in the embryonic zebrafish retina. Development 109:567-576.

Laurens H (1914) The reactions of normal and eyeless amphibian larvae to light. J Exp Zool 16:195-210.

Lerner AB, Case JD, Takahashi Y, Lee TH, Mori W (1958) Isolation of melatonin, the pineal factor that lightens melanocytes. J Am Chem Soc 80, 2857-2858.

Lerner AB, Case JD (1959) Pigment cell regulatory factors. J Invest Dermatol 32:211-221.

Lewis ER, Leverenz EL, Bialek WS (1985) The Vertebrate Inner Ear. Boca Raton:CRC Press.

Li C, Davletov BA, Südhof TC (1995) Distinct Ca2+ and Sr2+ binding properties of synaptotagmins. Definition of candidate Ca2+ sensors for the fast and slow components of neurotransmitter release. J Biol Chem 270:24898-24902.

Lim DJ (1987) Functional structure of the organ of Corti: a review. Hear Res 28:9-21.

Lingel A, Simon B, Izaurralde E, Sattler M (2003) Structure and nucleic-acid binding of the Drosophila Argonaute 2 PAZ domain. Nature 426:465-469.

LoGiudice L, Sterling P, Matthews G (2008) Mobility and turnover of vesicles at the synaptic ribbon. J Neurosci 28:3150-3158.

Londin ER, Niemiec J, Sirotkin HI (2005) Chordin, FGF signaling, and mesodermal factors cooperate in zebrafish neural induction. Dev Biol 279:1-19.

López-Schier H, Starr CJ, Kappler JA, Kollmar R, Hudspeth AJ (2004) Directional cell migration establishes the axes of planar polarity in the posterior lateral-line organ of the zebrafish. Dev Cell 7:401-412.

López-Schier H, Hudspeth AJ (2006) A two-step mechanism underlies the planar polarization of regenerating sensory hair cells. Proc Natl Acad Sci USA103:18615-18620.

Luo DG, Su CY, Yau KW (2009) Photoreceptors: physiology. In: Encyclopedia of Neurosciences (Squire LR, ed) San Diego:Academic Press.

Lupo G, Harris WA, Lewis KE (2006) Mechanisms of ventral patterning in the vertebrate nervous system. Nat Rev Neurosci 7:103-114.

Maerker T, van Wijk E, Overlack N, Kersten FF, McGee J, Goldmann T, Sehn E, Roepman R, Walsh EJ, Kremer H, Wolfrum U (2008) A novel Usher protein network at the periciliary reloading point between molecular transport machineries in vertebrate photoreceptor cells. Hum Mol Genet 17:71-86.

Magupalli VG, Schwarz K, Alpadi K, Natarajan S, Seigel GM, Schmitz F (2008) Multiple RIBEYE-RIBEYE interactions create a dynamic scaffold for the formation of synaptic ribbons. J Neurosci 28:7954-7967.

Malsam J, Seiler F, Schollmeier Y, Rusu P, Krause JM, Söllner TH (2009) The carboxy-terminal domain of complexin I stimulates liposome fusion. Proc Natl Acad Sci USA 106:2001-2006.

Marc RE, Sperling HG (1976) The chromatic organization of the goldfish cone mosaic. Vision Res 16:1211-1224.

Marc RE, Stell WK, Bok D, Lam DM (1978) GABA-ergic pathways in the goldfish retina. J Comp Neurol 182:221-244.

Marc RE (1999) The structure of vertebrate retinas. In: *The Retinal Basis of Vision* (Toyoda, J-I, Murkami M, Kaneko A, Saito T, eds) Amsterdam: Elsevier.

Marchiafava PL, Kusmic C (1993) The electrical responses of the trout pineal photoreceptors to brief and prolonged illumination. Prog Brain Res 95:3-13.

Masai I, Heisenberg CP, Barth KA, Macdonald R, Adamek S, Wilson SW (1997) floating head and masterblind regulate neuronal patterning in the roof of the forebrain. Neuron 18:43-57.

Masland RH (2001) The fundamental plan of the retina. Nat Neurosci 4:877-886.

Matthews G, Sterling P (2008) Evidence that vesicles undergo compound fusion on the synaptic ribbon. J Neurosci 28:5403-5411.

Matthews G, Fuchs P (2010) The diverse roles of ribbon synapses in sensory neurotransmission. Nat Rev Neurosci 11:812-822.

Maximov A, Tang J, Yang X, Pang ZP, Südhof TC (2009) Complexin controls the force transfer from SNARE complexes to membranes in fusion. Science 323:516-521.

Mbiene JP, Sans A (1986) Differentiation and maturation of the sensory hair bundles in the fetal and postnatal vestibular receptors of the mouse: a scanning electron microscopy study. J Comp Neurol 254:271-278.

McCord CP, Allen FP (1917) Evidences associating pineal gland function with alterations in pigmentation. J Exp Zool 23:207-224.

McGee J, Goodyear RJ, McMillan DR, Stauffer EA, Holt JR, Locke KG, Birch DG, Legan PK, White PC, Walsh EJ, Richardson GP (2006) The very large G-protein-coupled receptor VLGR1: a component of the ankle link complex required for the normal development of auditory hair bundles. J Neurosci 26:6543-6553.

McLaughlin T, Hindges R, O'Leary DD (2003) Regulation of axial patterning of the retina and its topographic mapping in the brain. Curr Opin Neurobiol 13:57-69.

McMahon HT, Missler M, Li C, Südhof TC (1995) Complexins: cytosolic proteins that regulate SNAP receptor function. Cell 83:111-119.

McNulty JA (1980) Ultrastructural obsevations on synaptic ribbons in the pineal organ of the goldfish. Cell Tissue Res 210:249-256.

Meissl H, Nakamura T, Thiele G (1986) Neural response mechanisms in the photoreceptive pineal organ of goldfish. J Comp Physiol 84A:467-473.

Meissl H, Ekström P (1988) Photoreceptor responses to light in the isolated pineal organ of the trout, Salmo gairdneri. Neurosci 25:1071-1076.

Meller K (1968) Histogenesis and cytogenesis of the developing retina. An electron microscopical study. Veroff Morphol Pathol 77:1-77.

Mellman I, Nelson WJ (2008) Coordinated protein sorting, targeting and distribution in polarized cells. Nat Rev Mol Cell Biol 9:833-845.

Mennerick S, Matthews G (1996) Ultrafast exocytosis elicited by calcium current in synaptic terminals of retinal bipolar neurons. Neuron 17:1241-1249.

Metcalfe WK, Kimmel CB, Schabtach E (1985) Anatomy of the posterior lateral line system in young larvae of the zebrafish. J Comp Neurol 233:377-389.

Michalski N, Michel V, Bahloul A, Lefèvre G, Barral J, Yagi H, Chardenoux S, Weil D, Martin P, Hardelin JP, Sato M, Petit C (2007) Molecular characterization of the ankle-link complex in cochlear hair cells and its role in the hair bundle functioning. J Neurosci 27:6478-6488.

Montgomery JC, Baker CF, and Carton AG (1997) The lateral line can mediate rheotaxis in fish. Nature 389:960-963.

Morgan JL, Dhingra A, Vardi N, Wong RO (2006) Axons and dendrites originate from neuroepithelial-like processes of retinal bipolar cells. Nat Neurosci 9:85-92.

Morgans CW, Brandstätter JH, Kellermann J, Betz H, Wässle H (1996) A SNARE complex containing syntaxin 3 is present in ribbon synapses of the retina. J Neurosci 16:6713-6721.

Morgans CW, Zhang J, Jeffrey BG, Nelson SM, Burke NS, Duvoisin RM, Brown RL (2009) TRPM1 is required for the depolarizing light response in retinal ON-bipolar cells. Proc Natl Acad Sci U S A 106:19174-19178.

Mui SH, Hindges R, O'Leary DD, Lemke G, Bertuzzi S (2002) The homeodomain protein Vax2 patterns the dorsoventral and nasotemporal axes of the eye. Development 129:797-804.

Mui SH, Kim JW, Lemke G, Bertuzzi S (2005) Vax genes ventralize the embryonic eye. Genes Dev 19:1249-1259.

Murakami SL, Cunningham LL, Werner LA, Bauer E, Pujol R, Raible DW, Rubel EW (2003) Developmental differences in susceptibility to neomycin-induced hair cell death in the lateral line neuromasts of zebrafish (Danio rerio). Hear Res 186:47-56.

Muresan V, Lyass A, Schnapp BJ (1999) The kinesin motor KIF3A is a component of the presynaptic ribbon in vertebrate photoreceptors. J Neurosci 19:1027-1037.

Nagiel A, Andor-Ardó D, Hudspeth AJ (2008) Specificity of afferent synapses onto plane-polarized hair cells in the posterior lateral line of the zebrafish. J Neurosci 228:8442-8453.

Nakajima Y, Iwakabe H, Akazawa C, Nawa H, Shigemoto R, Mizuno N, Nakanishi S (1993) Molecular characterization of a novel retinal metabotropic glutamate receptor mGluR6 with a high agonist selectivity for L-2-amino-4-phosphonobutyrate. J Biol Chem 268:11868-11873.

Nawrocki L (1985) Development of the neural retina in the zebrafish, Brachydanio rerio. PhD Thesis University of Oregon, Eugene.

Nayak GD, Ratnayaka HS, Goodyear RJ, Richardson GP (2007) Development of the hair bundle and mechanotransduction. Int J Dev Biol 51:597-608.

Neuhauss SC, Biehlmaier O, Seeliger MW, Das T, Kohler K, Harris WA, Baier H (1999) Genetic disorders of vision revealed by a behavioral screen of 400 essential loci in zebrafish. J Neurosci 19:8603-8615.

Negishi K, Kato S, Teranishi T (1988) Dopamine cells and rod bipolar cells contain protein kinase C-like immunoreactivity in some vertebrate retinas. Neurosci Lett 94:247-252.

Neuhauss SCF (2010) Zebrafish vision: Structure and function of the zebrafish visual system. Fish Physiol 29:81-122.

Nicolson T, Rusch A, Friedrich RW, Granato M, Ruppersberg JP, Nusslein-Volhard C (1998) Genetic analysis of vertebrate sensory hair cell mechanosensation: the zebrafish circler mutants. Neuron 20:271-283.

Nilsson SE (1964) Receptor cell outer segment development and ultrastructure of the disk membranes in the retina of the tadpole (rana pipiens). J Ultrastruct Res 11:581-602.

Northcutt RG *(1989)* The phylogenetic distribution and innervation of craniate mechanoreceptive lateral lines. In: The Mechanosensory Lateral Line: Neurobiology and Evolution (Coombs S, Görner P, Münz H, eds) New York: Springer-Verlag.

Nouvian R, Beutner D, Parsons TD, Moser T (2006) Structure and function of the hair cell ribbon synapse. J Mem Biol 209:153-165.

Obholzer N, Wolfson S, Trapani JG, Mo W, Nechiporuk A, Busch-Nentwich E, Seiler C, Sidi S, Söllner C, Duncan RN, Boehland A, Nicolson T (2008) Vesicular glutamate transporter 3 is required for synaptic transmission in zebrafish hair cells. J Neurosci 28:2110-2118.

Oikawa T (1971) Histochemical and physiological study of chromaffin cells in the skin of the medaka, Oryzias latipes. Dev Growth Differ 13:125-130.

Olney JW (1968) Centripetal sequence of appearance of receptor-bipolar synaptic structures in developing mouse retina. Nature 218:281-282.

Ono S, Baux G, Sekiguchi M, Fossier P, Morel NF, Nihonmatsu I, Hirata K, Awaji T, Takahashi S, Takahashi M (1998) Regulatory roles of complexins in neurotransmitter release from mature presynaptic nerve terminals. Eur J Neurosci 10:2143-2152.

Pabst S, Hazzard JW, Antonin W, Südhof TC, Jahn R, Rizo J, Fasshauer D (2000) Selective interaction of complexin with the neuronal SNARE complex. Determination of the binding regions. J Biol Chem 275:19808-19818.

Palmer MJ, Hull C, Vigh J, von Gersdorff H (2003) Synaptic cleft acidification and modulation of short-term depression by exocytosed protons in retinal bipolar cells. J Neurosci 23:11332-11341.

Parker GH (1948) Animal colour changes and their neurohumours; a survey of investigations, 1910-1943. Cambridge: Cambridge University Press.

Parsons TD, Sterling P (2003) Synaptic ribbon. Conveyor belt or safety belt? Neuron 37:379-382.

Petit C, Richardson GP (2009) Linking genes underlying deafness to hair-bundle development and function. Nat Neurosci 12:703-710.

Piatigorsky J (2001) Dual use of the transcriptional repressor (CtBP2)/ribbon synapse (RIBEYE) gene: how prevalent are multifunctional genes? Trends Neurosci 24:555-557.

Pickles JO, Comis SD, Osborne MP (1984) Cross-links between stereocilia in the guinea pig organ of Corti, and their possible relation to sensory transduction. Hear Res 15:103-112.

Pitcher TJ, Partridge BL, Wardle CS (1976) A blind fish can school. Science 194:963-965.

Polishchuk R, Di Pentima A, Lippincott-Schwartz J (2004) Delivery of raft-associated, GPI-anchored proteins to the apical surface of polarized MDCK cells by a transcytotic pathway. Nat Cell Biol 6:297-307.

Polyak SL (1941) The Retina. Chicago: The University of Chicago Press.

Popper AN, Fay RR (1993) Sound detection and processing by fish: critical review and major research questions. Brain Behav Evol 41:14-38.

Postlethwait JH, Yan YL, Gates MA, Horne S, Amores A, Brownlie A, Donovan A, Egan ES, Force A, Gong Z, Goutel C, Fritz A, Kelsh R, Knapik E, Liao E, Paw B, Ransom D, Singer A, Thomson M, Abduljabbar TS, Yelick P, Beier D, Joly JS, Larhammar D, Rosa F, Westerfield M, Zon LI, Johnson SL, Talbot WS (1998) Vertebrate genome evolution and the zebrafish gene map. Nat Genet 18:345-349.

Prokop A, Meinertzhagen IA (2006) Development and structure of synaptic contacts in Drosophila. Sem Cell Devel Biol 17:20-30.

Raible DW, Kruse GJ (2000) Organization of the lateral line system in embryonic zebrafish. J Comp Neurol 421:189-198.

Raymond PA, Barthel LK, Curran GA (1995) Developmental patterning of rod and cone photoreceptors in embryonic zebrafish. J Comp Neurol 359:537-550.

Redecker P (1996) Synaptotagmin I, synaptobrevin II, and syntaxin I are coexpressed in rat and gerbil pinealocytes. Cell Tiss Res 283:443-454.

Redecker P, Weyer C, Grube D (1996) Rat and gerbil pinealocytes contain the synaptosomal-associated protein 25 (SNAP-25). J Pineal Res 21:29-34.

Regus-Leidig H, Tom Dieck S, Specht D, Meyer L, Brandstätter JH (2009) Early steps in the assembly of photoreceptor ribbon synapses in the mouse retina: the involvement of precursor spheres. J Comp Neurol 512:814-824.

Regus-Leidig H, tom Dieck S, Brandstätter JH (2010) Absence of functional active zone protein Bassoon affects assembly and transport of ribbon precursors during early steps of photoreceptor synaptogenesis. Eur J Cell Biol 89:468-475.

Reim K, Regus-Leidig H, Ammermüller J, El-Kordi A, Radyushkin K, Ehrenreich H, Brandstätter JH, Brose N (2009) Aberrant function and structure of retinal ribbon synapses in the absence of complexin 3 and complexin 4. J Cell Sci 122:1352-1361.

Reiter RJ (1981-1982) The pineal gland. Boca Raton: CRC Press.

Retzius G (1884) Das Gehörorgan der Wirbelthiere. II. Das Gehörorgan der Reptilien, der Vogel und der Saügethiere. Stockholm: Samson and Wallin.

Reim K, Mansour M, Varoqueaux F, McMahon HT, Südhof TC, Brose N, Rosenmund C (2001) Complexins regulate a late step in Ca2+-dependent neurotransmitter release. Cell 104:71-

81.

Reim K, Wegmeyer H, Brandstätter JH, Xue M, Rosenmund C, Dresbach T, Hofmann K, Brose N (2005) Structurally and functionally unique complexins at retinal ribbon synapses. J Cell Biol 169:669-680.

Rieke F, Schwartz EA (1996) Asynchronous transmitter release: control of exocytosis and endocytosis at the salamander rod synapse. J Physiol (London) 493:1-8.

Riley BB, Zhu C, Janetopoulos C, Aufderheide KJ (1997) A critical period of ear development controlled by distinct populations of ciliated cells in the zebrafish. Dev Biol 191:191-201.

Risinger C, Salaneck E, Söderberg C, Gates M, Postlethwait JH, Larhammar D (1998) Cloning of two loci for synapse protein Snap25 in zebrafish: comparison of paralogous linkage groups suggests loss of one locus in the mammalian lineage. J Neurosci Res 54:563-573.

Roberts BL, Meredith GE (1989) The efferent system. In: The Mechanosensory Lateral Line: Neurobiology and Evolution (Coombs S, Görner P, Münz H, eds) New York: Springer-Verlag.

Rizo J, Rosenmund C (2008) Synaptic vesicle fusion. Nat Struct Mol Biol 15:665-674.

Roberts WM, Jacobs RA, Hudspeth AJ (1990) Colocalization of ion channels involved in frequency selectivity and synaptic transmission at presynaptic active zones of hair cells. J Neurosci 10:3664-3684.

Robinson J, Schmitt EA, Hárosi FI, Reece RJ, Dowling JE (1993) Zebrafish ultraviolet visual pigment: absorption spectrum, sequence, and localization. Proc Natl Acad Sci USA 90:6009-6012.

Rodieck RW (1973) The vertebrate retina: principles of structure and function. San Francisco: W. H. Freeman and Company.

Rouze NC, Schwartz EA (1998) Continuous and transient vesicle cycling at a ribbon synapse. J Neurosci 18:8614-8624.

Rzadzinska AK, Schneider ME, Davies C, Riordan GP, Kachar B (2004) An actin molecular treadmill and myosins maintain stereocilia functional architecture and self-renewal. J Cell Biol 164:887-897.

Safieddine S, Wenthold RJ (1999) SNARE complex at the ribbon synapses of cochlear hair cells: analysis of synaptic vesicle- and synaptic membrane-associated proteins. Eur J Neurosci 11:803-812.

Safieddine S, Ly CD, Wang YX, Wang CY, Kachar B, Petralia RS, Wenthold RJ (2002) Ocsyn, a novel syntaxin-interacting protein enriched in the subapical region of inner hair cells.

Mol Cell Neurosci 20:343-353.

Saito K (1980) Fine structure of the sensory epithelium of the guinea pig organ of Corti: afferent and efferent synapses of hair cells. J Ultrastruct Res 71:222-232.

Saisu H, Ibaraki K, Yamaguchi T, Sekine Y, Abe T (1991) Monoclonal antibodies immunoprecipitating omega-conotoxin-sensitive calcium channel molecules recognize two novel proteins localized in the nervous system. Biochem Biophys Res Commun 181:59-66.

Schaeffer SF, Raviola E (1978) Membrane recycling in the cone cell endings of the turtle retina. J Cell Biol 79:802-825.

Schaub JR, Lu X, Doneske B, Shin YK, McNew JA (2006) Hemifusion arrest by complexin is relieved by Ca2+-synaptotagmin I. Nat Struct Mol Biol 13:748-750.

Schier AF, Talbot WS (2005) Molecular genetics of axis formation in zebrafish. Annu Rev Genet 39:561-613.

Schmitz F, Konigstorfer A, Sudhof TC (2000) RIBEYE, a component of synaptic ribbons: a protein's journey through evolution provides insight into synaptic ribbon function. Neuron 28:857-872.

Schneider ME, Dosé AC, Salles FT, Chang W, Erickson FL, Burnside B, Kachar B (2006) A new compartment at stereocilia tips defined by spatial and temporal patterns of myosin IIIa expression. J Neurosci 26:10243-10252.

Schroeter EH, Wong RO, Gregg RG (2006) In vivo development of retinal ON bipolar cell axonal terminals visualized in nyx::MYFP transgenic zebrafish. Vis Neurosci 23:833-843.

Schulze FE (1861) Uber die Nervenendigung in den sogenannten Schleimkanalen der Fische und uber entsprechende Organe der durch Kiemenathmenden Amphibien. Arch Anat Physiol Lpz 759-769.

Schwander M, Kachar B, Müller U (2010) The cell biology of hearing. J Cell Biol 190:9-20.

Seiler C, Nicolson T (1999) Defective calmodulin-dependent rapid apical endocytosis in zebrafish sensory hair cell mutants. J Neurobiol 41:424-434.

Sejnowski TJ, Yodlowski ML (1982) A freeze-fracture study of the skate electroreceptor. J Neurocytol 11:897-912.

Shao X, Fernandez I, Südhof TC, Rizo J (1998) Solution structures of the Ca2+-free and Ca2+-bound C2A domain of synaptotagmin I: does Ca2+ induce a conformational change? Biochemistry 37:16106-16115.

Sheets L, Ransom DG, Mellgren EM, Johnson SL, Schnapp BJ (2007) Zebrafish melanophilin facilitates melanosome dispersion by regulating dynein. Curr Biol 17:1721-1734.

Shen Y, Heimel JA, Kamermans M, Peachey NS, Gregg RG, Nawy S (2009) A transient receptor potential-like channel mediates synaptic transmission in rod bipolar cells. J Neurosci 29:6088-6093.

Sherry DM, Yazulla S (1993) Goldfish bipolar cells and axon terminal patterns: a Golgi study. J Comp Neurol 329:188-200.

Sherry DM, Wang MM, Bates J, Frishman LJ (2003) Expression of vesicular glutamate transporter 1 in the mouse retina reveals temporal ordering in development of rod vs. cone and ON vs. OFF circuits. J Comp Neurol 465:480-498.

Shiraki T, Kojima D, Fukada Y (2010) Light-induced body color change in developing zebrafish. Photochem Photobiol Sci 9:1498-1504.

Sidi S, Busch-Nentwich E, Friedrich R, Schoenberger U, Nicolson T (2004) gemini encodes a zebrafish L-type calcium channel that localizes at sensory hair cell ribbon synapses. J Neurosci 24:4213-4223.

Siegel JH, Brownell WE (1986) Synaptic and Golgi membrane recycling in cochlear hair cells. J Neurocytol 15:311-328.

Siemens J, Lillo C, Dumont RA, Reynolds A, Williams DS, Gillespie PG, Müller U (2004) Cadherin 23 is a component of the tip link in hair-cell stereocilia. Nature 428:950-955.

Singer JH, Diamond JS (2006) Vesicle depletion and synaptic depression at a mammalian ribbon synapse. J Neurophysiol 95:3191-3198.

Singer JH, Lassova L, Vardi N, Diamond JS (2004) Coordinated multivesicular release at a mammalian ribbon synapse. Nat Neurosci 7:826-833.

Sjöstrand FS (1953) The ultrastructure of the retinal rod synapses of the guinea pig eye. J Appl Phys 24:1422-1429.

Sjöstrand F (1958) Ultrastructure of retinal rod synapses of the guinea pig eye as revealed by three-dimensional reconstructions from serial sections. J Ultrastruct Res 2:122-170.

Sobkowicz HM, Rose JE, Scott GL, Levenick CV (1986) Distribution of synaptic ribbons in the developing organ of Corti. J Neurocytol 15:693-714.

Söllner C, Rauch GJ, Siemens J, Geisler R, Schuster SC, Müller U, Nicolson T; Tübingen 2000 Screen Consortium (2004) Mutations in cadherin 23 affect tip links in zebrafish sensory hair cells. Nature 428:955-959.

Song JJ, Liu J, Tolia NH, Schneiderman J, Smith SK, Martienssen RA, Hannon GJ, Joshua-Tor L (2003) The crystal structure of the Argonaute2 PAZ domain reveals an RNA binding motif in RNAi effector complexes. Nat Struct Biol 10:1026-1032.

Spassova MA, Avissar M, Furman AC, Crumling MA, Saunders JC, Parsons TD (2004) Evidence that rapid vesicle replenishment of the synaptic ribbon mediates recovery from short-term adaptation at the hair cell afferent synapse. J Assoc Res Otolaryngol 5:376-390.

Spiwoks-Becker I, Maus C, tom Dieck S, Fejtová A, Engel L, Wolloscheck T, Wolfrum U, Vollrath L, Spessert R (2008) Active zone proteins are dynamically associated with synaptic ribbons in rat pinealocytes. Cell Tissue Res 333:185-195.

Stauffer EA, Scarborough JD, Hirono M, Miller ED, Shah K, Mercer JA, Holt JR, Gillespie PG (2005) Fast adaptation in vestibular hair cells requires myosin-1c activity. Neuron 47:541-553.

Stell WK (1967) The structure and relationships of horizontal cells and photoreceptor-bipolar synaptic complexes in goldfish retina. Am J Anat 121:401-423.

Sterling P (2004) How retinal circuits optimize the transfer of visual information. In: The Visual Neurosciences (Chalupa LM, Werner JS, eds) Cambridge: MIT Press.

Sterling P, Demb J (2004) Retina. In: The Synaptic Organization of the Brain, 5th edition (Shepherd GM ed), New York: Oxford University Press.

Strenzke N, Chanda S, Kopp-Scheinpflug C, Khimich D, Reim K, Bulankina AV, Neef A, Wolf F, Brose N, Xu-Friedman MA, Moser T (2009) Complexin-I is required for high-fidelity transmission at the endbulb of held auditory synapse. J Neurosci 29:7991-8004.

Stryer L (1986) Cyclic GMP cascade of vision. Annu Rev Neurosci 9:87-119.

Sung CH, Chuang JZ (2010) The cell biology of vision. J Cell Biol 190:953-963.

Sutton RB, Fasshauer D, Jahn R, Brunger AT (1998) Crystal structure of a SNARE complex involved in synaptic exocytosis at 2.4 A resolution. Nature 395:347-353.

Tachibana M, Kaneko A (1987) gamma-Aminobutyric acid exerts a local inhibitory action on the axon terminal of bipolar cells: evidence for negative feedback from amacrine cells. Proc Natl Acad Sci 84:3501-3505.

Takahashi S, Yamamoto H, Matsuda Z, Ogawa M, Yagyu K, Taniguchi T, Miyata T, Kaba H, Higuchi T, Okutani F, Fujimoto, S (1995) Identification of two highly homologous

presynaptic proteins distinctly localized at the dendritic and somatic synapses. FEBS Lett 368:455-460.

Takei K, Mundigl O, Daniell L, De Camilli P (1996) The synaptic vesicle cycle: a single vesicle budding step involving clathrin and dynamin. J Cell Biol 133:1237-1250.

Tang J, Maximov A, Shin OH, Dai H, Rizo J, Südhof TC (2006) A complexin/synaptotagmin 1 switch controls fast synaptic vesicle exocytosis. Cell 126:1175-1187.

Tanimoto M, Ota Y, Horikawa K, Oda Y (2009) Auditory input to CNS is acquired coincidentally with development of inner ear after formation of functional afferent pathway in zebrafish. J Neurosci 29:2762-2767.

Thoreson WB, Rabl K, Townes-Anderson E, Heidelberger R (2004) A highly Ca2+-sensitive pool of vesicles contributes to linearity at the rod photoreceptor ribbon synapse. Neuron 42:595-605.

Tokumaru H, Umayahara K, Pellegrini LL, Ishizuka T, Saisu H, Betz H, Augustine GJ, Abe T (2001) SNARE complex oligomerization by synaphin/complexin is essential for synaptic vesicle exocytosis. Cell 104:421-432.

Tomchik SM, Lu Z (2005) Octavolateral projections and organization in the medulla of a teleost fish, the sleeper goby (Dormitator latifrons). J Comp Neurol 481:96-117.

tom Dieck S, Altrock WD, Kessels MM, Qualmann B, Regus H, Brauner D, Fejtova A, Bracko O, Gundelfinger ED, Brandstätter JH (2005) Molecular dissection of the photoreceptor ribbon synapse: physical interaction of Bassoon and RIBEYE is essential for the assembly of the ribbon complex. J Cell Biol 168:825-836.

Ullrich B, Südhof TC (1994) Distribution of synaptic markers in the retina: implications for synaptic vesicle traffic in ribbon synapses. J Physiol (Paris) 88:249-257.

Usukura J, Yamada E (1987) Ultrastructure of the synaptic ribbons in photoreceptor cells of Rana catesbeiana revealed by freeze-etching and freeze-substitution. Cell Tiss Res 247:483-488.

Van Epps HA, Hayashi M, Lucast L, Stearns GW, Hurley JB, De Camilli P, Brockerhoff SE (2004) The zebrafish nrc mutant reveals a role for the polyphosphoinositide phosphatase synaptojanin 1 in cone photoreceptor ribbon anchoring. J Neurosci 24:8641-8650.

van Genderen MM, Bijveld MM, Claassen YB, Florijn RJ, Pearring JN, Meire FM, McCall MA, Riemslag FC, Gregg RG, Bergen AA, Kamermans M (2009) Mutations in TRPM1 are a common cause of complete congenital stationary night blindness. Am J Hum Genet 85:730-736.

Vigh B, Manzano MJ, Zádori A, Frank CL, Lukáts A, Röhlich P, Szél A, Dávid C (2002).

Nonvisual photoreceptors of the deep brain, pineal organs and retina. Histol Histopathol 17:555-590.

Vollrath L (1981) The pineal organ. New York: Springer-Verlag.

Vollrath L and Spiwoks-Becker I (1996) Plasticity of retinal ribbon synapses. Microsc Res Tech 35:472–487.

von Békésy G (1989) Experiments in Hearing. New York: McGraw-Hill.

von Frisch K (1911) Beitrage zur physiologie der pigmentzellen in der fischhaut, Pflugers Arch 138:319–387.

von Gersdorff H, Vardi E, Matthews G, Sterling P (1996) Evidence that vesicles on the synaptic ribbon of retinal bipolar neurons can be rapidly released. Neuron 16:1221-1227.

von Kriegstein K, Schmitz F (2003) The expression pattern and assembly profile of synaptic membrane proteins in ribbon synapses of the developing mouse retina. Cell Tissue Res 311:159-173.

Wan L, Almers W, Chen W (2005) Two ribeye genes in teleosts: the role of Ribeye in ribbon formation and bipolar cell development. J Neurosci 25:941-949.

Wässle H, Boycott BB (1991) Functional architecture of the mammalian retina. Physiol Rev 71:447-480.

Weil D, Blanchard S, Kaplan J, Guilford P, Gibson F, Walsh J, Mburu P, Varela A, Levilliers J, Weston MD, et al. (1995) Defective myosin VIIA gene responsible for Usher syndrome type 1B. Nature 374:60-61.

Weisz OA, Rodriguez-Boulan E (2009) Apical trafficking in epithelial cells: signals, clusters and motors. J Cell Sci 122:4253-4266.

Weninger K, Bowen ME, Choi UB, Chu S, Brunger AT (2008) Accessory proteins stabilize the acceptor complex for synaptobrevin, the 1:1 syntaxin/SNAP-25 complex. Structure 16:308-320.

Werblin FS, Dowling JE (1969) Organization of the retina of the mudpuppy, Necturus maculosus. II. Intracellular recording. J Neurophysiol 32:339-355.

Westerfield M: The Zebrafish Book. A guide for the Laboratory Use of Zebrafish (Danio rerio) Eugene: University of Oregon Press 2000.

Whitfield TT, Riley BB, Chiang MY, Phillips B (2002) Development of the zebrafish inner ear. Dev Dyn 223:427-458.

Wilson SW, Easter SS Jr (1991) A pioneering growth cone in the embryonic zebrafish brain. Proc Natl Acad Sci USA 88:2293-2296.

Wittig JH, Jr., Parsons TD (2008) Synaptic ribbon enables temporal precision of hair cell afferent synapse by increasing the number of readily releasable vesicles: a modeling study. J Neurophysiol 100:1724-1739.

Xue M, Reim K, Chen X, Chao HT, Deng H, Rizo J, Brose N, Rosenmund C (2007) Distinct domains of Complexin I differentially regulate neurotransmitter release. Nat Stuct Mol Biol 14:949-958.

Xue M, Stradomska A, Chen H, Brose N, Zhang W, Rosenmund C, Reim K (2008) Complexins are facilitators of neurotransmitter release at mammalian central excitatory and inhibitory synapses. Proc Natl Acad Sci USA 105:7875-7880.

Xue M, Lin YQ, Pan H, Reim K, Deng H, Bellen HJ, Rosenmund C (2009) Tilting the balance between facilitatory and inhibitory functions of mammalian and Drosophila complexins orchestrates synaptic vesicle exocytosis. Neuron 64:367-380.

Yamaguchi Y, Hearing VJ (2009) Physiological factors that regulate skin pigmentation. Biofactors 35:193-199.

Yan D, Liu XZ (2010) Genetics and pathological mechanisms of Usher syndrome. J Hum Genet 55:327-335.

Yan KS, Yan S, Farooq A, Han A, Zeng L, Zhou MM (2003) Structure and conserved RNA binding of the PAZ domain. Nature 426:468-474.

Yáñez J, Busch J, Anadón R, Meissl H (2009) Pineal projections in the zebrafish (Danio rerio): overlap with retinal and cerebellar projections. Neurosci 164:1712-1720.

Yazulla S, Studholme KM, Wu JY (1987) GABAergic input to the synaptic terminals of mb1 bipolar cells in the goldfish retina. Brain Res 411:400-405.

Yazulla S, Studholme KM (2001) Neurochemical anatomy of the zebrafish retina: an immunocytochemical analysis. J Neurocytol 30:551-592.

Yokoyama S, Oksche A, Darden TR, Farner DS (1978) The sites of encephalic photoreception in photoperiodic induction of the growth of testes in the white-crowed sparrow, *Zonotrichia leucophrys gambelii*. Cell Tissue Res 189:441-467.

Yoon TY, Lu X, Diao J, Lee SM, Ha T, Shin YK (2008) Complexin and Ca2+ stimulate SNARE-mediated membrane fusion. Nat Struct Mol Biol 15:707-713.

Young RW (1967) The renewal of photoreceptor cell outer segments. J Cell Biol 33:61-72.

Zanazzi G, Matthews G (2007) A doubleheader in endocytosis. Neuron 56:939-942.

Zanazzi G, Matthews G (2009) The molecular architecture of ribbon presynaptic terminals. Mol Neurobiol 39:130-148.

Zanazzi G, Matthews G (2010) Enrichment and differential targeting of complexins 3 and 4 in ribbon-containing sensory neurons during zebrafish development. Neural Dev Sep 1;5:24.

Zenisek D (2008) Vesicle association and exocytosis at ribbon and extraribbon sites in retinal bipolar cell presynaptic terminals. Proc Natl Acad Sci USA 105:4922-4927.

Zenisek D, Steyer JA, Almers W (2000) Transport, capture and exocytosis of single synaptic vesicles at active zones. Nature 406:849-854.

Zenisek D, Steyer JA, Feldman ME, Almers W (2002) A membrane marker leaves synaptic vesicles in milliseconds after exocytosis in retinal bipolar cells. Neuron 35:1085-1097.

Zenisek D, Davila V, Wan L, Almers W (2003) Imaging calcium entry sites and ribbon structures in two presynaptic cells. J Neurosci 23:2538-2548.

Zenisek D, Horst NK, Merrifield C, Sterling P, Matthews G (2004) Visualizing synaptic ribbons in the living cell. J Neurosci 24:9752-9759.

Zhang C, Song Y, Thompson DA, Madonna MA, Millhauser GL, Toro S, Varga Z, Westerfield M, Gamse J, Chen W, Cone RD (2010) Pineal-specific agouti protein regulates teleost background adaptation. Proc Natl Acad Sci USA 107:20164-20171.

Zhu Y, Xu J, Heinemann SF (2009) Two pathways of synaptic vesicle retrieval revealed by single vesicle imaging. Neuron 61:397-411.

Ziv L, Gothilf Y (2006) Circadian time-keeping during early stages of development. Proc Natl Acad Sci USA 103:4146-4151.